

An investigation of the properties of
large-conductance Ca^{2+} -activated K^{+}
channels of rat arterial smooth muscle
and their modulation by
vasoconstrictors.

Anna Sowerby

February 2009

PhD

ABSTRACT

Anna Sowerby

An investigation of the properties of large-conductance Ca^{2+} -activated K^+ channels of rat arterial smooth muscle and their modulation by vasoconstrictors

Large-conductance Ca^{2+} -activated K^+ (BK_{Ca}) channels play an important role in the regulation of vascular tone. They are activated by membrane depolarization and increases in local Ca^{2+} concentration ($[\text{Ca}^{2+}]$). Their location in the plasma membrane allows them to be activated by transient releases of Ca^{2+} from ryanodine receptors (RyR) in the sarcoplasmic reticulum, termed Ca^{2+} sparks, leading to the efflux of K^+ known as a spontaneous transient outward current (STOC). Activation of BK_{Ca} channels in this manner provides a negative feedback mechanism to regulate vasoconstriction by hyperpolarizing the cell membrane and so reducing Ca^{2+} influx through L-type voltage dependent Ca^{2+} channels. In this thesis I have investigated the relationship between $[\text{Ca}^{2+}]_i$ and membrane potential using inside-out patches excised from smooth muscle cells isolated from rat mesenteric artery. Whole-cell BK_{Ca} currents in these cells were also investigated both in the form of STOCs and by using voltage pulses to activate BK_{Ca} channels. The effects of the vasoconstrictors endothelin-1 (ET-1) and angiotensin II (Ang II) on both pulse-induced BK_{Ca} currents and STOC amplitude and frequency were investigated. Single BK_{Ca} channels with a slope conductance of 189 pA were recorded and their activation was shown to be dependent on $[\text{Ca}^{2+}]_i$ and membrane potential. Membrane depolarization also increased BK_{Ca} whole-cell current and the frequency and amplitude of STOCs. ET-1 and Ang II were found to inhibit pulse-induced BK_{Ca} currents and this effect of ET-1 could be inhibited using a peptide PKC inhibitor. ET-1 and Ang II also caused a decrease in both STOC amplitude and frequency, although the decrease in frequency may be the result of the reduction in amplitude. Finally, 1, 2-dioctanoyl-*sn*-glycerol (DOG), an analogue of the endogenous PKC activator diacylglycerol (DAG), was seen to inhibit both BK_{Ca} whole-cell and single channel currents, possibly due to direct inhibition of BK_{Ca} channels.

ACKNOWLEDGEMENTS

First of all I would like to thank my supervisor, Dr Noel Davies, for his support and guidance throughout the length of my project. I would also like to thank Dr Richard Rainbow for his help with the patch clamp technique and Prof. Nick Standen and Dr Martine Hamann for guidance provided as members of my thesis committee.

I would also like to mention my friends and colleagues at The University of Leicester, and to thank them for making my time at the university such an enjoyable experience.

Finally, I would like to thank my family, especially my fiancé Barry, for their patience, love, and support throughout this time.

ABBREVIATIONS

Abbreviation	Explanation
ACE	angiotensin converting enzyme
ADP	adenosine diphosphate
Ang II	angiotensin II
ANS	autonomic nervous system
ATP	adenosine triphosphate
BK _{Ca}	large-conductance Ca ²⁺ -activated K ⁺ channel
BTX	Batrachotoxin
cAMP	cyclic adenosine monophosphate
cGMP	cyclic guanosine monophosphate
CICR	calcium-induced calcium release
Cl _{Ca}	Ca ²⁺ -activated Cl ⁻ channels
CRAC	Ca ²⁺ -release activated Ca ²⁺ -entry
DAG	diacylglycerol
DOG	1, 2-dioctanoylglycerol
DTE	dithioerythritol
ET-1	endothelin-1
ET _A	endothelin type A receptor
GI	gastro-intestinal
HEK	human embryonic kidney
IbTx	iberiotoxin
IK _{Ca}	intermediate-conductance Ca ²⁺ -activated K ⁺ channel
IP ₃	inositol-1, 4, 5-trisphosphate
IP ₃ R	IP ₃ receptor
K _{ATP}	adenosine triphosphate-sensitive K ⁺ channel
Kir	inward rectifier K ⁺ channel
Kv	voltage-activated K ⁺ channel
MLCK	myosin light chain kinase
MLCP	myosin light chain phosphatase
NCX	Na ⁺ /Ca ²⁺ exchanger
P _i	inorganic phosphate molecule
PIP ₂	phosphatidylinositol-4, 5-bisphosphate
PKA	protein kinase A
PKC	protein kinase C
PKC-IP	PKC inhibitor peptide
PKG	protein kinase G

PLC	phospholipase C
PMCA	plasma membrane Ca^{2+} pump
P_{open}	open probability
RyR	ryanodine receptor
SEM	standard error of the mean
SERCA	sarcoplasmic or endoplasmic reticulum Ca^{2+} -ATPase
SK_{Ca}	small-conductance Ca^{2+} -activated K^{+} channel
SOC	store-operated channel
SR	sarcoplasmic reticulum
STOC	spontaneous transient outward current
TAT	transacting activator of transcription
TEA	Tetraethylammonium
TRPC	canonical transient receptor potential
VDCC	voltage-dependent Ca^{2+} channel

TABLE OF CONTENTS

ABSTRACT.....	ii
ACKNOWLEDGEMENTS.....	iii
ABBREVIATIONS	iv
TABLE OF CONTENTS.....	vi
TABLE OF FIGURES	x
1 INTRODUCTION	12
1.1 Muscle types and the regulation of contraction	12
1.1.1 Contractile machinery of skeletal and cardiac muscle.....	12
1.1.2 Contractile machinery of smooth muscle	14
1.1.3 Mechanism of contraction	15
1.1.4 Modulation of smooth muscle sensitivity to Ca^{2+}	18
1.2 Vascular smooth muscle	19
1.2.1 Regulation of vascular smooth muscle tone	20
1.2.1.1 Regulation by autonomic innervation	20
1.2.1.2 Regulation by vasoactive substances.....	21
1.2.1.3 Myogenic response	23
1.2.2 The role of protein kinases.....	24
1.3 The role of Ca^{2+} and its mobilization in vascular smooth muscle	25
1.3.1 Ca^{2+} influx through ion channels	25
1.3.2 Release of Ca^{2+} from intracellular stores	26
1.4 Membrane proteins involved in ion transport	31
1.4.1 Regulation of Ca^{2+}	31
1.4.2 Regulation of Na^{+}	34
1.4.3 Ca^{2+} -activated Cl^{-} channels.....	36
1.5 K^{+} channels	37
1.5.1 The role of K^{+} channels in vascular smooth muscle.....	37
1.5.2 Types of K^{+} channel found in vascular smooth muscle.....	38
1.5.2.1 K_v channels	38
1.5.2.2 K_{ATP} channels	39
1.5.2.3 K_{ir} channels.....	39
1.5.2.4 K_{Ca} channels	40

1.6	BK _{Ca} Channel Structure & Function	42
1.6.1	BK _{Ca} channel structure	42
1.6.1.1	The α -subunit.....	42
1.6.1.2	The β -subunit.....	45
1.6.2	The role of BK _{Ca} channels in vascular smooth muscle.....	46
1.6.2.1	The role of Ca ²⁺ sparks and STOCs.....	46
1.6.3	Regulation of BK _{Ca} channels by vasoactive substances	49
1.6.4	BK _{Ca} channels as drug targets.....	51
1.7	Aims of thesis.....	52
2	METHODS	53
2.1	Isolation of smooth muscle cells from rat mesenteric artery	53
2.2	Electrophysiology	56
2.2.1	The patch-clamp method	56
2.2.2	General principles of the patch-clamp technique	56
2.2.3	Fabrication of electrodes.....	57
2.2.4	Obtaining a seal	57
2.3	Solutions.....	59
2.3.1	Solutions for recording of single channel currents	59
2.3.2	Solutions for recording of pulse-induced whole-cell currents.....	60
2.3.3	Solutions for recording of STOCs	60
2.3.4	Drugs and solutions	61
2.4	Recording of Currents	62
2.4.1	Recording of BK _{Ca} single channel currents	62
2.4.2	Recording of BK _{Ca} whole-cell currents using voltage pulses.....	62
2.4.3	Recording of STOCs.....	63
2.5	Data analysis	65
2.5.1	Analysis of single BK _{Ca} channels	65
2.5.2	Analysis of whole-cell currents induced by voltage pulses.....	68
2.5.3	Analysis of STOCs	68
2.5.4	Statistical analyses	70
3	CHARACTERIZATION OF BK _{Ca} SINGLE CHANNEL PROPERTIES	71
3.1	Recording of single BK _{Ca} channels.....	71
3.2	Analysis of BK _{Ca} single channel activity.....	73

3.2.1	The effect of voltage on the activity of single BK _{Ca} channels.....	73
3.2.2	The effect of [Ca ²⁺] _i on the activity of single BK _{Ca} channels.....	78
3.3	Analysis of BK _{Ca} channel kinetics	83
3.3.1	The effect of voltage on BK _{Ca} channel kinetics.....	83
3.3.2	The effect of [Ca ²⁺] _i on BK _{Ca} channel kinetics.....	84
3.4	Modulation of BK _{Ca} channels by 1,2 dioctanoyl- <i>sn</i> -glycerol	88
3.4.1	The effect of 1, 2-dioctanoyl- <i>sn</i> -glycerol on the activity of single BK _{Ca} channels	88
3.4.2	The effect of 1,2-dioctanoyl- <i>sn</i> -glycerol on BK _{Ca} channel kinetics.....	89
3.5	Discussion	94
3.5.1	Recording BK _{Ca} single channel currents	94
3.5.2	The effect of Ca ²⁺ and voltage on BK _{Ca} single channel activity	94
3.5.3	The effect of Ca ²⁺ and voltage on BK _{Ca} single channel kinetics	96
3.5.4	The effect of 1, 2-dioctanoyl- <i>sn</i> -glycerol on BK _{Ca} single channel activity	96
4	MODULATION OF VOLTAGE PULSE-INDUCED BK _{Ca} CURRENTS	98
4.1	Recording of BK _{Ca} whole-cell currents	98
4.1.1	Ryanodine reduces fluctuations in BK _{Ca} whole-cell current caused by the presence of STOCs	100
4.1.2	The effects of membrane potential and [Ca ²⁺] _i on BK _{Ca} whole-cell current	101
4.1.3	The effects of ET-1 on whole-cell BK _{Ca} current	107
4.1.4	The effects of PKC activation on BK _{Ca} whole-cell current.....	108
4.1.5	The effects of ET-1 is inhibited by pre-incubation of the cells with PKC-IP.....	110
4.1.6	The effects of Ang II on BK _{Ca} whole-cell current.....	114
4.2	Discussion	116
4.2.1	Recording of BK _{Ca} whole-cell currents	116
4.2.2	Ryanodine reduces fluctuations in BK _{Ca} whole-cell current caused by the presence of STOCs	116
4.2.3	The effects of membrane potential and [Ca ²⁺] _i on BK _{Ca} whole-cell current	118
4.2.4	The effects of ET-1 on BK _{Ca} whole-cell current	119
4.2.5	The effects of 1, 2-dioctanoyl- <i>sn</i> -glycerol on BK _{Ca} whole-cell currents.....	120

4.2.6	The effects of Ang II on BK _{Ca} whole-cell current	120
5	MODULATION OF SPONTANEOUS TRANSIENT OUTWARD CURRENTS.....	122
5.1	Analysis of STOCs.....	123
5.2	Recording of STOCs	125
5.2.1	STOCs in mesenteric artery smooth muscle cells are due to	
	activation of BK _{Ca} channels.....	125
5.2.2	The effect of Ca ²⁺ buffering on STOC activity	128
5.2.3	Ca ²⁺ -release is from the SR.....	130
5.2.4	The effect of membrane potential on STOC activity.....	135
5.2.5	The effect of [Ca ²⁺] _i on STOC activity.....	136
5.2.6	The effects of vasoconstrictors on STOCs	143
5.3	Discussion	150
5.3.1	Analysis of STOCs	150
5.3.2	STOCs in mesenteric artery smooth muscle cells are due to	
	activation of BK _{Ca} channels.....	150
5.3.3	The effect of Ca ²⁺ buffering on STOC activity	151
5.3.4	Ca ²⁺ -release is from the SR.....	152
5.3.5	The effect of membrane potential on STOC activity.....	153
5.3.6	The effect of [Ca ²⁺] _i on STOC activity.....	157
5.3.7	Modulation of STOCs by ET-1 & Ang II.....	159
6	DISCUSSION.....	163
6.1	Future work	170
	REFERENCES	172

TABLE OF FIGURES

Figure 1.1 <i>The sarcomere of striated muscle.</i>	13
Figure 1.2 <i>The cross-bridge mechanism of muscle contraction.</i>	16
Figure 1.3 <i>K⁺ channel nomenclature tree.</i>	41
Figure 1.4 <i>Schematic diagram illustrating the structure of the α- and β-subunits of the BK_{Ca} channel.</i>	44
Figure 2.1 <i>Photographs of smooth muscle cells isolated from rat mesenteric artery.</i> .	55
Figure 2.2 <i>Patch clamp cell configurations.</i>	58
Figure 2.3 <i>Protocols used for the recording of currents.</i>	64
Figure 2.4 <i>The method used by the in-house software programme to detect STOCs.</i> ...	70
Figure 3.1 <i>Possible presence of subconductance states and a voltage-dependent channel.</i>	72
Figure 3.2 <i>Fitting of Boltzmann equation to show the effect of membrane potential on BK_{Ca} single channel activity.</i>	75
Figure 3.3 <i>Plot of V_{1/2} against [Ca²⁺]_i.</i>	75
Figure 3.4 <i>Effect of membrane potential on BK_{Ca} single channel activity.</i>	76
Figure 3.5 <i>Effect of membrane potential on BK_{Ca} single channel amplitude.</i>	77
Figure 3.6 <i>Concentration-response curve to show the effect of [Ca²⁺]_i on BK_{Ca} single channel activity.</i>	79
Figure 3.7 <i>Effect of [Ca²⁺]_i on BK_{Ca} single channel activity.</i>	80
Figure 3.8 <i>Effect of [Ca²⁺]_i on BK_{Ca} single channel activity.</i>	81
Figure 3.9 <i>Hill plot showing the relationship between [Ca²⁺]_i and the P_{open} of the channel.</i>	82
Figure 3.10 <i>Effect of membrane potential on BK_{Ca} channel kinetics.</i>	85
Figure 3.11 <i>Effect of membrane potential on BK_{Ca} channel kinetics.</i>	86
Figure 3.12 <i>Effect of [Ca²⁺]_i on BK_{Ca} channel kinetics.</i>	87
Figure 3.13 <i>Effect of DOG on BK_{Ca} single channel activity.</i>	90
Figure 3.14 <i>Effect of DOG on BK_{Ca} single channel amplitude.</i>	91
Figure 3.15 <i>Effect of the application of 10 μM DOG on the kinetics of the BK_{Ca} channel.</i>	92
Figure 3.16 <i>Effect of the application of 1 μM DOG on the kinetics of the BK_{Ca} channel.</i>	93
Figure 4.1 <i>BK_{Ca} control currents.</i>	99
Figure 4.2 <i>Effect of BK_{Ca} channel blockers on whole-cell current.</i>	99
Figure 4.3 <i>Effect of ryanodine on BK_{Ca} whole-cell current.</i>	103
Figure 4.4 <i>Effect of [Ca²⁺]_i on BK_{Ca} whole-cell current.</i>	104
Figure 4.5 <i>Current-voltage plot showing effect of [Ca²⁺]_i and voltage on BK_{Ca} whole-cell current.</i>	105
Figure 4.6 <i>Effect of [Ca²⁺]_i and membrane potential on BK_{Ca} tail currents.</i>	106
Figure 4.7 <i>Effect of ET-1 on BK_{Ca} whole-cell current in the absence and presence of PKC-IP.</i>	112

Figure 4.8 <i>Effect of 1,2-dioctanoyl-sn-glycerol on BK_{Ca} whole-cell current.</i>	113
Figure 4.9 <i>Effect of 100 nM Ang II on BK_{Ca} whole-cell current.</i>	115
Figure 5.1 <i>Use of in-house software to analyse STOCs.</i>	126
Figure 5.2 <i>Effect of BK_{Ca} channel blockers on STOCs.</i>	127
Figure 5.3 <i>Effect of EGTA on STOCs.</i>	129
Figure 5.4 <i>Effect of EGTA on the frequency of STOCs.</i>	129
Figure 5.5 <i>Effect of 10 μM ryanodine on STOCs.</i>	132
Figure 5.6 <i>Effect of 10 mM caffeine on STOCs.</i>	133
Figure 5.7 <i>Effect of 1 mM caffeine on STOCs.</i>	134
Figure 5.8 <i>Effect of membrane potential on STOCs</i>	138
Figure 5.9 <i>Effect of [Ca²⁺]_i on STOCs</i>	139
Figure 5.10 <i>Effect of [Ca²⁺]_i and voltage on the frequency and amplitude of STOCs.</i> 140	
Figure 5.11 <i>Graph showing the effect of membrane potential on the slope of STOC activation.</i>	141
Figure 5.12 <i>Graph showing the effect of an increase in STOC rise time on the activation slope of simulated STOCs.</i>	141
Figure 5.13 <i>Graph showing the effect of [Ca²⁺]_i on the slope of STOC activation.</i> ..	142
Figure 5.14 <i>Effect of ET-1 on STOCs.</i>	145
Figure 5.15 <i>Effect of ET-1 on the amplitude and frequency of STOCs.</i>	145
Figure 5.16 <i>Effect of TEA on STOCs.</i>	146
Figure 5.17 <i>Effect of TEA on the amplitude and frequency of STOCs.</i>	146
Figure 5.18 <i>Graph showing the effect of application of 10 nM ET-1 on the slope of STOC activation.</i>	147
Figure 5.19 <i>Effect of Ang II on STOCs.</i>	148
Figure 5.20 <i>Effect of Ang II on the frequency and amplitude of STOCs.</i>	149
Figure 5.21 <i>Graph showing the effect of application of 100 nM Ang II on the slope of STOC activation.</i>	149

1 INTRODUCTION

1.1 Muscle types and the regulation of contraction

There are 3 distinct types of muscle found in the body: cardiac, skeletal and smooth muscle. Cardiac muscle cells are found only in the heart, as their name suggests, and provide the powerful contractile force required to pump blood around the body. Skeletal muscle is attached to the skeleton and is required for the movement of the body. Smooth muscle cells form the walls of hollow organs such as bronchi, the urinary bladder, arteries and veins. Skeletal muscle is under voluntary control by the somatic nervous system, whereas smooth and cardiac muscles are controlled by the non-voluntary autonomic nervous system (ANS). They share similarities and differences in their structure that allows them to perform their own specific function.

1.1.1 Contractile machinery of skeletal and cardiac muscle

Cardiac and skeletal muscles are structurally very different but the contractile mechanism contained within them is similar. They are both striated muscle types, with the striation banding pattern being formed by the arrangement of thick and thin filaments within the cells. The thick filaments are composed primarily of myosin filaments whilst the thin filaments are formed mainly from actin. Myosin is a protein with ATPase activity that is composed of a “tail” region and two “heads” and plays an important role in the contractile mechanism. It is the tail region that forms the bulk of the thick filament body, whilst the heads are required to bind to the actin molecules of thin filaments to form what is known as a “cross-bridge” between the thick and thin filaments. Thin filaments are attached at one end to the “Z line”. A single Z line has

thin filaments projecting outwards in both directions and the area between two Z lines where thin filaments and thick filaments overlap is known as the sarcomere (figure 1.1). The degree of overlap between thick and thin filaments is what regulates muscle contraction. An increase in overlap causes the length of the H zone to decrease and so the sarcomere shortens and the muscle contracts.

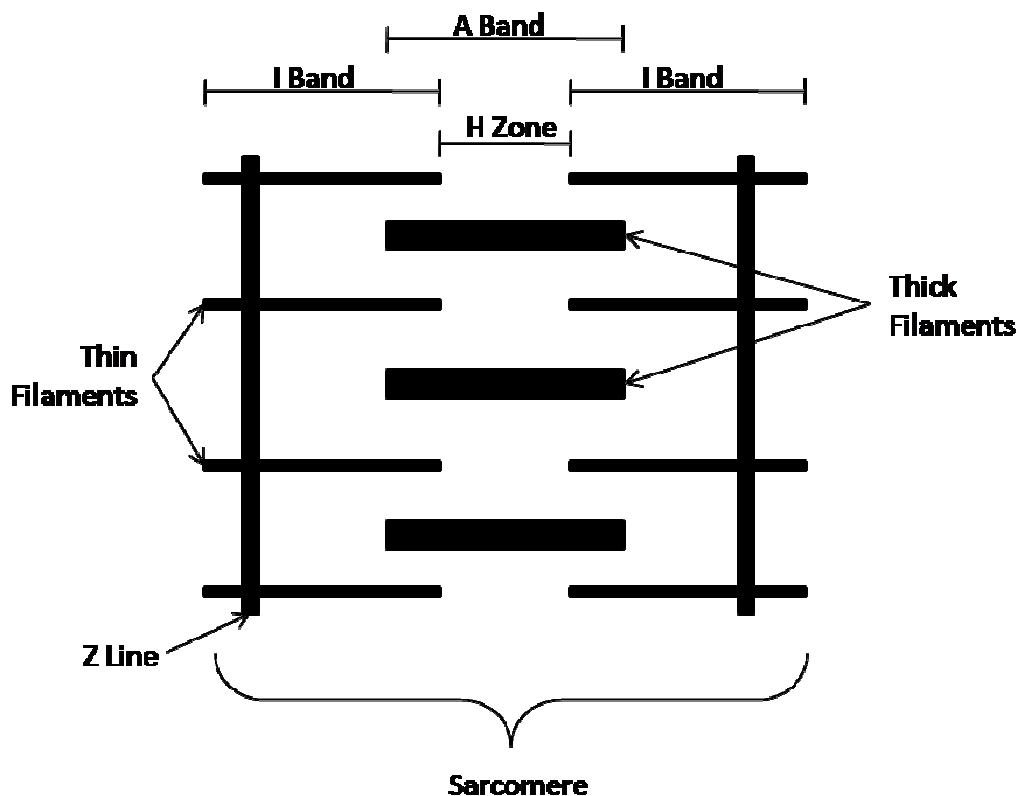


Figure 1.1 The sarcomere of striated muscle. Thin filaments protrude outwards from the Z line to overlap the thick filaments slightly. An increase in the amount of overlap causes the sarcomere to shorten and the muscle to contract. The H zone shortens as a result of this but the I bands and A band remain the same length.

1.1.2 Contractile machinery of smooth muscle

Much of the contractile machinery contained in smooth muscle cells is the same as that of skeletal and cardiac muscles but the striation pattern is lacking, suggesting that the machinery is perhaps arranged differently. It is this lack of striation that gives this type of muscle its name. Smooth muscle cells contain actin and myosin filaments, as in other muscle types, but they are organised differently within the cell. The filaments are arranged in a similar fashion to the sarcomeres of skeletal and cardiac muscles, but they run laterally across the cell rather than longitudinally as in these other muscle types. It is this orientation that results in the lack of striation. Smooth muscle cells contain dense bodies, the equivalent of Z lines, positioned at opposite ends of the cell. These bodies are formed largely from α -actinin, just like Z lines, and connect the actin filaments to the plasma membrane. The sites where the dense bodies attach to the plasma membrane are often arranged in opposition to the dense bodies of neighbouring cells to form connections between adjacent cells and allow maximum transmission of contractile force. Filaments in smooth muscle cells overlap as in striated muscle types, and this overlap increases during contraction. In the case of vascular smooth muscle, smooth muscle cells are positioned around the lumen of the vessel and the cells contract longitudinally so as to cause vasoconstriction. Visceral smooth muscle cells of organs such as the urinary bladder contract in a uniform manner to reduce organ volume.

1.1.3 Mechanism of contraction

The mechanism of actual contraction is also very similar between muscle types, with only slight differences as required by function. When the muscle is at rest, there is only a slight overlap between the filaments and no cross-bridges are formed. When the cell is activated by an increase in intracellular Ca^{2+} levels ($[\text{Ca}^{2+}]_i$), this is sensed within the cell and cross-bridges between actin and myosin filaments are allowed to form. As the myosin head attaches to actin of the thin filaments, it rotates. This movement is known as the “power stroke” and it generates enough force to slide the thin filament along the thick filament, leading to a shortening of the sarcomere. Adenosine triphosphate (ATP) then binds to the head of myosin and this breaks the strong bond of the cross-bridge. The ATP molecule is then hydrolysed, allowing the myosin head to return to its original position, and the contractile machinery is then ready for the cycle to repeat (figure 1.2).

In all muscle types, it is an increase in $[\text{Ca}^{2+}]_i$ sensed by the cell that leads to the activation of muscle contraction. The mechanism by which Ca^{2+} activates the contractile machinery, however, differs between striated muscles and smooth muscle.

In cardiac and skeletal muscle cells it is the thin filaments that ultimately sense changes in $[\text{Ca}^{2+}]_i$. These filaments contain regulatory proteins known as troponin and tropomyosin that play an important role in the initiation of contraction by Ca^{2+} . When the muscle is at rest, adenosine diphosphate (ADP) and an inorganic phosphate molecule (P_i) are bound to the heads of the myosin filaments which protrude out towards the actin of thin filaments. At this time, tropomyosin covers the myosin binding sites of actin, preventing cross-bridge formation between thick and thin filaments. As $[\text{Ca}^{2+}]_i$ increases within the cell it binds to troponin. This leads to the

movement of the tropomyosin molecules, uncovering the myosin binding sites, and so making it possible for cross-bridge formation to occur.

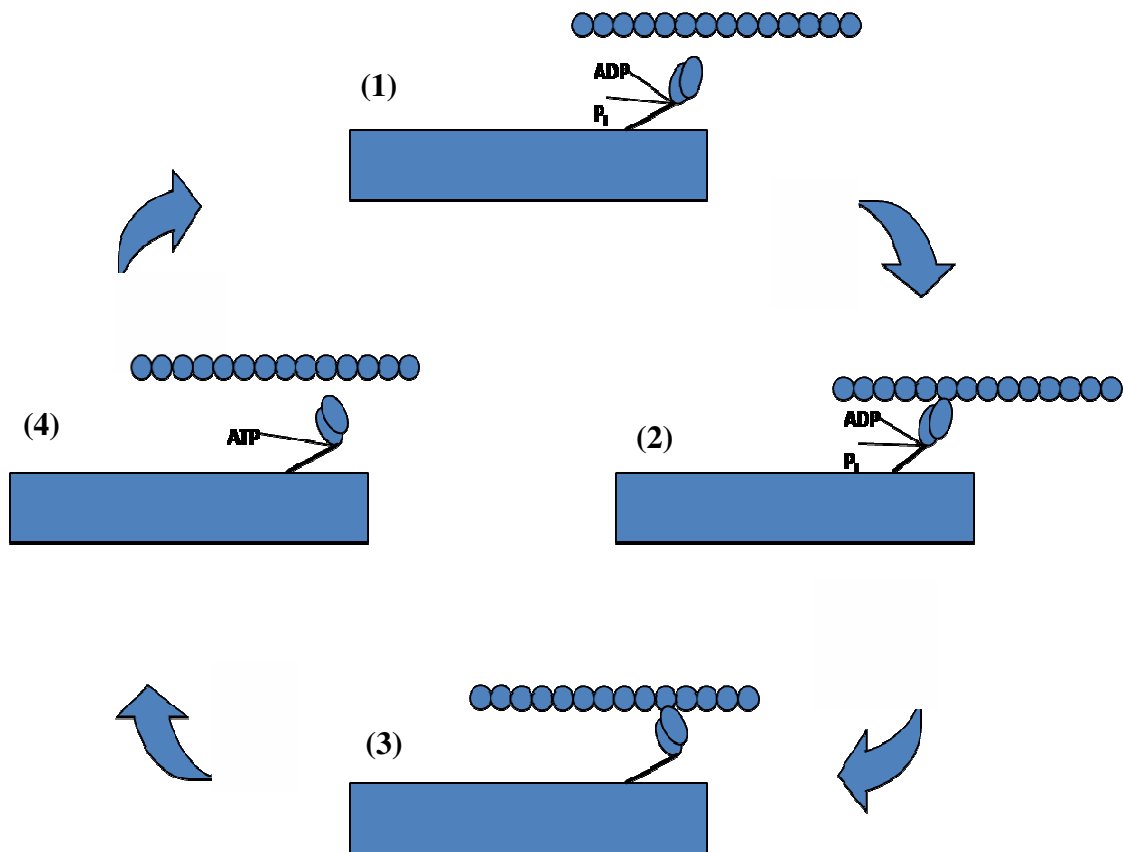


Figure 1.2 *The cross-bridge mechanism of muscle contraction. (1) The cross-bridge in relaxed muscle. The myosin heads are not bound to actin. (2) Myosin and actin bind as a result of increased $[Ca^{2+}]_i$. (3) The head rotates as ADP and P_i are released. This movement causes the thin filament to slide. (4) ATP binds and the cross-bridge detaches. Hydrolysis of ATP then occurs and the myosin head returns to the resting position (1).*

Smooth muscle does not contain troponin and so increases in $[Ca^{2+}]_i$ must be sensed by a different mechanism in order for contraction to occur. Smooth muscle cells utilise the cross-bridge mechanism of contraction as described above (figure 1.2) but, without the presence of troponin or tropomyosin in the thin filaments, an increase in $[Ca^{2+}]_i$ is instead sensed by a calcium-modulating protein, known as calmodulin, which binds to calcium and modulates many different cellular functions. Up to 4 Ca^{2+} ions can bind to a single molecule of calmodulin to form a calcium-calmodulin complex (reviewed by Walsh, 1994). This calcium-calmodulin complex binds to and activates myosin light chain kinase (MLCK), a serine/threonine protein kinase that then catalyses the phosphorylation of the myosin regulatory light chain, causing a conformational change in the myosin (reviewed by Walsh, 1994). This allows the myosin head to bind to actin and cross-bridge formation continues as described above.

Cross-bridge cycling continues until myosin light chain phosphatase (MLCP) dephosphorylates the myosin regulatory light chains. This dephosphorylation is able to occur whether or not the cross-bridges are still attached, but the state of the cross-bridge at the time of phosphorylation is thought to have an important role in the maintenance of contraction of smooth muscle. One of the important functions of many types of smooth muscle is that they must perform a constant level of contraction, known as basal tone, in order to maintain a constant organ volume. If the cross-bridges are still attached when this dephosphorylation occurs, then their detachment proceeds at a slower rate than usual, and it is possibly this that regulates basal tone. This slow mechanism of cross-bridge recycling often causes the cross-bridge to remain on a “latch” which provides a very efficient mechanism of contraction as it uses less energy for contraction and allows the organ to avoid muscle fatigue (reviewed by Murphy & Rembold, 2005). Elevated Ca^{2+} levels are thought to be required to maintain this basal

tone as if $[Ca^{2+}]_i$ declines back below the threshold required to activate contraction, cross-bridges detach and no new cross-bridges are able to form.

1.1.4 Modulation of smooth muscle sensitivity to Ca^{2+}

A variety of substances have the ability to modulate the calcium sensitivity of smooth muscle, including cyclic adenosine monophosphate (cAMP), cyclic guanosine monophosphate (cGMP), and RhoA and Rho kinase. This means that the contractile force initiated by any given $[Ca^{2+}]_i$ can be increased or decreased depending on the particular molecule. For example, nitric oxide-induced vasorelaxation of resistance arteries has been seen to occur without any effect on $[Ca^{2+}]_i$ (Bolz *et al*, 1999). This effect was found to be reliant upon MLCP and cGMP, and antagonized by pathways involving RhoA and Rho kinase (Bolz *et al*, 2003).

1.2 Vascular smooth muscle

The role of vascular smooth muscle is to control the diameter of the blood vessel through the contraction or relaxation of the individual smooth muscle cells. Each of the cells acts independently of one another but more or less cells may become activated depending on how the conditions change. In this way smooth muscle cells act together to regulate blood vessel size. For example, contraction of the smooth muscle decreases the diameter of the internal lumen of the vessel increasing the resistance against blood flow. This regulates the flow of blood through the vessels and so increases blood pressure. Conversely, relaxation of the smooth muscle increases internal lumen diameter, allowing blood to flow through more easily and decreasing blood pressure.

Most arterial blood vessels are composed of 3 layers or “tunics”. The tunica intima is composed of endothelial cells; the tunica media contains smooth muscle and connective tissue; and the tunica adventitia contains connective tissue. Small arterioles however, such as third and fourth order mesenteric arteries, are made up of only smooth muscle and endothelium. The main function of vessels of this size is to control the flow of blood to specific tissues. Large arteries are the most elastic blood vessels in the body. This is in order to allow them to absorb a large amount of pressure from the heartbeat. However, these vessels do not play a major role in the short term adjustment of blood pressure. Smaller arteries are more muscular in structure and their role is to carry blood to the specific organs of the body. It is these blood vessels that play a major role in blood pressure regulation through constriction or dilation. It is possible to direct blood flow to specific areas of the body by selectively dilating or constricting smaller blood vessels within the body. Blood flow is equal to the change in pressure divided by the resistance. Therefore as blood pressure increase, blood flow is decreased.

1.2.1 Regulation of vascular smooth muscle tone

Vascular smooth muscle is different to visceral smooth muscle such as the bladder, as changes in membrane potential are gradual (termed “tonic”) rather than the quicker “phasic” change caused by the action potentials of visceral smooth muscle. This gradual change allows the muscle to maintain its state of contraction (as mentioned briefly earlier, some smooth muscle types are always found in a state of partial contraction known as basal tone) rather than the pulsing contractions of other smooth muscles. Basal tone ensures that the pressure within the blood vessels is enough to ensure that organs receive an adequate supply of blood. This level of contraction can then be increased or decreased as necessary according to the needs of the body. Total peripheral resistance plays an important role in the regulation of systemic arterial blood pressure. The regulation of this will be discussed in further detail in the following section.

$$\text{Total peripheral resistance} = \frac{(\text{mean arterial pressure} - \text{mean venous pressure})}{\text{cardiac output}}$$

where mean arterial pressure is the average of diastolic and systolic pressures and mean venous pressure is as measured at the right atrium.

1.2.1.1 Regulation by autonomic innervation

A variety of stimuli may act on the vessel in order to regulate blood pressure through alteration of the total peripheral resistance. Extensive innervation of vascular smooth muscle by neurons of the autonomic nervous system (ANS) allows blood vessels to react to the needs of the animal. For example, activation of sympathetic neurons of the ANS gives rise to the body’s “fight or flight” response. Vessels feeding the skin and

gastro-intestinal (GI) tract vasoconstrict to divert blood flow away from these organs, while blood vessels serving the heart, lungs and skeletal muscle vasodilate to promote blood flow in that direction. Autonomic neurons contain many sites of transmitter release, called varicosities, along their axons, and synaptic vesicles gather in these areas until stimulation of the neuron leads to their contents being released. Neuronal varicosities and smooth muscle receptors are found in very close proximity to each other, approximately 20-150 nM apart depending on the tissue (reviewed by Bennett, 1996). When the synaptic vesicles fuse with the membrane at the neuron bouton, the neurotransmitter is released and is able to have an effect on the appropriate receptor.

1.2.1.2 Regulation by vasoactive substances

The autonomic nervous system may also stimulate the release of vasoactive substances, such as circulating peptides, that can also modulate vascular smooth muscle tone. These substances can have either vasoconstrictory or vasodilatory effects by binding to their specific receptors on the plasma membrane of the cell to alter ion conductance through a variety of intracellular signalling pathways. Endothelin-1 (ET-1) and Angiotensin II (Ang II) are both examples of endogenous vasoconstrictors. ET-1 is a peptide produced in the endothelium from its precursor, big endothelin, and secreted by endothelial cells into the vasculature. This release may be stimulated by the autonomic nervous system or by substances such as Ang II, anti-diuretic hormone (ADH), and cytokines. Release of ET-1 can lead to vasoconstriction of arterial blood vessels by either acting on its receptors on vascular smooth muscle cells, or through the release of aldosterone and a reduction in renal blood flow. Aldosterone release causes Na⁺ and water to be retained. Ang II is produced from the inactive angiotensinogen in 2 steps. The first is the conversion of angiotensinogen to angiotensin-I by renin, and the second

is the conversion of this newly produced substance to angiotensin-II by angiotensin converting enzyme (ACE). Angiotensinogen is produced and released by the liver whilst renin is released by the kidneys upon autonomic nervous system stimulation. Ang II is primarily produced in the lungs but has also been found to be released from endothelial cells. It can cause the release of ET-1 as well as the activation of the renin-angiotensin system, the main effects of which are to cause vasoconstriction through an increase in Na^+ reabsorption and the release of aldosterone and ADH. ET-1, for example, acts upon its specific G-protein coupled receptor leading to the activation of intracellular signalling pathways. ET_A , thought to be the predominant ET-1 receptor in vascular smooth muscle, is coupled to the $\text{G}\alpha_{q/11}$ G-protein. This initiates a signalling pathway involving activation of an isoform of phospholipase C (PLC), known as $\text{PLC}\beta$, and leads to the production of inositol-1, 4, 5-trisphosphate (IP_3) and diacylglycerol (DAG). Phosphatidylinositol-4, 5-bisphosphate (PIP_2), found in the plasma membrane of the cell, is broken down to produce these two substances. IP_3 then migrates to the sarcoplasmic reticulum (SR) of the cell to stimulate Ca^{2+} -release from this intracellular store through the activation of IP_3 -sensitive Ca^{2+} channels, whilst DAG activates protein kinase C (PKC). Ang II is thought to have the dual effect of activating PKC and inhibiting protein kinase A (PKA) (Hayabuchi *et al*, 2001a; Hayabuchi *et al*, 2001b).

Many vasodilators have their effect through the activation of $\text{GTP}\alpha_s$. This stimulates adenylate cyclase, found in the plasma membrane of the cell, which in turn leads to an increase in cAMP and activation of PKA. Nitric oxide is a vasodilator produced by the endothelium of blood vessels and activates guanylate cyclase. This leads to an increase in cGMP and activation of protein kinase G (PKG).

1.2.1.3 Myogenic response

Vascular smooth muscle may also be regulated by a “myogenic response”, first described by Bayliss (Bayliss, 1902). Increased pressure within the vessel leads to depolarisation of the smooth muscle, Ca^{2+} entry and vasoconstriction. Conversely, a reduction in pressure leads to hyperpolarisation of the cell membrane, reduced Ca^{2+} entry, and vasodilation. This mechanism therefore enables the blood vessel to keep blood flow relatively constant even though blood pressure may vary, and it is likely to play an important role in regulating blood flow to tissue through small resistance arteries such as the cerebral arteries of the brain. In fact, a myogenic response has been observed in a wide range of blood vessels, in small veins as well as arteries (even though myogenic response in veins is rather weak), although the strength of the response has been seen to vary between different kinds of vascular beds. The size of the vessel is thought to be a deciding factor in determining the strength of myogenic response, as vessels at extreme ends of the size scale display quite a weak vascular response, whilst the stronger myogenic responses are seen in vessels that are intermediate in size. However, size cannot be the only determining factor, as arteries of a similar size may also exhibit varying responses. For example, cerebral arteries and mesenteric arteries are both small vessel types, but a much stronger myogenic response is seen in the cerebral artery. It is thought that a change in the tension of the arterial wall induced by pressure provides the stimulus for myogenic response rather than the change in pressure itself (reviewed by Davis & Hill, 1999).

1.2.2 The role of protein kinases

As mentioned, a variety of protein kinases play a role in vasoregulation. PKA, PKC and PKG are all present in vascular smooth muscle and their activation may govern a variety of responses within the cell. In general, activation of PKC tends to lead to vasoconstriction whereas activation of either PKA or PKG will lead to vasodilation. This can be complicated further by apparent cross-activation between pathways involving cAMP and cGMP, as the adenylate cyclase activator, forskolin, has been seen to stimulate PKG activity in coronary arteries without elevating cGMP levels (White *et al*, 2000).

Protein kinases phosphorylate intracellular proteins to have a wide range of effects, including regulation of gene expression, cell differentiation and apoptosis. They may also phosphorylate ion channels to modulate their function. PKC and PKA for example, are both thought to be able to phosphorylate ryanodine receptors (RyRs) of the SR to either decrease or increase the release of Ca²⁺ from intracellular stores, respectively (Bonev *et al*, 1997; Marx *et al*, 2000), and they may also modulate the activity of plasma membrane ion channels.

1.3 The role of Ca^{2+} and its mobilization in vascular smooth muscle

In a resting vascular smooth muscle cell, the free $[\text{Ca}^{2+}]_i$ is approximately 100 nM, but the total $[\text{Ca}^{2+}]_i$ is closer to 1 mM as a large amount of Ca^{2+} is stored in intracellular stores such as the sarcoplasmic reticulum (SR) and mitochondria. This low free $[\text{Ca}^{2+}]_i$ within the cell means that Ca^{2+} will readily move down its concentration gradient into the cytoplasm when the cell is activated by membrane depolarization, leading to a rise in the $[\text{Ca}^{2+}]_i$. It is this rise in $[\text{Ca}^{2+}]_i$ that is often the common factor linking the main mechanisms leading to vasoconstriction of vascular smooth muscle, as this initial step is required in order to bind to calmodulin and initiate the complex signalling pathway described previously.

1.3.1 Ca^{2+} influx through ion channels

The main mechanism of increasing $[\text{Ca}^{2+}]_i$ in vascular smooth muscle is through the activation of L-type voltage-dependent Ca^{2+} channels (VDCCs) by membrane depolarisation. These channels are found on the plasma membrane of the cell and allow extracellular Ca^{2+} to enter the cell. The relationship between membrane depolarisation and these ion channels is thought to be so strong that depolarization by as little as 3 mV can as much as double Ca^{2+} entry into the cell through this mechanism alone (Nelson *et al*, 1990; Nelson *et al*, 1988).

Calcium may also enter the cell through store-operated channels (SOCs). These non-selective cation channels are also found on the plasma membrane and are often activated by the depletion of intracellular Ca^{2+} stores, allowing Ca^{2+} to enter the cell.

Very little is known about these channels and their mechanism of activation, but they will be discussed in a little more detail in section 1.4.1.

1.3.2 Release of Ca^{2+} from intracellular stores

Ca^{2+} can also be released from intracellular stores. Stimulation of the cell leads to the release of this Ca^{2+} and contraction of the cell may occur. Two different types of Ca^{2+} -release channel are also present on the membrane of the SR, allowing the release of Ca^{2+} from intracellular stores to raise free $[\text{Ca}^{2+}]_i$. The first of these channels, the IP_3 -sensitive channel (IP_3R), is opened by the PIP_2 hydrolysis product, IP_3 , acting upon its receptor on the SR. However channel activation is not thought to be able to occur in the presence of IP_3 alone, the binding of Ca^{2+} is also thought to be required for channel activation (Suematsub *et al*, 1984; Iino, 1990a; Finch *et al*, 1991; Bezprozvanny *et al*, 1991). The second type of channel is the ryanodine-sensitive Ca^{2+} -release channel (RyR), a channel that is modulated by Ca^{2+} alone, without any need for the binding of an additional agonist as in the case of IP_3Rs .

The IP_3R channel consists of 4 subunits, each containing 6 transmembrane domains. The N-termini is large and found in the cytoplasm but the C-termini domains are smaller (Ross *et al*, 1992; Michikawa *et al*, 1994). Three mammalian IP_3R isoforms have so far been discovered ($\text{IP}_3\text{R1}$, $\text{IP}_3\text{R2}$ and $\text{IP}_3\text{R3}$). These channels appear to be found in clusters, with approximately 25-35 receptors grouping together (Shuai *et al*, 2006). The RyR Ca^{2+} release channel also has a tetrameric structure, but is larger in size than the IP_3R , with each subunit consisting of 10 transmembrane domains. It also has a large cytoplasmic N-terminal and smaller C-terminal. Three isoforms of RyR are known to exist (RyR1 , RyR2 and RyR3) with all three having been found in smooth

muscle (Neylon *et al*, 1995). RyRs may also be found in clusters on the SR. While IP₃Rs require the presence of IP as a ligand in order to activate, RyRs do not. However, it is possible to pharmacologically manipulate the activity of RyRs using compounds such as ryanodine or caffeine. Ryanodine is a plant alkaloid that was originally used to identify the RyR. When applied at low micromolar concentrations, ryanodine stimulates the release of Ca²⁺ stores from the SR. At concentrations of approximately 50 μM, however, ryanodine blocks the RyR so that no Ca²⁺ can be released from these channels (Iino, 1990b; Nelson *et al*, 1995; White & McGeown, 2000). Caffeine is a compound that is thought to increase the Ca²⁺ sensitivity of the RyR, stimulating the release of Ca²⁺.

The simultaneous activation of a group of ryanodine channels is thought to be responsible for the transient release of packets of Ca²⁺ from the sarcoplasmic reticulum, termed Ca²⁺ “sparks”, whilst the releases of Ca²⁺ from a cluster of the IP₃ channels were given the name of Ca²⁺ “puffs” (Parker & Yao, 1991). Ca²⁺ puffs are thought to be smaller in amplitude than Ca²⁺ sparks, and this may be the reason why they are rarely detected unless the smooth muscle has been stimulated. When several different clusters of IP₃ receptors are activated to release Ca²⁺ from the SR, a Ca²⁺ “wave” passes through the cell to cause a detectable rise in global Ca²⁺ concentration (Parker & Yao, 1991).

Both IP₃Rs and ryanodine receptors (RyRs) are thought to be sensitive to [Ca²⁺], both in the cytosol and in the SR, and this gives rise to the theory that IP₃Rs and RyRs may actually be able to regulate each other’s activity, as well as the activity of neighbouring receptors of the same type. Activation in this manner would mean that Ca²⁺ waves within the cell would be able to propagate and the Ca²⁺ signal could be amplified. However, investigations into the effect of [Ca²⁺] on the open probabilities (P_{open}) of IP₃ and ryanodine channels have shown that the Ca²⁺ dependence of both receptor types is

bell-shaped, meaning that at both low and high levels of $[Ca^{2+}]_i$ the channel may be inhibited. In general, RyRs are activated by free $[Ca^{2+}]_i$ that are in the micromolar range or above (Fill & Copello, 2002), while IP₃R_s are activated by $[Ca^{2+}]_i$ below 1 μ M (Iino, 1990a; Fill & Copello, 2002). However, the concentration at which maximal channel activation occurs differs, not only between the two different types of receptor, but also between various receptor isoforms. Other factors affecting channel activation may be the amount of Ca^{2+} within the SR (SR load), intracellular ATP and/or Mg^{2+} levels, or local IP₃ concentration (Iino & Endo, 1992). The idea that SR load can affect Ca^{2+} release is an interesting one as it is much more complicated than one might expect. It might be easily presumed that Ca^{2+} release is proportional to SR load, with the release of Ca^{2+} slowly decreasing in line with $[Ca^{2+}]_i$ in the store. In reality, Ca^{2+} release may be inhibited even when there is still a large amount of Ca^{2+} stored within the SR. For example, in the case of uterine smooth muscle, the release threshold for IP₃ channels is 80% of the usual storage level. Once the $[Ca^{2+}]_i$ stored within the SR drops below this threshold, Ca^{2+} release through IP₃ channels is inhibited (Shmygol & Wray, 2005). This suggests that there are other factors alongside SR load that determine Ca^{2+} release through these channels.

It is thought that Ca^{2+} sparks released by ryanodine channels could activate other RyRs nearby to cause an increase in $[Ca^{2+}]_i$ by a process known as calcium-induced calcium release (CICR). This phenomenon has been seen in a variety of muscle types but is still a controversial subject in smooth muscle research, as the influx of Ca^{2+} observed during depolarisation of the cell membrane is thought to be enough to account for the increases in $[Ca^{2+}]_i$ in colonic and portal vein myocytes (Kamishima & McCarron, 1996; Bradley *et al*, 2002; McCarron *et al*, 2004). CICR has been reported in some smooth muscles such as cerebral artery myocytes and the smooth muscle cells from the urinary bladder

(Kamishima & McCarron, 1997; Burdyga *et al*, 1995), but not in others (Guerrero *et al*, 1994; Kohda *et al*, 1997). It is thought that the coupling between VDCCs and RyRs in some types of smooth muscle could be quite loose, and so CICR may not always occur. Ji (Ji *et al*, 2006) observed that the local photorelease of Ca^{2+} led not only to Ca^{2+} release as Ca^{2+} sparks, but also as Ca^{2+} waves that spread throughout the cell. They therefore hypothesized that RyRs are found throughout the cell where they aid in the propagation of Ca^{2+} release. This is as opposed to the theory that RyRs are only found in certain local areas where Ca^{2+} sparks can activate calcium-activated channels such as large-conductance Ca^{2+} -activated K^+ channels (BK_{Ca}) and Ca^{2+} -activated Cl^- channels (Cl_{Ca}), where it can have an indirect effect on membrane depolarization and Ca^{2+} entry through VDCCs. The role of Ca^{2+} sparks in the activation of BK_{Ca} channels will be explained in more detail later (section 1.6.2.1). As mentioned briefly, it is thought that cross-talk between RyRs and IP_3Rs could lead to them modulating each other's activity. There is evidence that release of Ca^{2+} through ryanodine channels by a mechanism such as CICR has a positive effect on Ca^{2+} release through IP_3Rs but that Ca^{2+} release through ryanodine channels is unlikely to be affected by IP_3Rs (MacMillan *et al*, 2005; Ji *et al*, 2006).

Ca^{2+} sparks provide evidence both for and against a positive-feedback mechanism for Ca^{2+} release. When SR load is above the threshold of 80% total capacity, there is a strong relationship between $[\text{Ca}^{2+}]$ of the SR and the release of Ca^{2+} (Zhuge *et al*, 1999). An increase in spark frequency is proof of this. This suggests that an increase in Ca^{2+} within the SR has a positive effect on Ca^{2+} release. However, Ca^{2+} sparks themselves are contradictory of Ca^{2+} release because a Ca^{2+} spark involves the activation and fast deactivation of RyRs, therefore limiting their own activity. The mechanism for this inactivation is unclear, but it has been suggested that high Ca^{2+} flux through the RyR

may have an inhibitory effect on the cytoplasmic side of the receptor, as has been seen in skeletal muscle (Tripathy & Meissner, 1996). The Ca^{2+} chelator BAPTA may prevent this high flux being sensed by the channel as RyR activity is not inhibited when BAPTA is present (Xu & Meissner, 1998).

There is much debate as to whether these 2 types of receptor share a common Ca^{2+} pool within the sarcoplasmic reticulum, or whether the stores are independent of one another. Reports suggesting that the release of Ca^{2+} induced by one receptor may be modulated by the other support the idea that Ca^{2+} pools are shared. Boittin (Boittin *et al*, 1998) and Bayguinov (Bayguinov *et al*, 2000) both reported that the release of Ca^{2+} from ryanodine receptors can enhance the release of Ca^{2+} by IP_3 , in vascular myocytes and colonic myocytes respectively. Other work carried out by a number of different groups has also shown that it is possible for this to occur vice versa, with IP_3 Rs modulating Ca^{2+} sparks in a variety of smooth muscle types that includes portal vein (Gordienko & Bolton, 2002), the pulmonary blood vessels (Zhang *et al*, 2003), and the vas deferens (White & McGeown, 2003). This could prove to be very important as vasoconstrictors such as ET-1 and Ang II cause the release of Ca^{2+} through IP_3 Rs through PLC-dependent pathways.

1.4 Membrane proteins involved in ion transport

The role of SR Ca^{2+} channels in Ca^{2+} mobilization was discussed in the previous section, along with a brief mention of plasma membrane channels that can lead to an increase in Ca^{2+} when activated. In this section, the plasma membrane channels will be discussed in more detail, and other membrane proteins involved in regulating intracellular concentrations of Ca^{2+} and other ions will also be considered.

1.4.1 Regulation of Ca^{2+}

There are only two types of VDCCs present in vascular smooth muscle (reviewed by Horowitz *et al*, 1996). L-type VDCCs are activated at high membrane potentials, whereas T-type VDCCs are activated at lower membrane potentials and inactivate at higher potentials. Only L-type VDCCs are thought to play a role in the vasoconstriction of vascular smooth muscle cells; the role of T-type VDCCs is unclear and will not be considered further. Activation of L-type VDCCs leads to Ca^{2+} influx and muscle contraction as described earlier (section 1.1.3). It is also believed that these VDCCs are involved in CICR in the smooth muscle types that display this form of Ca^{2+} release, and are distributed throughout the cell in a similar pattern to RyRs (Carrington *et al*, 1995). Their activation may also be indirectly regulated by vasoconstrictors as these substances often lead to membrane depolarization and so Ca^{2+} entry.

Another type of channel, the vanilloid transient receptor potential channel, TRPV4, is also thought to form a signalling complex with RyRs and BK_{Ca} channels (Earley *et al*, 2005). Ca^{2+} entry through TRPV4 is believed to activate RyR to increase Ca^{2+} release as sparks, and this can then activate BK channels to cause hyperpolarisation of the cell membrane through an increase in STOC activity.

A group of channels known as store-operated channels (SOCs) are also likely to be present in vascular smooth muscle. These channels are activated by a reduction in intracellular Ca^{2+} stores and so Ca^{2+} enters the cell and is able to replenish the stores. Casteels and Droogmans were the first to observe the entry of Ca^{2+} in this manner, as they found that traditional calcium antagonists had no effect on this type of Ca^{2+} influx (Casteels & Droogmans, 1981). They also observed that this Ca^{2+} did not lead to cell contraction, indicating that SOCs and Ca^{2+} stores are tightly coupled. The actual channels involved in store-mediated entry are not known, although various channels have been put forward as possible candidates. The Ca^{2+} release activated Ca^{2+} entry (CRAC) channels are one possibility, as are members of the canonical transient receptor potential (TRPC) family at least one of which, TRPC6, is thought to be present in rat mesenteric artery smooth muscle (Hill et al, 2006). Both of these types of channels have been seen to play a role in other cells but it is not clear which of these are present and may play a role in vascular smooth muscle.

So far the discussion has been largely orientated towards proteins involved in Ca^{2+} entry into cells however there must also be mechanisms that transport Ca^{2+} back out of the cytoplasm, either into stores or the extracellular fluid, in order to regulate $[\text{Ca}^{2+}]_i$ and so limit the contraction of the cell. Regulation of free $[\text{Ca}^{2+}]_i$ is performed by a variety of Ca^{2+} pumps present in the plasma membrane and the membrane of the SR and each of these will be discussed in turn.

The $\text{Na}^+/\text{Ca}^{2+}$ exchanger (NCX) is found in the plasma membrane of the cell. This protein uses the transport of Na^+ from the extracellular side down its ionic gradient into the cell to provide the energy required to move Ca^{2+} against its gradient back out of the cell. The stoichiometry of this protein is 3 Na^+ :1 Ca^{2+} , meaning that the movement of three Na^+ into the cell are required to move one Ca^{2+} out. The NCX has been seen to be

reversible; it can move Na^+ out of the cell and Ca^{2+} into the cell, conditions permitting. The direction in which ions move through this exchanger is therefore dependent upon their concentration gradients. Membrane potential appears to be the main influencing factor, as Ca^{2+} may be forced into the cell when the membrane is depolarized but removes excess Ca^{2+} to the extracellular solution when the cell is hyperpolarized. Extracellular Na^+ may also play a role in the function of the exchanger as removal of Na^+ from the extracellular medium leads to an increase in Ca^{2+} entry and a decrease in its exit.

The plasma membrane Ca^{2+} pump (PMCA) is also involved in the removal of Ca^{2+} from the cytoplasm. PMCA is an ATPase and so requires the breakdown of ATP in order to provide the energy to remove Ca^{2+} from the cell. It is found in an inactive state, due to an autoinhibitory process, until Ca^{2+} -calmodulin levels within the cell increase and bind with the autoinhibitory domain, relieving the inhibition. The NCX and PMCA are believed to work in parallel and complement each other in the regulation of $[\text{Ca}^{2+}]_i$. The NCX has low affinity for Ca^{2+} but a very high rate of transport (10-fold higher than that of the PMCA) and so plays the dominant role when $[\text{Ca}^{2+}]_i$ is raised. PMCA has a higher affinity for intracellular Ca^{2+} and so its role may be to regulate smaller increases in $[\text{Ca}^{2+}]_i$ when Ca^{2+} levels are at a basal level (around 100 nM).

A second Ca^{2+} -ATPase found in the cell is the sarcoplasmic or endoplasmic reticulum Ca^{2+} -ATPase (SERCA) situated in the membrane of the SR. SERCA belongs to the same family of ATPases as the PMCA but there is very little sequence homology between the two. SERCA appears to be more efficient at removing Ca^{2+} than PMCA, requiring the breakdown of only one ATP molecule to provide the energy to transport two Ca^{2+} into the SR, as opposed to the hydrolysis of one or two ATP molecules required by the PMCA to transport Ca^{2+} out of the cell. An increase in cytoplasmic

Ca^{2+} is likely to lead to an increase in the activity of the SERCA pump, whereas an increase in the $[\text{Ca}^{2+}]$ of the SR is expected to cause a reduction in SERCA activity (Wu et al., 2001).

These three transport mechanisms work together to ensure that free $[\text{Ca}^{2+}]_i$ is tightly regulated. However, there is also a wide range of other membrane proteins present in both the plasma membrane and the SR of the vascular smooth muscle cell. Many of these proteins are known to play a vital role in maintaining homeostasis in the cells, whilst the presence of others is still controversial and their role is unclear.

1.4.2 Regulation of Na^+

The Na^+/K^+ -ATPase present in the plasma membrane is important for regulating Na^+ and K^+ levels. It transports these two ions against their concentration gradients, with a stoichiometry of 3 Na^+ :2 K^+ to keep the $[\text{Na}^+]_i$ of the cell low and the $[\text{K}^+]_i$ high. Activity of the Na^+/K^+ -ATPase may be regulated by elevated extracellular K^+ levels as well as metabolic products of arachidonic acid.

The Na^+/H^+ exchanger is another membrane protein. Its role is to regulate intracellular pH as changes are thought to have an effect on a variety of cellular mechanisms including ion channel function.

There is also a variety of ion channels present in the plasma membrane. Voltage-gated Na^+ channels are found in abundance in the membrane of neurons, where their major role is to facilitate the upstroke of the action potential. Vascular smooth muscle cells, however, are not activated by action potentials as it is the entry of Ca^{2+} into these cells, rather than Na^+ , that largely serves to depolarise the membrane. The presence of

voltage-gated Na⁺ channels and their role in smooth muscle cells such as these is therefore a somewhat controversial subject.

Voltage-gated Na⁺ channels have reportedly been recorded in a variety of smooth muscle types, including guinea pig ureter (Muraki *et al*, 1991), rat myometrium (Amedee *et al*, 1986), and rat portal vein (Mironneau *et al*, 1990), although these earlier works suggested that they were unlikely to play a significant role in depolarisation and contractility. When currents have been found, this has largely been in cultured smooth muscle cells which may have different properties to freshly isolated myocytes. There has also been disagreement over whether these currents have been recorded in particular cell types such as those isolated from rat mesenteric artery (Ohya *et al*, 1997; Berra-Romani *et al*, 2005). It has been suggested that this contradiction may be down to differing conditions in the enzymatic isolation of the single smooth muscle cells (Berra-Romani *et al*, 2005).

One investigation that did suggest that Na⁺ channels had an effect on membrane depolarization was a study looking into the effects of activators of these channels, such as Veratridine and Batrachotoxin (BTX). The results showed that activation of the Na⁺ channel led to a gradual increase in the contraction of rat aortic rings (Shinjoh *et al*, 1991), suggesting that Na⁺ entry may depolarize the membrane and cause vasoconstriction through the entry of Ca²⁺ through VDCCs. Saleh (Saleh *et al*, 2005) also reported that activation of Na⁺ channels lead to the contraction of portal vein myocytes.

1.4.3 Ca^{2+} -activated Cl^- channels

Ca^{2+} -activated Cl^- (Cl_{Ca}) channels have been observed in a wide of variety vascular smooth muscle cells, including mesenteric artery (Peng *et al*, 2001), cerebral artery (Large & Wang, 1996), and portal vein (Saleh & Greenwood, 2005), and their activation is likely to play a role in membrane depolarisation and increased cell excitability. These cells may be activated by Ca^{2+} release from stores in the SR, causing Cl^- to leave the cell, and so leading to membrane depolarisation. Cl_{Ca} channels are active when the cell is at rest and so are likely to play a role in setting the resting membrane potential of these cells.

The ion channels discussed so far all lead to membrane depolarization upon their activation. The activation of K^+ channels in vascular smooth muscle cells lead to membrane hyperpolarization and so are believed to play an important role in the dampening of cell excitability. This role will be explained in more detail in the following section.

1.5 K⁺ channels

K⁺ channels are the most diverse group of ion channels known and make up their own “superfamily” of ion channels. They are broadly classified according to the structure of the pore-forming subunit, separating the channels into groups that generally contain two, four or six transmembrane domains. The selectivity filter of the pore ensures that they are highly selective for K⁺, which moves down its concentration gradient upon activation to exit the cell.

1.5.1 The role of K⁺ channels in vascular smooth muscle

K⁺ channels play a role in the functioning of many types of both excitable and non-excitable cells where they regulate a variety of cell signalling processes, including neuronal excitability and insulin secretion, as well as smooth muscle contraction. In the case of vascular smooth muscle contraction, activation of K⁺ channels leads to hyperpolarization of the cell membrane, which in turn leads to the closing of VDCCs, decreasing Ca²⁺ entry into the cell, and so limiting cell contraction. Activation of K⁺ channels therefore leads to vasodilation of vascular smooth muscle. Conversely, the inhibition of K⁺ channels tends to lead to a depolarization of the cell membrane, Ca²⁺ influx and vasoconstriction. As mentioned earlier, small changes in membrane potential can have a large effect on Ca²⁺ entry. Regulation of membrane potential by K⁺ channels can therefore have a major effect on blood vessels, providing an important mechanism to regulate arterial diameter and blood flow. Many K⁺ channels are therefore targets of vasoregulatory substances that act to regulate membrane potential. The functioning of K⁺ channels has been found to be altered in a variety of pathological conditions including hypertension and ischaemia.

1.5.2 Types of K⁺ channel found in vascular smooth muscle

Four different types of K⁺ channels have been identified in vascular smooth muscle cells, each playing their own important role in the regulation of vasoconstriction by responding to its specific stimuli (reviewed by Standen & Quayle, 1998; figure 1.3). The proportion of each channel present depends on the vascular bed, and may also differ between larger arteries and smaller resistance arteries.

1.5.2.1 Kv channels

Voltage-activated K⁺ (Kv) channels react to depolarisation of the cell membrane. Their activation therefore plays an important role in responding to the stimuli that can cause this depolarisation in order to limit it. They may also play an important role in regulating myogenic tone by responding to the depolarization induced by increases in the tension of the arterial wall. However, depolarization does not lead to the activation of K⁺ channels indefinitely, as sustained depolarization leads to inactivation of the Kv channel. Holding rat mesenteric artery smooth muscle cells at a membrane potential of -20 mV will inactivate over 80 % of Kv channels within a few seconds (Davies NW, oral communication). The pore-forming α -subunit of Kv consists of six transmembrane domains, and four of these subunits come together to form the channel pore. The S4 region of the α -subunit contains the voltage sensor that allows the channel to respond to changes in membrane potential, and the linker between S5 and S6 lines the selectivity filter of the pore. Regulatory β -subunits may interact with the α -subunits to modulate the activity of the channel.

1.5.2.2 K_{ATP} channels

The ATP-sensitive K⁺ channel (K_{ATP}) responds to changes in cell metabolism. The ratio of ATP to adenosine diphosphate (ADP) is important in the regulation of this channel, and so K_{ATP} provides a link between the metabolism and excitability of the cell. These channels are composed of four pore-forming α -subunits in association with four sulphonylurea subunits that regulate their function. They are inhibited by raised intracellular ATP levels.

1.5.2.3 Kir channels

Inward rectifier K⁺ (Kir) channels are found in great abundance in small resistance arteries. They are open at negative membrane potentials and have been shown to play a role in regulating the resting membrane potential of vascular smooth muscle by the specific inhibition of their activity using Ba²⁺, which led to vasoconstriction of the vessel (Park *et al*, 2007). As their name suggests, these channels are inwardly rectifying, meaning that their conductance is greater at membrane potentials negative to E_K where they permit the inward movement of K⁺, than it is membrane potentials positive to E_K where they pass only a small amount of outward current. The membrane potential of vascular smooth muscle is usually positive to E_K and so these channels permit the outward movement of K⁺. Kir channels are tetramers with each subunit consisting of only two transmembrane domains.

1.5.2.4 K_{Ca} channels

Ca²⁺-activated K⁺ (K_{Ca}) channels are also found in vascular smooth muscle cells. Three types of K_{Ca} channels have been discovered and they are classified according to their conductance. The small-conductance Ca²⁺-activated K⁺ channel (SK_{Ca}) has a conductance of 2-25 pS; the intermediate-conductance Ca²⁺-activated K⁺ channel (IK_{Ca}) has a conductance of 25-100 pS; and the large-conductance Ca²⁺-activated K⁺ channel (BK_{Ca}) has a conductance of 100-300 pS (reviewed by Ghatta *et al.*, 2006). Only SK_{Ca} and BK_{Ca} channels are thought to be present in vascular smooth muscle (Brayden, 1996). Both are activated by [Ca²⁺]_i as their names suggest, but the activity of BK_{Ca} channels is also strongly regulated by membrane potential whereas SK_{Ca} channels are not influenced by voltage. BK_{Ca} channels will be covered in more detail in the following section.

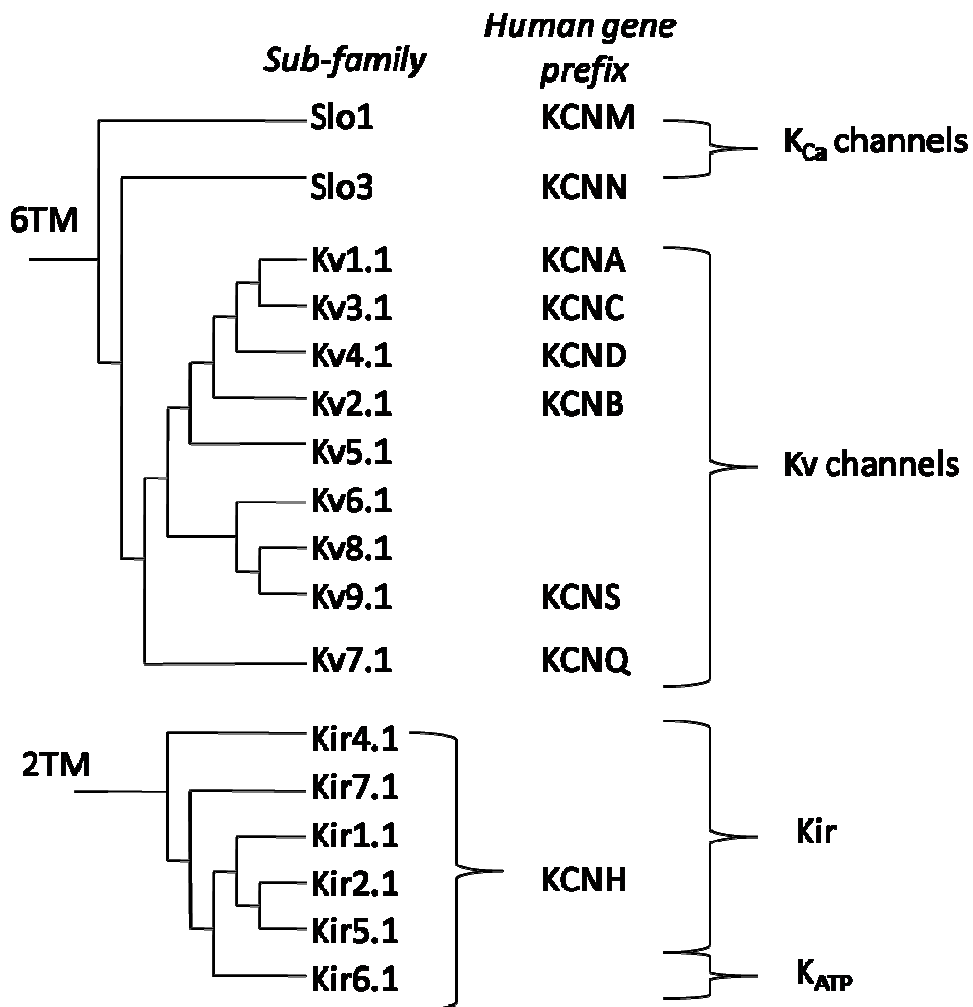


Figure 1.3 K^+ channel nomenclature tree displaying the K^+ channel gene families, many of which have been found to be expressed in smooth muscle. Adapted from Hille, 2001.

1.6 BK_{Ca} Channel Structure & Function

BK_{Ca} channels are the predominant K⁺ channel in most arteries (Nelson & Quayle, 1995). Their large-conductance means that the activation of only a handful of channels is able to have a significant effect on membrane potential.

1.6.1 BK_{Ca} channel structure

1.6.1.1 The α -subunit

The BK_{Ca} channel is formed by four α -subunits that come together to form the channel pore. Each of these subunits have six transmembrane domains that are similar in structure to the α -subunit of the Kv channel but that also contain certain structural differences in order to allow for its sensitivity to Ca²⁺ and to aid in the binding of auxiliary subunits (figure 1.4). As is the case for Kv, it is the S4 region of the α -subunit that contains the voltage sensor required in order for the channel to respond to increases in membrane depolarisation. Many positively-charged arginine residues reside in this area, and depolarization causes them to move, leading to a conformational change in the protein, and the opening of the channel pore (Stefani *et al*, 1997). It is also the S5-S6 linker that lines the pore of this channel and that contains the binding sites for BK_{Ca} channel pore blockers such as iberiotoxin (IbTX) and charybdotoxin (ChTX).

A major difference between BK_{Ca} and Kv channel structure is the inclusion of an additional transmembrane domain (S0) at the N-terminus of the BK_{Ca} channel, making this region extracellular and providing the binding site for the auxiliary β -subunits to associate with the pore-forming subunit (Wallner *et al*, 1996). It is also thought that this extra N-terminal domain may provide a region with which vasoactive substances such

as nitric oxide may bind and have their effect. Another difference is that the BK_{Ca} channel has a very large intracellular region at the C-terminal end of the protein, with further domains numbered S7-S10. This region is thought to make up approximately two thirds of the channel and the domains found here contain the Ca²⁺-sensing region, also known as the calcium bowl. This sensing region is just before the S10 domain and contains a number of negatively-charged aspartate residues thought to be important in Ca²⁺-binding (Wei *et al*, 1996; Schreiber & Salkoff, 1997). A regulator of conductance for K⁺ (RCK) domain found in S7-S8 also confers some sensitivity to Ca²⁺. Other Ca²⁺-sensing regions must also exist as experiments involving the removal of the C-terminal did not prevent the channel opening, and even retained wild-type Ca²⁺-sensitivity, under physiological conditions (Piskorowski and Aldrich, 2002). The C-terminus region also contains phosphorylation sites for possible modulation of the channel by PKA, PKG (Zhou *et al*, 2001), PKC and tyrosine kinase (Wang *et al*, 1999).

The pore-forming α -subunit of the channel is encoded by a single gene yet despite this, BK_{Ca} channels in different tissues display a great amount of diversity. This variation is believed to partly come from alternative splicing of the gene. The Ca²⁺ bowl is one such region thought to contain numerous alternative splicing sites.

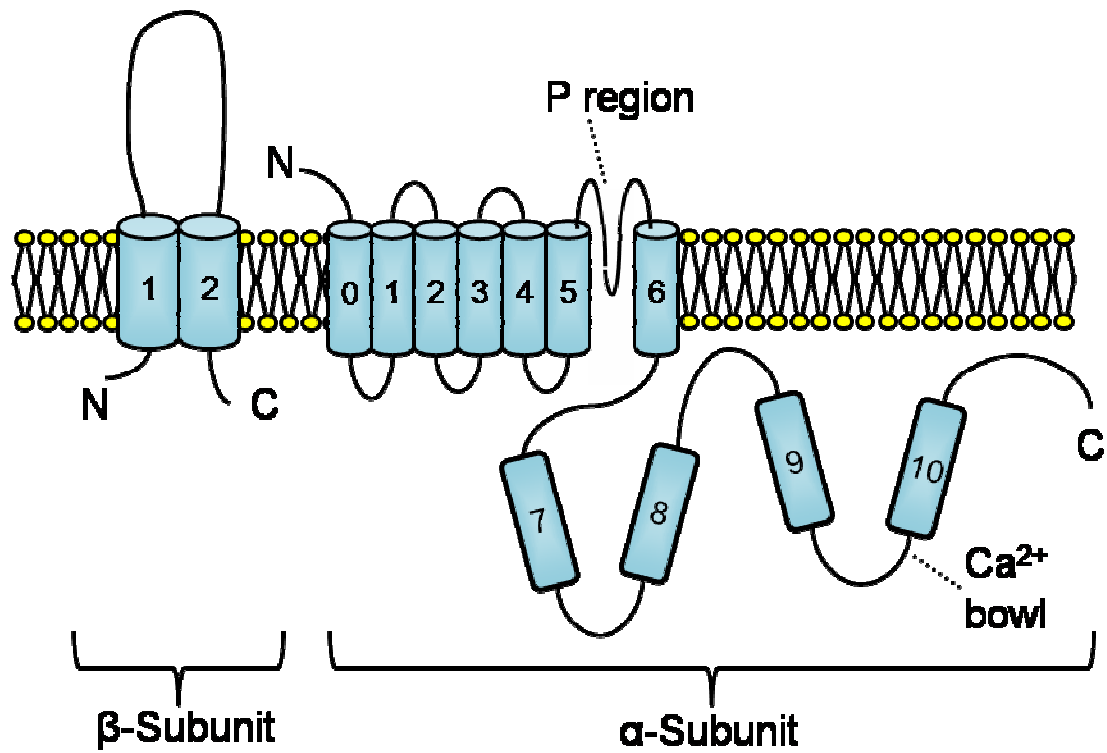


Figure 1.4 Schematic diagram illustrating the structure of the α - and β -subunits of the BK_{Ca} channel. The domains of the subunits are numbered, and the N-terminus, C-terminus, pore region (P region) and Ca^{2+} bowl are labelled.

1.6.1.2 The β -subunit

As mentioned, auxiliary β -subunits can interact with the α -subunit in order to modulate its function. The ratio with which β -subunits bind with α -subunits is 1:1 (Toro *et al*, 1998). Four β -subunit isoforms have been cloned so far, named β 1- β 4, and their interaction with the pore-forming subunit has an effect on the gating of K^+ current. β -subunits are composed of two transmembrane domains, linked by an extracellular loop, and with their N- and C-termini located in the cytoplasm (McManus *et al*, 1995).

The association of the α -subunit with a β -subunit can lead to the regulation of the channel in a number of different ways, depending on the actual β -subunit isoforms involved (McManus *et al*, 1995; Wallner *et al*, 1995; Meera *et al*, 2000). β 1 is the predominant isoform of the β -subunit found in vascular smooth muscle (Jiang *et al*, 1999; Tanaka *et al*, 2004). The binding of the β 1-subunit to the α -subunit increases the apparent calcium sensitivity of the channel compared to the α -subunit alone so that, at a given voltage, less Ca^{2+} -binding energy is required to open the channel (Cox & Aldrich, 2000). The binding of the β 1-subunit also affects channel gating in such a way that these channels do not inactivate (Meera *et al*, 2000). β 2- and β 3- subunits prevent sustained activation of the channel and cause inactivation to occur (Wallner *et al*, 1999; Xia *et al*, 1999). β 4 has a biphasic effect on the channel's sensitivity to Ca^{2+} . It appears to decrease the channel's apparent Ca^{2+} -sensitivity when $[Ca^{2+}]_i$ is low, but causes an increase in apparent Ca^{2+} sensitivity when $[Ca^{2+}]_i$ is raised. Like β 1, β 4-modulated channels do not show any sign of inactivation (Wallner *et al*, 1999).

The importance of the beta-subunit has become clearer in recent years. Recently, there has been a growing amount of evidence suggesting that reduced activity of BK_{Ca} channels plays a role in the vascular complications that are often associated with diabetes (Dimitropoulou *et al*, 2002; Burnham *et al*, 2006). It is thought that this may

be due to a downregulation of the β -1 subunit leading to a decrease in the Ca^{2+} sensitivity of the channel (McGahon *et al*, 2007).

1.6.2 The role of BK_{Ca} channels in vascular smooth muscle

The role of BK_{Ca} channels in vascular smooth muscle is to provide a negative feedback mechanism to combat depolarization and increased Ca^{2+} entry. By responding to changes in both membrane potential and $[\text{Ca}^{2+}]_i$, these channels are able to react to the causes of vasoconstriction and so dampen cellular excitability and reduce contractility of the cell. Their activation is also thought to play a role in the regulation of myogenic tone.

1.6.2.1 The role of Ca^{2+} sparks and STOCs

The formation of microdomains allows Ca^{2+} to have a particular effect in a small area without affecting the whole of the cell. The cell structure is highly organised in order to facilitate this. In particular, membranes of the cell, such as the plasma membrane and that of the SR, can be found in close proximity to one another, and this may inhibit the free movement of Ca^{2+} (Bradley *et al*, 2004). The viscosity of the cytoplasm may also help by slowing down Ca^{2+} diffusion. Ca^{2+} channels such as L-type VDCCs, TRPV4 channels, and RyRs are found in cluster within these area, allowing them to interact in order to regulate $[\text{Ca}^{2+}]_i$ (DeFelice, 1993). The random release of packets of Ca^{2+} from the SR, termed Ca^{2+} sparks, were mentioned briefly earlier. Ca^{2+} release in this manner is a novel way of activating BK_{Ca} channels in order to provide this negative feedback mechanism. This release of Ca^{2+} is through RyR channels on the membrane of the SR that are found in very close proximity to BK_{Ca} channels of the plasma membrane.

These channels are believed to be within 1 μm , with figures of around 20 nm also being reported (Wallner *et al*, 1999; Devine *et al*, 1972; Bennett, 1996). The local $[\text{Ca}^{2+}]$ in these regions is therefore much higher than the global $[\text{Ca}^{2+}]$ in the cytoplasm. It is in this manner that Ca^{2+} sparks can raise local $[\text{Ca}^{2+}]_i$ high enough to allow activation of BK_{Ca} channels without affecting other calcium-dependent mechanisms within the cell. It is thought that these sparks can in fact increase the local $[\text{Ca}^{2+}]_i$ to the order of 10 μM (Zhuge *et al*, 2002). The activation of BK_{Ca} channels in this manner, and the resulting efflux of K^+ , has been termed a spontaneous transient outward current, or STOC (Benham & Bolton, 1986). At global $[\text{Ca}^{2+}]_i$ and membrane potentials the P_{open} of the BK_{Ca} channels is thought to be close to zero. The activation of BK_{Ca} channels by Ca^{2+} sparks is therefore of great importance for BK_{Ca} function. It has been reported that the activation of BK_{Ca} channels by a single Ca^{2+} spark can hyperpolarize isolated cells by up to 20 mV (Ganitkevich & Isenberg, 1990), and therefore have a great influence on the membrane potential of cells (Nelson *et al*, 1988).

The activation of IP_3Rs may also lead to the development of Ca^{2+} microdomains in these areas. Ca^{2+} trapped within this area is also likely to be taken up into the SR, increasing SR load, and so leading to the further release of Ca^{2+} from these stores through RyR and IP_3R activation and, in the case of RyR activation, an increase in spark activity. It is believed that IP_3Rs and RyRs may be able to interact as the activation of receptors that lead to the production of IP_3 have also been found to increase spark activity (Gordienko *et al*, 1998). This is of interest because both ET-1 and Ang II act on their receptors leading to IP_3 production and so they may be able to modulate Ca^{2+} spark release in this way. RyRs may also be able to affect IP_3R -mediated Ca^{2+} release as inhibition of the RyR using ryanodine or a RyR antibody has been shown to reduce Ca^{2+} oscillations induced by acetylcholine and noradrenaline, two substances that activate Ca^{2+} release through the IP_3R .

There is a complex relationship between RyRs on the membrane of the SR, and BK_{Ca} channels and VDCCs of the plasma membrane, with these proteins all working closely together. More recently, TRPV4 channels have also been included in this relationship (Earley *et al*, 2005). This co-localisation of RyR and BK_{Ca} with these plasma membrane Ca²⁺ influx channels means that, upon activation of the plasma membrane channels during depolarization, high local [Ca²⁺] may arise through this mechanism also. The influx of Ca²⁺ is thought to stimulate the release of Ca²⁺ from the SR through RyRs which is then likely to lead to the activation of BK_{Ca} channels (Jaggar *et al*, 1998a). This co-localisation is of great physiological importance as it allows BK_{Ca} channels to play their role of providing a negative feedback mechanism.

Despite the fact that STOCs can barely be seen at holding potentials of -50 mV and below (Benham & Bolton, 1986; Hogg *et al*, 1993; Pluger *et al*, 2000), they are still believed to play an important physiological role in isolated smooth muscle cells. This may be because very few BK_{Ca} channels actually need to open in order to hyperpolarize the cell membrane potential. It is possible that STOC frequency at resting membrane potentials is greater than has been reported but that they are difficult to resolve above the noise seen in the recordings due to the small current amplitude of BK_{Ca} channels at these potentials. The physiological importance of BK_{Ca} channels has been shown in current clamp experiments on rat mesenteric arterial smooth muscle cells where the application of Ang II led to a depolarization of the cell membrane. This depolarization of the membrane was interrupted intermittently by “spikes” of hyperpolarization, preventing a continuous increase in membrane potential. Application of the BK_{Ca} blocker penitrem A inhibited this hyperpolarization and so Ang II was able to depolarize the membrane potential at a faster rate (Rainbow RD, unpublished data). Another experiment demonstrating the physiological importance of BK_{Ca} channels

involved knockout mice lacking the $\beta 1$ -subunit gene which led to altered BK_{Ca} functionality in these animals due to a reduction in Ca^{2+} sensitivity. BK_{Ca} channels of the cerebral artery displayed decreased sensitivity to Ca^{2+} sparks, and the coupling between this form of Ca^{2+} release and the activation of the BK_{Ca} channel was diminished. These animals therefore exhibited symptoms of hypertension, including high blood pressure and increased arterial tone (Brenner *et al*, 2000), thus demonstrating the importance of BK_{Ca} function in the regulation of vascular smooth muscle tone.

1.6.3 Regulation of BK_{Ca} channels by vasoactive substances

Like many types of K^+ channels, BK_{Ca} channels can be regulated by a number of vasoactive compounds such as the vasodilator nitric oxide, and vasoconstrictors like ET-1 and Ang II. The general consensus is that these endogenous substances have their effect by activating protein kinase signalling pathways. The mechanisms involved are complicated, and different groups have reported varying effects of ET-1 and Ang II on BK_{Ca} channels of smooth muscle. In general, ET-1 and Ang II are both thought to inhibit BK_{Ca} channels through the activation of PKC. Ang II has also been found to modulate K_V and K_{ATP} currents through the inhibition of PKA (Hayabuchi *et al*, 2001a; Hayabuchi *et al*, 2001b), and so it is possible that it may also modulate BK_{Ca} currents through the same signalling pathway. PKC is thought to have this effect by reducing the frequency of Ca^{2+} sparks from the SR and also inhibiting the coupling between sparks and BK_{Ca} channels by reducing the Ca^{2+} sensitivity of the BK_{Ca} channel (Bayguinov *et al*, 2001). In other vascular smooth muscle, such as the rat pulmonary artery, PKC has actually been seen to increase Ca^{2+} spark and BK_{Ca} activity (Barman *et*

al, 2004). However, this increase in BK_{Ca} activity still leads to vasoconstriction of the vessel, and is thought to involve PKG in some manner. Differences in response to protein kinases in this manner could be due to the tissue specific actions of varying PKC isoforms, and also differences in BK_{Ca} channel function due to alternative splicing (Zhou *et al*, 2001).

It is possible that protein kinases may actually interact with their specific phosphorylation sites that have been found in the α -subunit in order to affect BK_{Ca} channel activity directly. This is in addition to any effects that they may have through the further activation of intracellular signalling pathways and through the phosphorylation of other channel proteins, such as the RyR, that could modulate Ca²⁺ spark activity and so indirectly alter BK_{Ca} channel activity. Possible phosphorylation sites for PKA and PKG have also been found on the β -subunit in smooth muscle (Toro *et al.*, 1998), but very little has since been reported on whether these protein kinases interact directly with the β -subunit. Experiments performed by Schubert (Schubert *et al*, 1999) suggest that PKC could affect BK_{Ca} channel activity directly in rat tail artery smooth muscle cells.

1.6.4 BK_{Ca} channels as drug targets

BK_{Ca} channels have the potential to be useful targets for drugs to treat hypertension, and as they are not found in the heart, the chances of serious side effects on the heart associated with the drug would be lower than with drugs targeting other K⁺ channels such as K_{ATP} channels for example. It may even be possible to target smooth muscle BK_{Ca} channels especially if drugs could be targeted to the specific β -subunit present, such as the β 1-subunit in smooth muscle, in order to reduce the chances of any side effects on the central nervous system.

1.7 Aims of thesis

The main aim of my thesis was to investigate how endogenous vasoconstrictors regulate the resting membrane potential of smooth muscle through the modulation of BK_{Ca} channels. BK_{Ca} channel currents were recorded in rat isolated mesenteric artery smooth muscle cells using a variety of patch-clamp configurations. The relationship between membrane potential and cytoplasmic [Ca²⁺] was investigated using inside-out excised patches. Whole-cell BK_{Ca} currents were examined using voltage-pulses, and spontaneous transient outward currents (STOCs), which were shown to result from BK_{Ca} activation, were also recorded. I found that the vasoconstrictors ET-1 and Ang II affected both pulse-induced BK_{Ca} currents and STOC amplitude and frequency. The role of PKC activation in this modulation of BK_{Ca} channels was investigated using peptide PKC inhibitors.

2 METHODS

All experiments for this thesis were performed on smooth muscle cells isolated from the small branches of rat mesenteric artery by enzymatic dissociation of the tissue. The protocol for this procedure is as explained below.

2.1 Isolation of smooth muscle cells from rat mesenteric artery

Male adult Wistar rats were killed by cervical dislocation. The care and killing of these animals followed the regulations laid out in the UK Animals (Scientific Procedures) Act 1986. As often as possible the animal was “shared” with colleagues isolating cardiac myocytes so that no animals were used unnecessarily. The mesenteric artery was carefully removed and placed into a petri dish of zero calcium solution containing (mM) 137 NaCl, 5.4 KCl, 0.42 Na₂HPO₄, 0.44 NaH₂PO₄, 1 MgCl₂, 10 HEPES, and 10 Glucose, adjusted to pH 7.4 with NaOH. Any surrounding fat and connective tissue was stripped off using small forceps and the mesenteric vein was identified and removed. The mesenteric vein is composed of less elastic fibres and smooth muscle than the mesenteric artery and pulling gently on the vein causes it to break away. It is important to take great care not to over-stretch the artery during the dissection as this can damage the vessel.

A great deal of time was spent developing the enzymatic digestion stage of the isolation. The original protocol (Rainbow *et al*, 2006) had to be constantly adapted as the specific activity of the enzymes used varied between batches. The first enzyme solution was a low calcium solution (zero calcium solution as described above but with the addition of

0.1 mM Ca²⁺) containing (mg/ml) 0.9 albumin (Sigma; A7030), 0.9 dithioerythritol (DTE; Sigma; D8255), and varying amounts of papain (0.9-1.4; Sigma; P4762), depending on the specific activity of the batch of papain used. The total specific activity of the enzyme was kept constant at approximately 40 units. This solution was warmed to 35°C for 10 min whilst the mesenteric dissection was taking place and the vessel was then added to this solution for the first digestion stage lasting 31 minutes. 10 minutes before this first digestion period was due to end, a second low calcium solution (enzyme solution 2) containing (mg/ml) 0.9 albumin, 0.55-1.4 collagenase type F (Sigma; C7926) and 0.65-0.9 hyaluronidase type I-S (Sigma; H3506) was placed in the water bath to warm for 10 minutes. The artery was transferred to this solution, taking care not carry too much solution with it, for the second part of the enzymatic digestion stage. Again, it was necessary to vary the amount of enzyme used according to the differing specific activity between batches, but the total specific activity remained constant at approximately 7.5 units for caseinase, a component of collagenase type F, and 810 units for hyaluronidase. The vessel appeared to be particularly vulnerable at this stage and it was sometimes necessary to alter the length of the second digestion in order to isolate a sufficient number of healthy looking cells. This second phase therefore lasted 11.5-12.5 minutes, depending upon the concentrations of the enzymes used that day, in order to achieve the best isolation possible. If higher enzyme concentrations were used then the state of the vessel was checked after 10.5 minutes to ensure that it was not over-digesting. 1 minute before the digestion was due to finish the enzyme solution was slowly and carefully removed, so that, at the scheduled finish time, no solution remained and the washout stage could begin immediately. The artery was washed 3-4 times in a low calcium solution containing 0.9 mg/ml albumin, discarding the solution between each wash. The artery was then transferred to the low

calcium solution and the small branches were removed by gentle trituration using a 3 ml Pasteur pipette. The main branch was then discarded and single smooth muscle cells were obtained from the small branches of mesenteric arteries by further trituration with a 1 ml Pasteur pipette (figure 2.1). The isolated smooth muscle cells were stored on ice at approximately 4°C throughout the day. Cells were freshly prepared each day on the morning of the experiment using the method described.

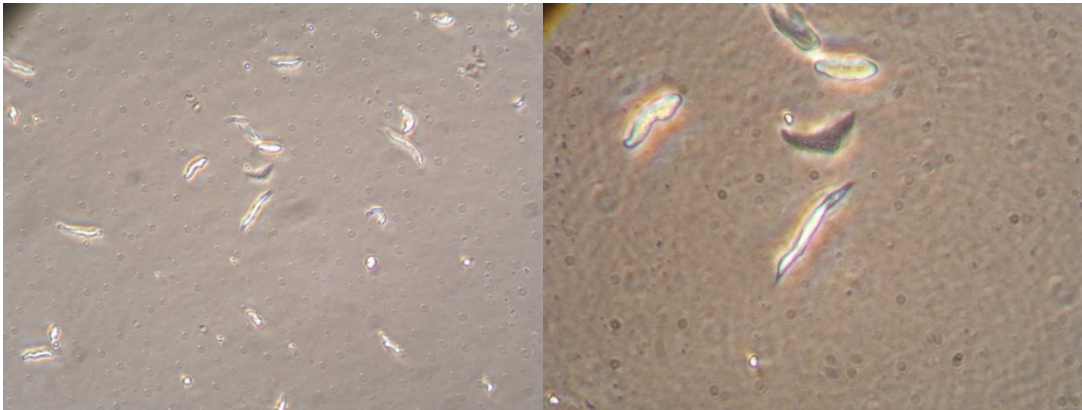


Figure 2.1 Photographs of smooth muscle cells isolated from rat mesenteric artery. Healthy cells appear elongated in comparison to others.

2.2 Electrophysiology

2.2.1 The patch-clamp method

The development of the patch-clamp technique changed the way in which we could study cell activity at the individual ion channel level as it allows the current across the cell membrane to be accurately measured in cells that were too small to be studied previously.

2.2.2 General principles of the patch-clamp technique

The patch clamp technique enables the electrical isolation of a patch of membrane from the extracellular solution. Once a high resistance seal has been achieved (section 2.2.4) it is possible to record currents using any one of a variety of patch configurations (figure 2.2). Single-channel recordings were filtered at 2 kHz and digitized at 10 kHz. Whole-cell currents were filtered at 2 kHz. Whole-cell recordings are prone to errors due to its design and continuous use of a single electrode. It is assumed that the pipette voltage is equal to the membrane voltage however this is not the case as current flowing through the pipette meets a resistance in series with the cell membrane. This must be compensated for in order to minimize errors. For voltage pulse experiments a P/6 leak subtraction protocol was used. This protocol was designed not to activate any current so that the leak pulses contain only the capacitive and linear leak of the membrane. For all experiments, the perfusion bath was grounded using a silver chloride wire.

2.2.3 Fabrication of electrodes

Electrodes were fabricated from thick-walled borosilicate glass using a Narishige two-stage vertical puller. The electrode resistances after filling with the appropriate electrolytic solution were approximately 4-6 M Ω for experiments using the whole-cell patch configuration, and 8-12 M Ω for excised patches. The electrodes used for excised patches were also fire-polished using a Narishige microforge to encourage seal formation and so reduce noise in the recordings.

2.2.4 Obtaining a seal

The patch pipette (containing appropriate electrolytic solution) was pressed lightly against the cell surface. The resistance of the patch was monitored by the continuous use of a 5 mV test pulse of 10 ms in length. Coming into contact with the cell causes the size of the current produced by the test pulse to decrease slightly, due to an increase in the resistance of the patch, indicating that a weak seal between the cell and the electrode has been formed. Applying a small amount of suction to the cell at this point improves the quality of the seal until a tight gigaohm seal is formed. This step is aided by the application of a negative membrane potential (-50 to -65 mV) to the electrode. The term “gigaohm” means that this is the minimum resistance of the patch; the actual resistance is usually much greater. This serves to electrically isolate a patch of membrane from the bath solution and so reducing noise and preventing the leak of current. Once a high seal resistance has been achieved, various patch configurations can be employed according to the requirements of the experiment (figure 2.2).

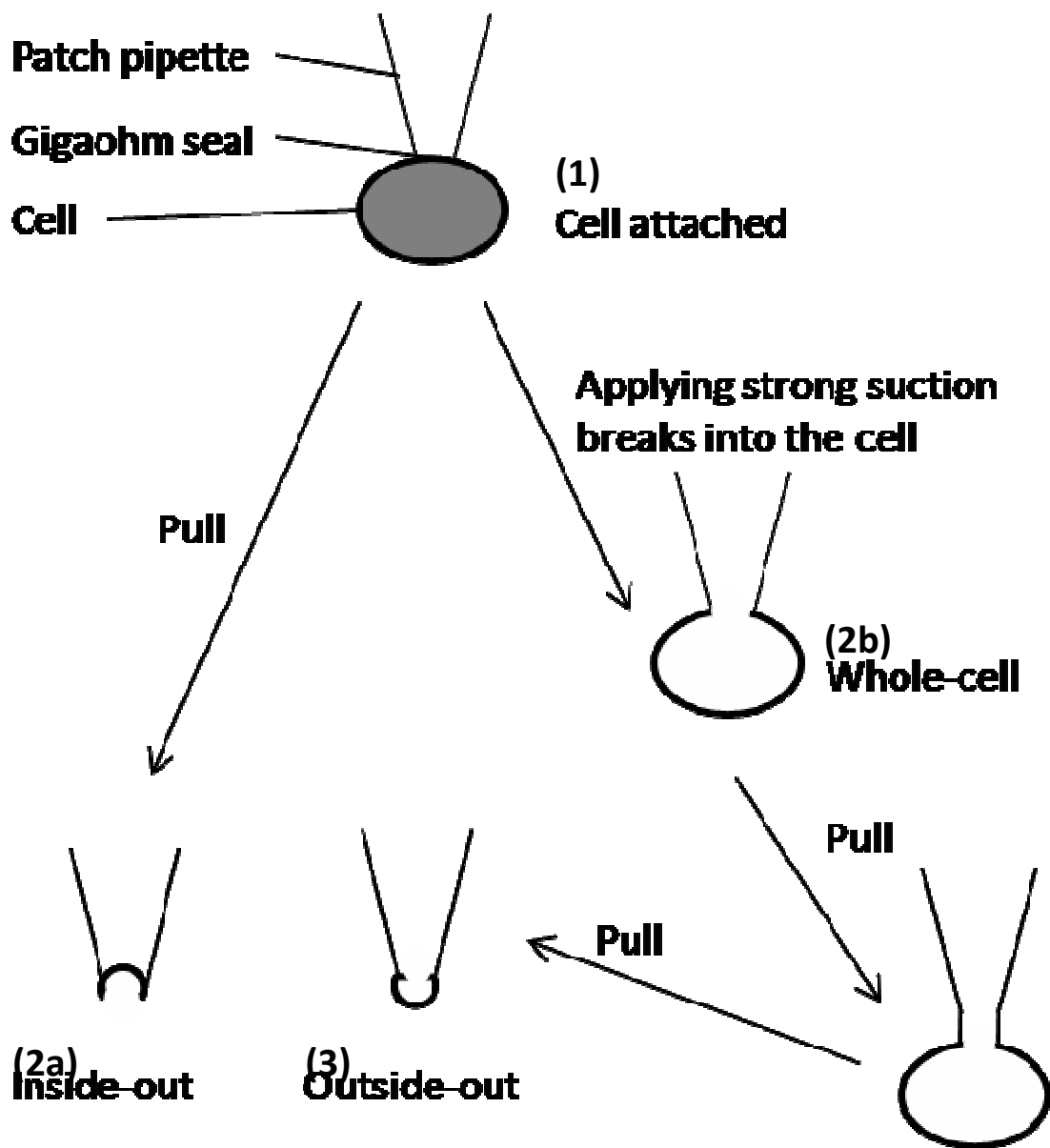


Figure 2.2 Patch clamp cell configurations. Once a gigaohm seal has been achieved, a variety of patch configurations may be used. (1) Cell attached, (2a) inside-out, (2b) whole-cell, and (3) outside-out.

2.3 Solutions

2.3.1 Solutions for recording of single channel currents

The intracellular solution (used as bath solution for inside-out experiments) consisted of (mM) 110 KCl, 30 KOH, 1 MgCl₂, 10 HEPES, and various CaCl₂ concentrations: 0 (buffered with 10 EGTA), 1.33, 3.15, 6.06, 8.24 (buffered with 10 HEDTA), and 0.1 (no buffer present). These varying concentrations of CaCl₂ gave free Ca²⁺ concentrations of (μM) 0, 1, 3, 10, 30, and 100 respectively, as calculated using Maxchelator (Patton, 2003). HEPES is a buffer used to regulate the pH of the solution. EGTA and HEDTA are Ca²⁺ chelators that were included in the intracellular solution to buffer any changes in [Ca²⁺]_i. HEDTA is a very effective Ca²⁺ chelator and was used to buffer [Ca²⁺]_i at the micromolar level. EGTA is more effective at buffering lower [Ca²⁺] and in these experiments was used to buffer the Ca²⁺-free intracellular solution. The pH of these solutions was adjusted to 7.2 with KOH

The extracellular solution (used as the pipette solution) consisted of (mM) 134 NaCl, 6 KCl, 0.33 NaH₂PO₄, 5 Na-pyruvate, 1 MgCl₂, 2 CaCl₂, 10 HEPES, 4 glucose, and 6 mannitol, adjusted to pH 7.4 with NaOH. For experiments involving 1, 2-dioctanoyl-*sn*-glycerol (DOG) the extracellular solution was similar but a total of 10 mM glucose was used instead of mannitol. This was in order to maintain consistency with previous work carried out in the lab investigating the effects of DOG on Kv channels. The total concentration of glucose and mannitol added was kept constant in order to maintain osmolarity.

The experimental chamber had a volume of 0.4 ml, and the external solution was changed by continuous perfusion of the whole bath, with complete exchange taking approximately 60 s. All of the cells in the bath were replaced in between experiments in

order to prevent repeated exposure to the compounds tested. Using the Nernst equation, E_K is -82 mV under these conditions.

2.3.2 Solutions for recording of pulse-induced whole-cell currents

The intracellular solution consisted of (mM) 110 KCl, 30 KOH, 1 MgCl₂, 4.04 CaCl₂, 10 HEPES, 10 EGTA, 3 Na₂ATP, 0.5 GTP, and the pH was adjusted to 7.2 with KOH. HEPES is a buffer used to regulate the pH of the solution and EGTA is a Ca²⁺ chelator that was included in the intracellular solution to buffer any changes in [Ca²⁺]_i.

The concentration of free Ca²⁺ was 100 nM (calculated using Maxchelator). For experiments investigating the effect of [Ca²⁺] on BK_{Ca} current, total CaCl₂ concentrations of (mM) 1.19 and 6.70 were also used to give free Ca²⁺ concentrations of 20 nM and 300 nM respectively. The extracellular solution consisted of (mM) 134 NaCl, 6 KCl, 0.33 NaH₂PO₄, 5 Na-pyruvate, 1 MgCl₂, 2 CaCl₂, 10 HEPES, 4 glucose, and 6 mannitol, adjusted to pH 7.4 with NaOH. For experiments involving 1, 2-dioctanoyl-*sn*-glycerol the extracellular solution was similar but a total of 10 glucose was used instead of mannitol.

2.3.3 Solutions for recording of STOCs

For the recording of STOCs, the intracellular solution was modified slightly so that it contained (mM) 1 EGTA and 0.40 CaCl₂ to again give a free Ca²⁺ concentration of 100 nM. A variety of Ca²⁺ concentrations were investigated and so the concentration of CaCl₂ added was modified appropriately. Total CaCl₂ concentrations were therefore adjusted to (mM) 0.12 and 0.67, in the presence of 1 mM EGTA, in order to give free

Ca²⁺ concentrations of 20 nM and 300 nM respectively as calculated using Maxchelator. The extracellular solution was the same as that used to study pulse-induced BK_{Ca} currents. The experimental chamber had a volume of 0.4 ml, and the external solution was changed by continuous perfusion of the whole bath, with complete exchange taking approximately 60 s. For all recordings made in the whole-cell patch configuration, all of the cells were replaced between experiments in order to avoid repeated exposure to the compounds tested. Using the Nernst equation, E_K is -82 mV under these conditions.

2.3.4 Drugs and solutions

Albumin bovine serum, DTE, papain, collagenase and hyaluronidase that were required for the cell isolation were all obtained from Sigma-Aldrich (Poole-UK), as were all reagents used to make the recording solutions and all drugs and compounds used experimentally. The only exception to this was protein kinase C inhibitor peptide 20-28 (PKC-IP 20-28) which was obtained from Calbiochem (Nottingham, UK) and linked to a TAT peptide by Dr R. I. Norman (University of Leicester). The isolation enzymes were aliquoted out into smaller measures upon arrival so that they could then be frozen and only a small amount was freeze/thawed for use at any one time. This was done to keep the enzymes as fresh and active as possible for as long as possible as they tend to go off quite quickly with repeated thawing and freezing. DOG was made up in DMSO (final DMSO concentration of $\leq 0.1\%$). A control solution containing DMSO of the same final concentration as before but without any DOG present was also used as a vehicle control and this was not seen to have any effect on BK_{Ca} activity. Stock solutions of penitrem A, Ang II and ET-1 were all made up in distilled water.

2.4 Recording of Currents

2.4.1 Recording of BK_{Ca} single channel currents

Single channel currents were also recorded from smooth muscle cells using the patch clamp technique. The patch pipette (containing the external solution) formed a tight gigaohm seal as described previously, but the membrane patch was then pulled away from the cell so that the inside of the cell membrane was facing outwards towards the bath solution. This is known as the inside-out patch configuration (figure 2.2). With the intracellular side of the membrane facing the bath solution, it was possible to easily change the intracellular conditions of the cell during recording, so that the effects of various Ca²⁺ concentrations, for example, could be studied while the cell membrane was held at a constant potential (figure 2.3C). All experiments were carried out at 30°C.

2.4.2 Recording of BK_{Ca} whole-cell currents using voltage pulses

In order to record pulse-induced BK_{Ca} currents, a gigaohm seal was formed as described in section 2.2.4, and then strong suction was applied in order to rupture the cell membrane within the pipette. This allowed control of the intracellular solution whilst at the same time permitting the study of all channels within the cell. This is known as the whole-cell patch clamp configuration (figure 2.2).

The Ca²⁺-voltage relationship for BK_{Ca} channels was investigated using a voltage step protocol (figure 2.3A). Cells were held at -65 mV at first before being held at -20 mV for a minimum of 5 sec in order to inactivate Kv channels. From this new holding potential, the membrane potential was then stepped to various membrane potentials, ranging from -10 to +80 mV, before decreasing to 0 mV in order to measure tail

currents. The membrane potential was then hyperpolarized to -20 mV before finally returning to the initial holding potential of -65 mV.

In order to investigate the effect of various BK_{Ca} inhibitors and vasoconstrictors on BK_{Ca} whole-cell current, the membrane potential of the cells were pulsed from the holding potential to a more positive potential in a single step (figure 2.3B). This was repeated so that a total of 20 pulses were obtained which could then be averaged. For all compounds except 1, 2-dioctanoyl-*sn*-glycerol (DOG), the membrane potential was pulsed from a holding potential of -20 mV to +60 mV. For DOG, 0 mV to +80 mV was used instead. All experiments were carried out at 30°C.

2.4.3 Recording of STOCs

STOCs were recorded using the whole-cell patch clamp configuration (figure 2.2). The cell membrane was held at a constant potential and the appearance of spontaneous currents was observed (figure 2.3C). The effects of changes in membrane potential and the external application of vasoconstrictors could then be investigated.

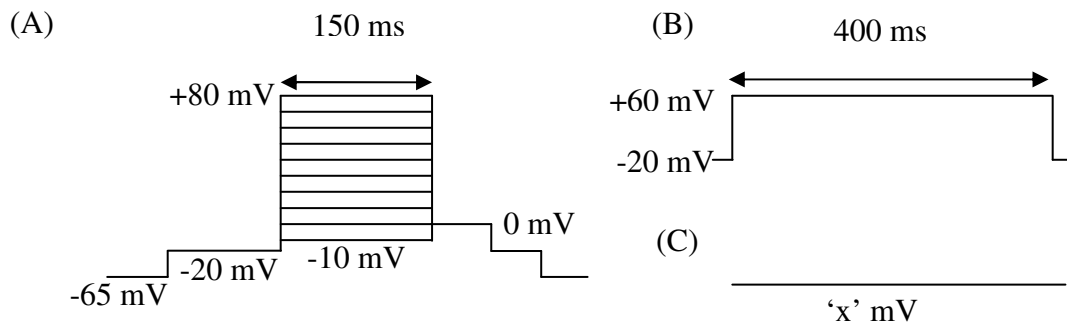


Figure 2.3 Protocols used for the recording of currents. **(A)** Voltage step protocol for Ca^{2+} -voltage relationship experiments (not to scale). The prepulse at -20 mV lasted for 5 seconds. **(B)** An example of the pulse protocol used to investigate the effect of a variety of BK_{Ca} inhibitors. The membrane potential was increased from a holding potential of -20 mV to +60 mV in a single step. **(C)** Protocol used for the recording of STOCs. The membrane potential was held at the required voltage for the necessary period of time.

2.5 Data analysis

2.5.1 Analysis of single BK_{Ca} channels

BK_{Ca} single channel data was analysed using an in-house software programme. Only recordings with a steady baseline, a good signal to noise ratio, and without any other type of channels present in the patch were considered for the analysis of single channel activity.

The 50%-threshold-crossing technique was used to analyse the BK_{Ca} single channel recordings. The threshold was placed halfway between open and closed states and was used to measure P_{open} and to detect the duration of each opening and closing event. It can be difficult to measure the maximum number of channels in a patch, all we can go on is the maximum number of channels seen under what could be considered to be near-optimal conditions for channel opening. However, it has been reported by McManus & Magleby (1988) that BK_{Ca} channels can remain closed or “silent” for periods of longer than 1 minute. This may make it difficult to measure the actual maximum number of channels in a patch without recording for very long periods of time. However, it is important to note that the recordings carried out by that group were of BK_{Ca} channels of cultured rat skeletal muscle which may have very different properties to freshly isolated cells. Without recording for very long periods of time, which is difficult to do with freshly isolated vascular smooth muscle cells, it is therefore necessary to assume that the maximum number of channels observed is equal to the maximum number of channels present in the patch as it is not possible to know whether there are any silent channels present if they do not become active at some point during the recording. This assumption has also been made by other groups that have investigated the properties of

BK_{Ca} channels by recording activity for a similar length of time as I have in this study (Mistry & Garland, 1998; Sun *et al*, 1999). Therefore, in order to estimate the number of channels present in a patch, the patch was held at a pipette potential of -40 mV (membrane potential therefore equal to +40 mV) in the presence of 100 μM [Ca²⁺]_i so that the P_{open} of the BK_{Ca} channel was close to 1. The largest number of open channels observed in the patch under these conditions was assumed to be equal to the total number of channels in the patch, and this figure was then used to calculate the P_{open} under various conditions using the following equation:

$$P_{open} = \left(\frac{\sum_{j=1}^N t_j j}{TN} \right) \quad (\text{Equation 1})$$

where N is the number of channels in the patch, t_j is the time spent at level j and T the total duration of the recording.

In patches where only single channels were recorded, the mean open and closed times of the channel could also be measured and analysed. The 50%-threshold-crossing technique was used to measure channel dwell times. Data was plotted as number of events (square root scale) against dwell times (log scale). The dwell time data was plotted on a log scale to enable display and fitting of components with widely different time constants on the same histogram (Sigworth & Sine, 1987). Exponentials were then fitted to the data by the maximum likelihood method. This method attempts to determine the parameters that give the highest probability that the data observed will be obtained. Parameter values are chosen in order to make the fit of the data more likely to

be correct than the fits obtained using any other parameter values. The time constants obtained by this method for each of the components can then be compared to see how they are affected by changes in experimental conditions such as $[Ca^{2+}]_i$ and membrane potential.

In order to investigate the relationship between $[Ca^{2+}]_i$ and voltage and its effect on BK_{Ca} single channel activity, the data was analysed as described above and a single channel iV curve was constructed to measure the conductance of the channel. The open probability of the channel (P_{open}) with various $[Ca^{2+}]_i$ was also plotted against the membrane potential and a Boltzmann curve was fitted in order to study the relationship between the two and the effect of varying $[Ca^{2+}]_i$ on this relationship:

$$P_{open} = \frac{1}{\left\{1 + \exp\left(\frac{V - V_{1/2}}{k}\right)\right\}} \quad (\text{Equation 2})$$

where V is the assumed membrane potential, $V_{1/2}$ is the potential at which half-maximal activation is achieved, and k is the slope factor representing the voltage-dependence.

In patches where only single channels were recorded, the effect of $[Ca^{2+}]_i$ and voltage on channel dwell times were analysed as described above.

The effect of DOG on the properties of BK_{Ca} single channels was also analysed as described, and P_{open} , and mean open and closed times were compared to control.

2.5.2 Analysis of whole-cell currents induced by voltage pulses

The same in-house software programme was used to analyse BK_{Ca} whole-cell current. In the case of the voltage pulse protocol used to study the Ca²⁺-voltage relationship and its effect on BK_{Ca} channels, the steady state current and tail currents were analysed and then used to produce iV curves. Steady state current was defined as the current exhibited at the end of the voltage pulse and exponentials were fitted to the tail currents to give an indication of the P_{open} of the channel under the appropriate conditions. Cell capacitance was measured by compensation of the capacity transients that appear upon rupturing the cell membrane. This was used as an indication of the size of the cell and so enabled normalisation of current density

The effects of BK_{Ca} inhibitors and vasoconstrictors such as penitrem A, ET-1 and DOG were analysed by measuring the steady state current in the absence of the compound and then at various time points after application. This was done by averaging the 20 sweeps in order to measure the mean steady state current at each time point. This was then used to calculate the percentage of control current that was recorded in the presence of each individual compound, and so conversely, the percentage of current inhibition achieved by each (\pm standard error of the mean; SEM).

2.5.3 Analysis of STOCs

Conventional threshold detection methods, such as those used to detect single channels are not suitable for detecting STOCs due to the presence of an uneven and noisy baseline. In order to overcome this problem STOCs were detected using the method shown in figure 2.4. First, a seven point window was used to obtain a running mean. This served to reduce the noise in the trace while still maintaining the overall profile of

the current. The time derivative (slope) and a running variance (using a seven point window) of this trace were then obtained. Variance is a measure of the spread of data points around their mean and is equal to the square of the standard deviation. Obtaining the variance in this way accentuates the transients contained within the trace. Since it is the upstroke of the STOCs that need detecting this variance was then multiplied with the time derivative to give positive values for the upward transients alone, and the point at which this value crosses the threshold was taken as the start of the STOC (see figure 2.4). Note that even moderately fast changes in the baseline do not affect this detection method.

Once STOCs had been detected in this way, each STOC was aligned to a common point and written to file so that this new file contained the same number of records as STOCs that had been detected. Each record contained a section of the original trace made up of 512 data points. STOCs were aligned at a starting point of 150 data points (75 ms at a digitization rate of 2 kHz) into the record. Durations between successive STOCs were stored during the detection process and could be exported to create a frequency histogram. The file containing the aligned STOCs was used to measure parameters such as maximum amplitudes, rate of rise etc. as described in chapter 5.

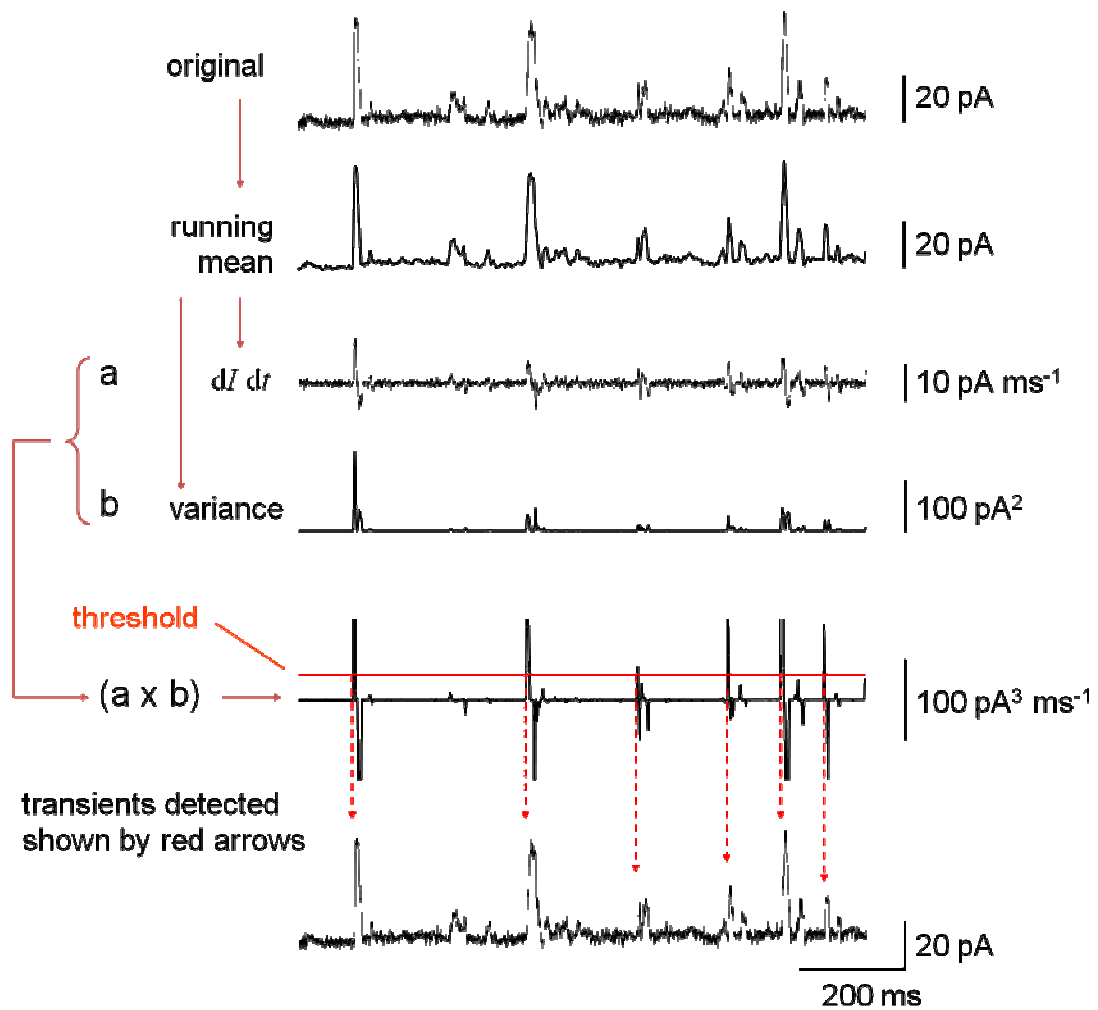


Figure 2.4 The method used by the in-house software programme to detect STOCs. See section 2.5.3 for description.

2.5.4 Statistical analyses

All data was expressed as mean \pm the standard error of the mean (SEM). As Gaussian distributions could be fitted to the data, it was possible for parametrical statistical tests to be carried out. It was assumed that all observations were independent. Statistical analyses were performed using one-way ANOVA, or paired or unpaired Student's *t* test as appropriate. Statistical significance was assumed where $P = <0.05$.

3 CHARACTERIZATION OF BK_{Ca} SINGLE CHANNEL PROPERTIES

3.1 Recording of single BK_{Ca} channels

Single BK_{Ca} channels were recorded in vascular smooth muscle cells isolated from rat mesenteric arteries. These experiments were performed in the presence of physiological K⁺ concentrations (140 mM [K⁺]_i/6 mM [K⁺]_o) rather than symmetrical K⁺ so that the results could be compared to recordings performed in the whole-cell patch configuration more easily. Single channel currents were recorded using the inside-out excised patch technique, as described in the previous chapter, enabling the [Ca²⁺]_i facing the cytoplasmic side of the membrane to be easily changed by switching the bath solution. The greatest number of channels seen in any one patch was 6, but more frequently 1-3 channels were observed.

The channel observed in these cells was Ca²⁺ and voltage dependent, and current-voltage data showed that the channel had a large unitary conductance of 189.4 ± 12.0 pS ($n = 5$). This value is consistent with those recorded previously for BK_{Ca} channels (Jackson & Blair, 1998; Mistry & Garland, 1998; Singer & Walsh, 1987; Zhou *et al*, 2005). Channel openings were usually observed at a single current level, but various subconductance could sometimes be seen (figure 3.1A). These subconductance levels appear to be at either one third or one half of the single channel current. Occasionally, a different channel could be seen in the patch (figure 3.1B). This channel appeared to be voltage-dependent, as it was present when the membrane potential of the cell was held at +40 mV but not at 0 mV. Changes in [Ca²⁺]_i did not appear to have any effect on the

activity of this channel and so it is possible that it was a type of voltage-dependent K^+ channel. This channel was rarely observed and so was not investigated any further.

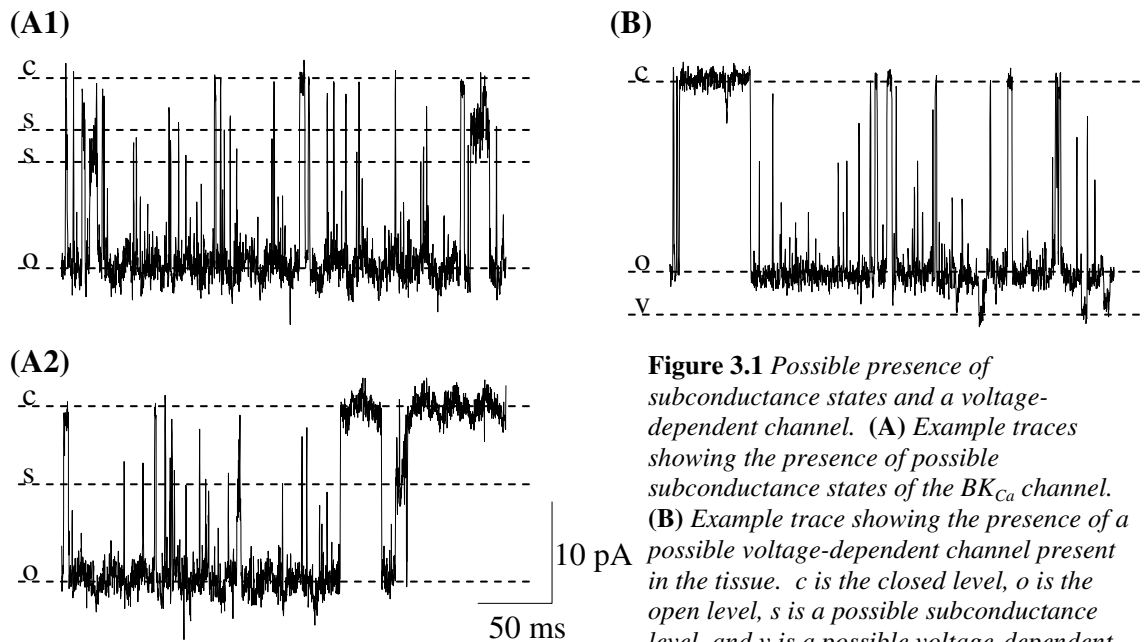


Figure 3.1 Possible presence of subconductance states and a voltage-dependent channel. (A) Example traces showing the presence of possible subconductance states of the BK_{Ca} channel. (B) Example trace showing the presence of a possible voltage-dependent channel present in the tissue. c is the closed level, o is the open level, s is a possible subconductance level, and v is a possible voltage-dependent channel. $[K^+]_i = 140$ mM. $[K^+]_o = 6$ mM.

3.2 Analysis of BK_{Ca} single channel activity

3.2.1 The effect of voltage on the activity of single BK_{Ca} channels

The effect of voltage on BK_{Ca} single channel properties was investigated. It could perhaps be said that this has been studied in enough detail in the past, however, I felt that it was important to determine how BK_{Ca} single channels in mesenteric arterial smooth muscle cells were modulated by voltage under the particular conditions that I used. One major difference between the experimental work that I carried out and much of that previously reported in the literature, is that the experiments described here were performed in near physiological K⁺ as opposed to the symmetrical K⁺ solutions often used. Various [Ca²⁺]_i (0, 1, 3, 10, 30, and 100 μM) were used across a range of voltages (-60 - +60 mV) and the results at each [Ca²⁺]_i were plotted as P_{open} against membrane potential (figure 3.2). P_{open} was calculated according to equation 1 (section 2.5.1). Each recording used to obtain P_{open} was of at least 45 s in length. The data obtained was fitted using the Boltzmann equation (equation 2; section 2.5.1). The information from this graph was then used to plot V_{1/2} against log [Ca²⁺]_i (figure 3.3). As was expected, the relationship between V_{1/2} and log [Ca²⁺]_i was linear within this range. This is in agreement with reports in the literature (Cui *et al*, 1997; Lin *et al*, 2003). The voltage shift for a ten-fold change in [Ca²⁺]_i was approximately 50 mV. This is slightly lower than that reported in ovine basilar artery, where a value of ~67 mV was stated (Lin *et al*, 2003).

For all [Ca²⁺]_i, an increase in depolarisation was accompanied by an increase in the P_{open} of the channel. This initial activation occurred at more negative potentials when a high [Ca²⁺]_i was present. As expected, depolarisation caused an increase in the current amplitude of the channel (figures 3.4 & 3.5).

The voltage at which half maximal activation of the channel occurs is known as $V_{1/2}$. When the Boltzmann equation has been fitted to the data, $V_{1/2}$ shifts to more hyperpolarised potentials as the $[Ca^{2+}]_i$ is increased. When a 10 μM Ca^{2+} solution faced the cytoplasmic side of the membrane, half-maximal activation of the channel was seen at -15.25 mV. As the $[Ca^{2+}]_i$ was increased, this value shifted to more negative potentials, whilst a decrease in $[Ca^{2+}]_i$ shifted $V_{1/2}$ to more positive potentials. This shift appears to be more pronounced at lower Ca^{2+} concentrations, as can be seen in the table in figure 3.2. This data shows that $V_{1/2}$ shifts by only a few millivolts when $[Ca^{2+}]_i$ is increased from 10 μM to 30 μM or from 30 μM to 100 μM . However, when $[Ca^{2+}]_i$ is decreased from 10 μM to 3 μM , there appears to be quite a large shift in $V_{1/2}$ from -15.25 mV to +40.26 mV. This suggests that this small increase in $[Ca^{2+}]_i$ could have a greater effect on the voltage-activation of the channel. However, the plot of $V_{1/2}$ against $\log [Ca^{2+}]_i$ suggests that the relationship between the two is actually linear, and there is not a larger shift between 3 μM and 10 μM . Previous studies have also reported a linear relationship between $V_{1/2}$ and $[Ca^{2+}]_i$ (Jackson & Blair, 1998; Lippiat *et al*, 2003).

Even with very high intracellular Ca^{2+} (100 μM) at very high membrane potentials (+40 mV), P_{open} does not quite reach unity. In the case of 30 μM and 100 μM , P_{open} approaches very close to 1, with the channel only closing very briefly throughout. It is interesting to note that the open probability of the channel in the presence of lower intracellular Ca^{2+} does not quite achieve these high levels; there appears to be a slight decrease in the maximal P_{open} achieved as Ca^{2+} concentration decreases. Even at the very depolarised potential of +80 mV, the P_{open} of the channel in the presence of 3 μM $[Ca^{2+}]_i$ is noticeably lower than that of 100 μM at much more hyperpolarised potentials. There is a further decrease in maximum P_{open} as the $[Ca^{2+}]_i$ is lowered to 1 μM , but this

may be because 1 μM Ca^{2+} could not be tested at high enough potentials for its true maximum to be reached.

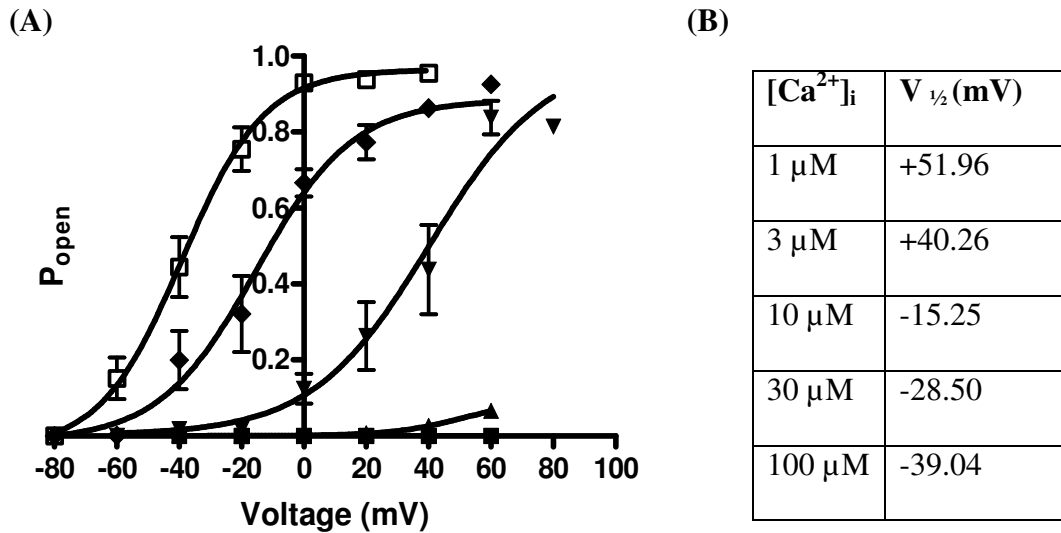


Figure 3.2 Fitting of Boltzmann equation to show the effect of membrane potential on BK_{Ca} single channel activity. (A) Graph showing a Boltzmann fit of P_{open} against voltage for a range of $[\text{Ca}^{2+}]_i$. $\square = 100 \mu\text{M}$, $\blacklozenge = 10 \mu\text{M}$, $\blacktriangledown = 3 \mu\text{M}$, and $\blacktriangle = 1 \mu\text{M}$, and $\blacksquare = 0 \mu\text{M}$ $[\text{Ca}^{2+}]_i$. The data for 30 μM $[\text{Ca}^{2+}]_i$ was removed for clarity. (B) Table showing $V_{1/2}$ values for each $[\text{Ca}^{2+}]_i$ as calculated from the Boltzmann curves.

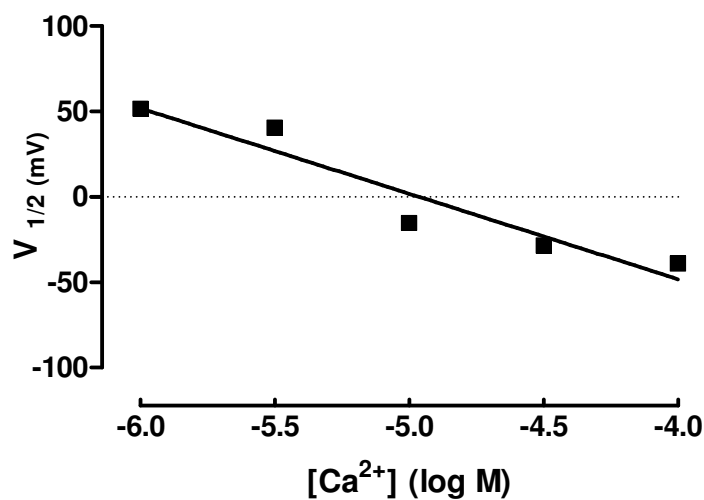


Figure 3.3 Plot of $V_{1/2}$ against $[\text{Ca}^{2+}]_i$. Graph showing a plot of $V_{1/2}$ against $[\text{Ca}^{2+}]_i$ as determined from the data fitted in figure 3.2.

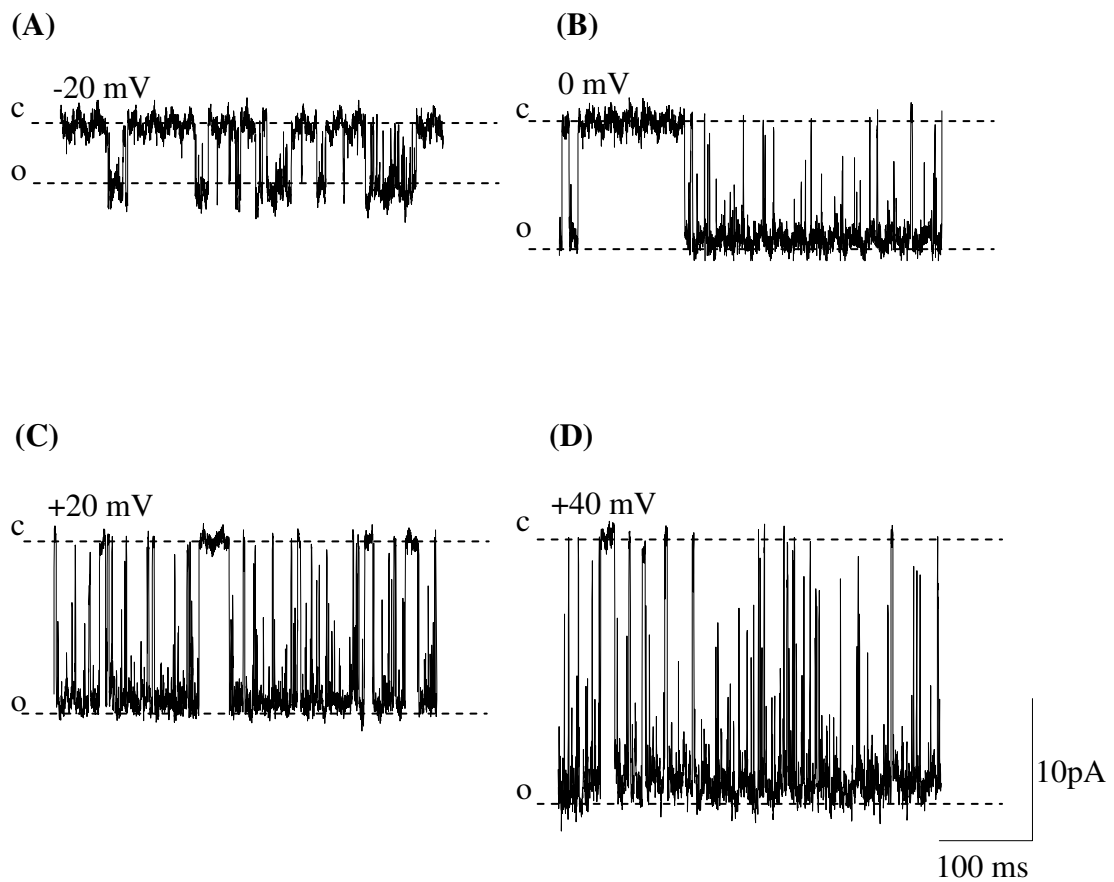


Figure 3.4 Effect of membrane potential on BK_{Ca} single channel activity. Example traces showing BK_{Ca} single channel activity at (A) -20 mV ($P_{open} = 0.23$), (B) 0 mV ($P_{open} = 0.65$), (C) $+20$ mV ($P_{open} = 0.76$), and (D) $+40$ mV ($P_{open} = 0.86$). The open (o) and closed (c) states of the channel are indicated. Recordings were made in the presence of $10 \mu\text{M}$ $[\text{Ca}^{2+}]_i$, $[\text{K}^+]_i = 140$ mM, $[\text{K}^+]_o = 6$ mM.

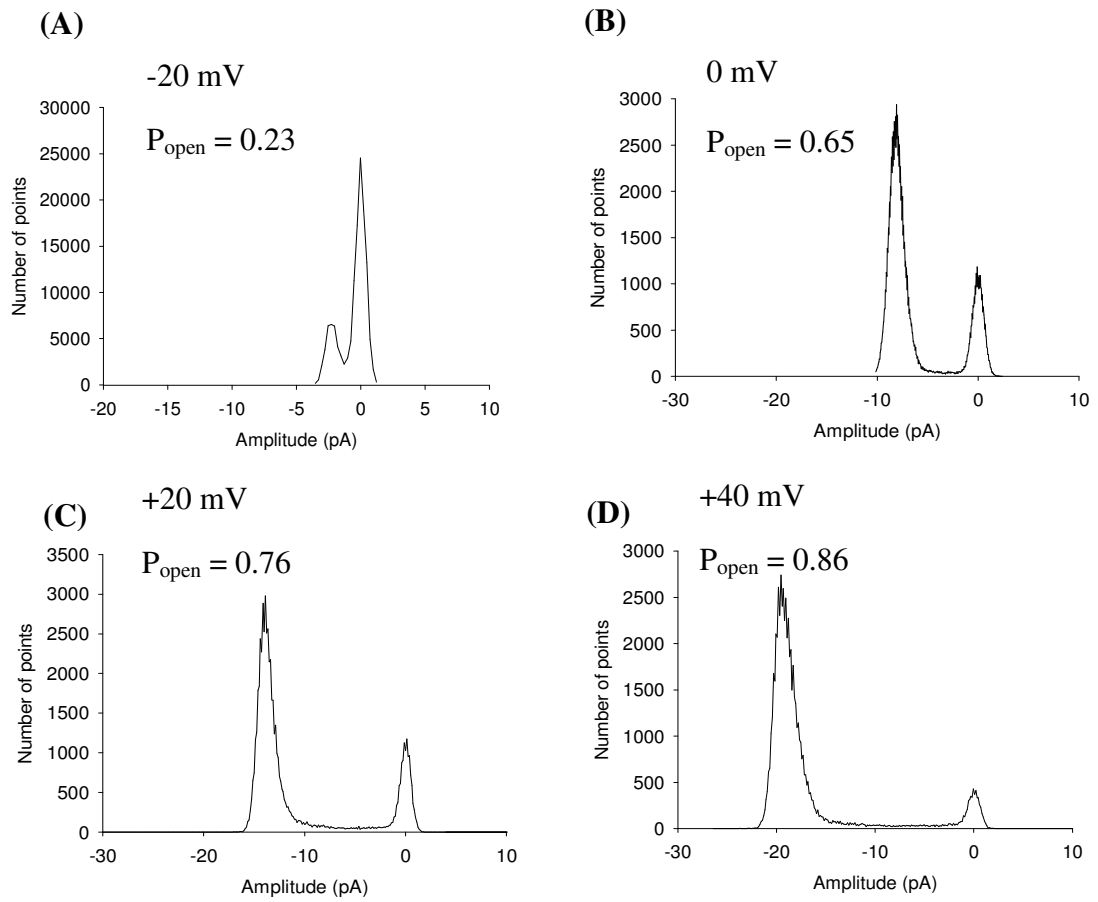


Figure 3.5 Effect of membrane potential on BK_{Ca} single channel amplitude. Histograms showing BK_{Ca} single channel amplitude at (A) -20 mV, (B) 0 mV, (C) +20 mV, and (D) +40 mV. Recordings were made in the presence of $10 \mu\text{M}$ $[\text{Ca}^{2+}]_i$, $[\text{K}^+]_i = 140 \text{ mM}$, $[\text{K}^+]_o = 6 \text{ mM}$.

3.2.2 The effect of $[Ca^{2+}]_i$ on the activity of single BK_{Ca} channels

The effect of $[Ca^{2+}]_i$ on BK_{Ca} single channel was investigated using a variety of $[Ca^{2+}]_i$ (0, 1, 3, 10, 30, and 100 μM) over a range of membrane potentials. Again, I felt that it was important to perform these experiments under my own particular conditions, for the reasons described in section 3.2.1, rather than to rely on solely on what had previously been reported in the literature. This data was plotted as a concentration-response curve so that the dissociation constant for Ca^{2+} (K_d) could be determined at each membrane potential (figure 3.6A). Depolarization of the cell membrane led to a decrease in the K_d for Ca^{2+} suggesting that lower $[Ca^{2+}]_i$ was required to half-maximally activate the channel at more depolarized membrane potentials (figure 3.6B). Increasing the $[Ca^{2+}]_i$ across this range of Ca^{2+} concentrations led to an increase in the activity of the channel but had no effect on single channel amplitude (figures 3.7 & 3.8).

The Hill equation can be used to estimate the number of Ca^{2+} ions bound to the BK_{Ca} channel. The open probability, P_{open} , as a function of $[Ca^{2+}]_i$ was fitted to this equation:

$$P_{open} = \frac{[Ca^{2+}]_i^H}{(K_d^H + [Ca^{2+}]_i^H)} \quad \text{(Equation 3)}$$

where H is the Hill coefficient and K_d is the dissociation constant.

P_{open} was normalised and then $\log [P_{open}/(1-P_{open})]$ was plotted against $[Ca^{2+}]_i$ (log M). The data point for 100 μM had to be omitted due to this normalisation of the data. This graph was then used to estimate the Hill coefficient by fitting a straight line to the slope of the log-log plot. A straight line should fit the Hill plot adequately, however, it is probable that more data points would give a better fit of this data. The Hill plot of the data can be seen in figure 3.9 and the slope of this graph gives a Hill coefficient of 3.2.

This number suggests co-operative binding of four Ca^{2+} ions in order to maximally activate the channel. Hill coefficients of two to five are typically observed in muscle (Barrett *et al*, 1982; Golowasch *et al*, 1986; McManus & Magleby, 1991; Jahromi *et al*, 2008), including values of 2.9 and 3.2 in ovine basilar artery and canine colonic circular muscle respectively (Lin *et al*, 2003; Carl *et al*, 1996). It is thought that the Hill coefficient calculated in this way is usually an underestimation of the co-operativity shown by Ca^{2+} , and so it is quite possible that four Ca^{2+} ions bind to the BK_{Ca} channel. As four alpha subunits come together to form what is thought to be a homotetramer, this could theoretically mean that one Ca^{2+} ion binds to each α -subunit of the BK_{Ca} channel. However, it is important to note that there is more than one Ca^{2+} binding site per α -subunit, and that the Hill coefficient only gives an idea of the minimum number of Ca^{2+} ions that are required to maximally activate the channel.

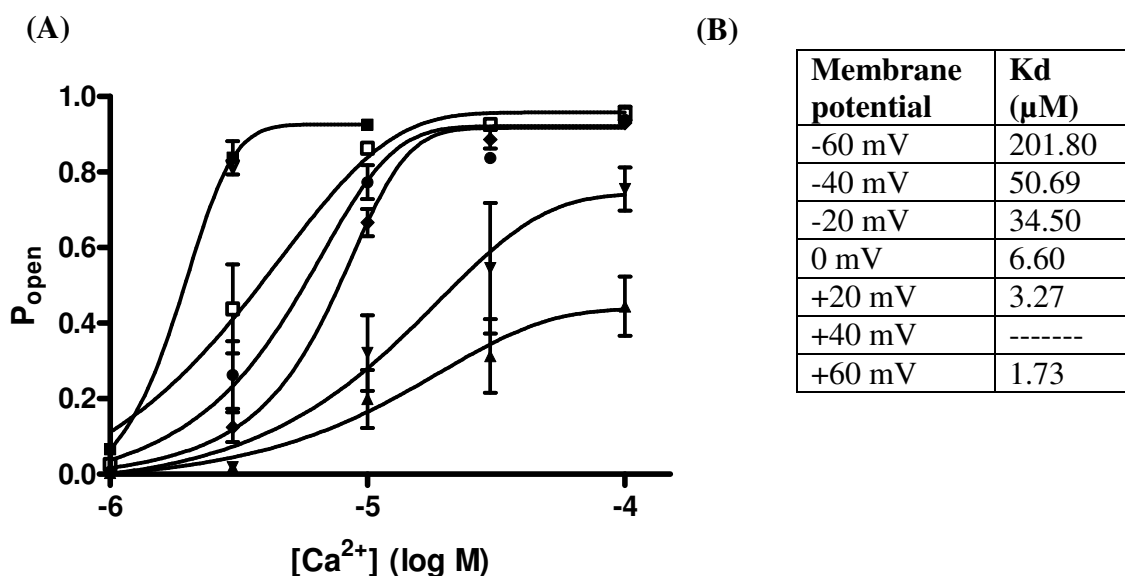


Figure 3.6 Concentration-response curve to show the effect of $[\text{Ca}^{2+}]_i$ on BK_{Ca} single channel activity. (A) Graph showing concentration-response curves for BK_{Ca} channels over a range of membrane potentials. ■ = +60 mV, □ = +40 mV, ● = +20 mV, ◆ = 0 mV, ▼ = -20 mV, and ▲ = -40 mV. (B) Table showing K_d values for Ca^{2+} at each membrane potential as calculated from the concentration-response curves.

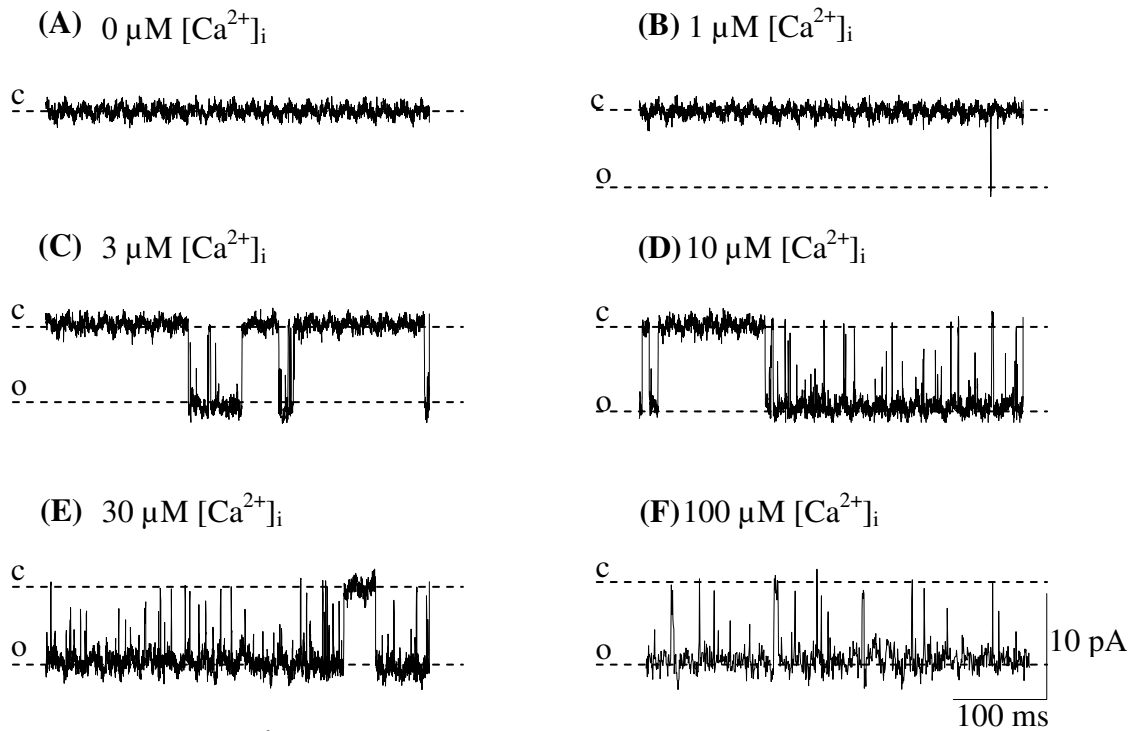


Figure 3.7 Effect of $[Ca^{2+}]_i$ on BK_{Ca} single channel activity. Example traces showing BK_{Ca} single channel activity in the presence of (A) $0 \mu M$ ($P_{open} = 0$), (B) $1 \mu M$ ($P_{open} = 0.001$), (C) $3 \mu M$ ($P_{open} = 0.16$), (D) $10 \mu M$ ($P_{open} = 0.65$), (E) $30 \mu M$ ($P_{open} = 0.87$), and (F) $100 \mu M$ $[Ca^{2+}]_i$ ($P_{open} = 0.92$). The open (o) and closed (c) states of the channel are indicated. Recordings were made at a membrane potential of 0 mV . $[K^+]_i = 140 \text{ mM}$. $[K^+]_o = 6 \text{ mM}$.

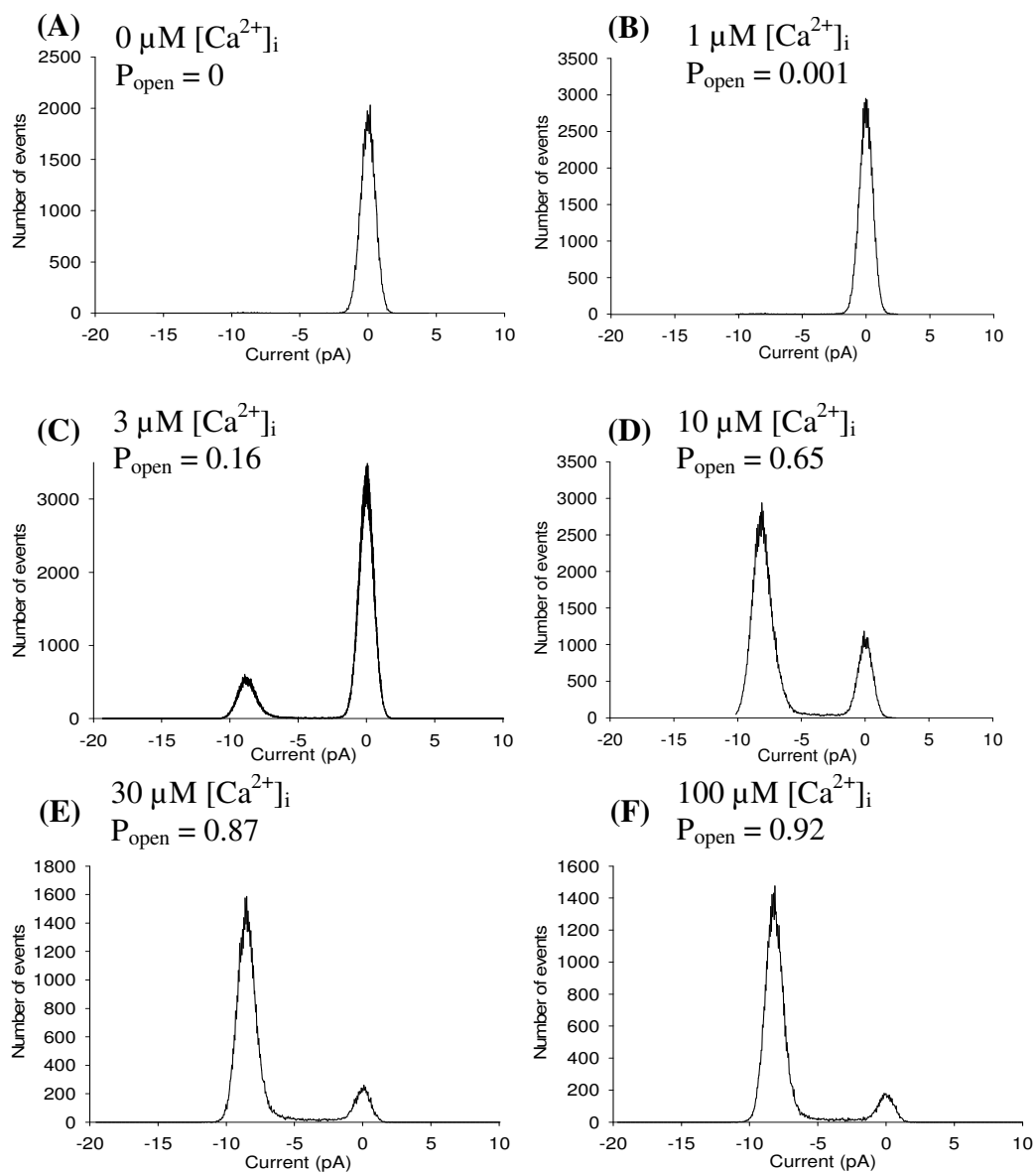


Figure 3.8 Effect of $[\text{Ca}^{2+}]_i$ on BK_{Ca} single channel activity. Histograms showing BK_{Ca} single channel amplitude in the presence of (A) $0 \mu\text{M}$, (B) $1 \mu\text{M}$, (C) $3 \mu\text{M}$, (D) $10 \mu\text{M}$, (E) $30 \mu\text{M}$, and (F) $100 \mu\text{M}$ $[\text{Ca}^{2+}]_i$. Recordings were made at a membrane potential of 0 mV . $[\text{K}^+]_i = 140 \text{ mM}$. $[\text{K}^+]_o = 6 \text{ mM}$.

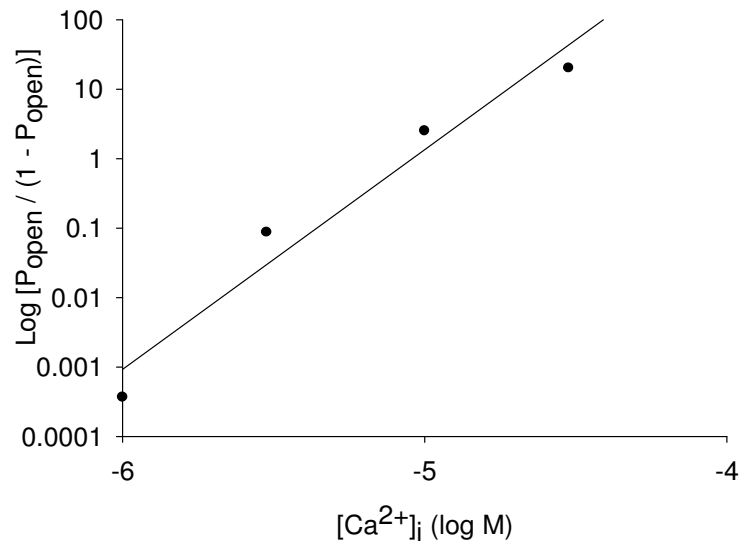


Figure 3.9 Hill plot showing the relationship between $[Ca^{2+}]_i$ and the P_{open} of the channel. A straight line was fitted to the data with a gradient of 3.2.

3.3 Analysis of BK_{Ca} channel kinetics

The study of ion channel kinetics is important as it provides a means with which to study the effect that a particular manipulation has on channel gating. The effect that a particular compound has on open and closed times can often give an indication of the type of ion channel block that that compound has. The kinetics of single BK_{Ca} channels were investigated in patches that contained only one active channel. Dwell times were measured using the 50% threshold method described previously and the effect of changes in Ca²⁺ and voltage were studied. Data was acquired at 10 kHz with 2 kHz filtering. The minimum duration of an event that would just reach 50% at this filter setting was 90 μs, while the duration of an event that at the 50% level would be equal to its true duration was 120 μs. Any event of less than 120 μs would therefore be too brief for its correct or “true” duration to be accurately measured. A minimum resolution of 100 μs was imposed during the analysis of single channel dwell times. Although this did not limit events to those with a true duration only at 50%, it did remove most of the events that were much briefer than their true duration. Two open states and three closed states accurately described channel behaviour whether or not these brief channel events were included in the fitting of data.

3.3.1 The effect of voltage on BK_{Ca} channel kinetics

The effect of voltage on channel kinetics was investigated as for P_{open} above. Channel kinetics were analysed in the presence of 10 μM Ca²⁺ across the same range of voltages, however, channel kinetics could only be analysed at membrane potentials of -40 mV and above due to the difficulty in resolving channel events below this level. At this membrane potential, the single channel current was equal to approximately 2.4 pA. It is

possible that increasing the signal:noise ratio by spending more time grounding the equipment would enable currents of this size to be resolved more precisely. As membrane potential was increased, the duration of the slowest open state increased whilst the duration of the slowest closed state was dramatically decreased (figures 3.10 & 3.11; 0 mV is shown in both figures for clear comparison).

3.3.2 The effect of $[Ca^{2+}]_i$ on BK_{Ca} channel kinetics

The effect of free $[Ca^{2+}]_i$ on single channel kinetics was investigated in the same manner as for τ_{open} above. The cell was held at a constant voltage of 0 mV whilst the $[Ca^{2+}]_i$ was increased. Only channel kinetics in the presence of 3 μ M Ca^{2+} or above could be analysed due to the lack of channel activity below this concentration. As was the case for membrane potential, increases in $[Ca^{2+}]_i$ were accompanied by an increase in the duration of the open state and a marked decrease in the duration of the second component of the closed state (figure 3.12).

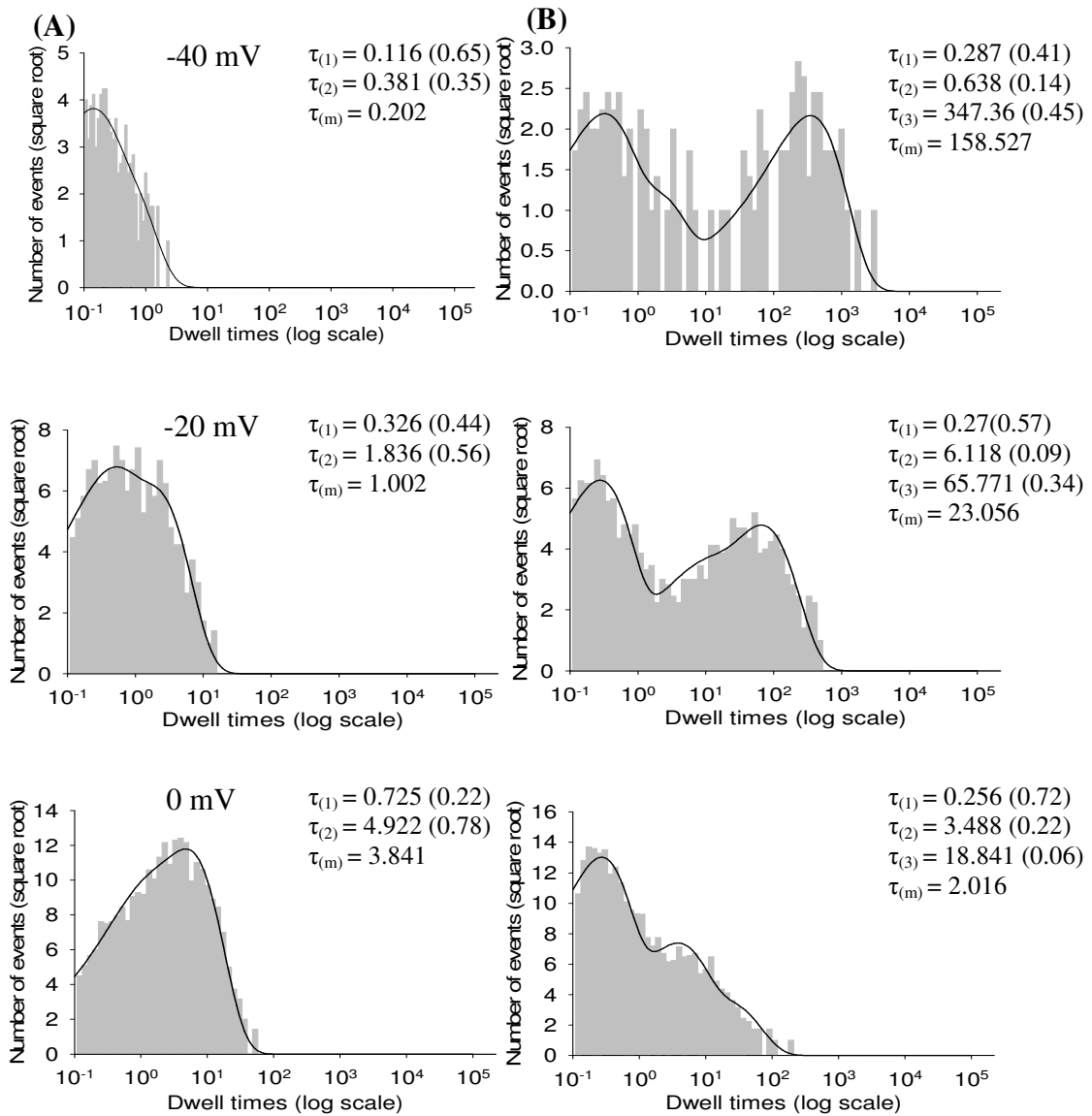


Figure 3.10 Effect of membrane potential on BK_{Ca} channel kinetics. **(A)** Open time constants and **(B)** Closed time constants. The time constants (in ms) for each are numbered with 1 being the fastest and 2 to 3 being the slowest. The proportion of the plot that that component makes up is in brackets. $\tau_{(m)}$ is the mean time constant for closed components and the corrected mean time constant for open components. Recordings were made in the presence of $10 \mu M [Ca^{2+}]_i$, $[K^+]_i = 140 \text{ mM}$, $[K^+]_o = 6 \text{ mM}$.

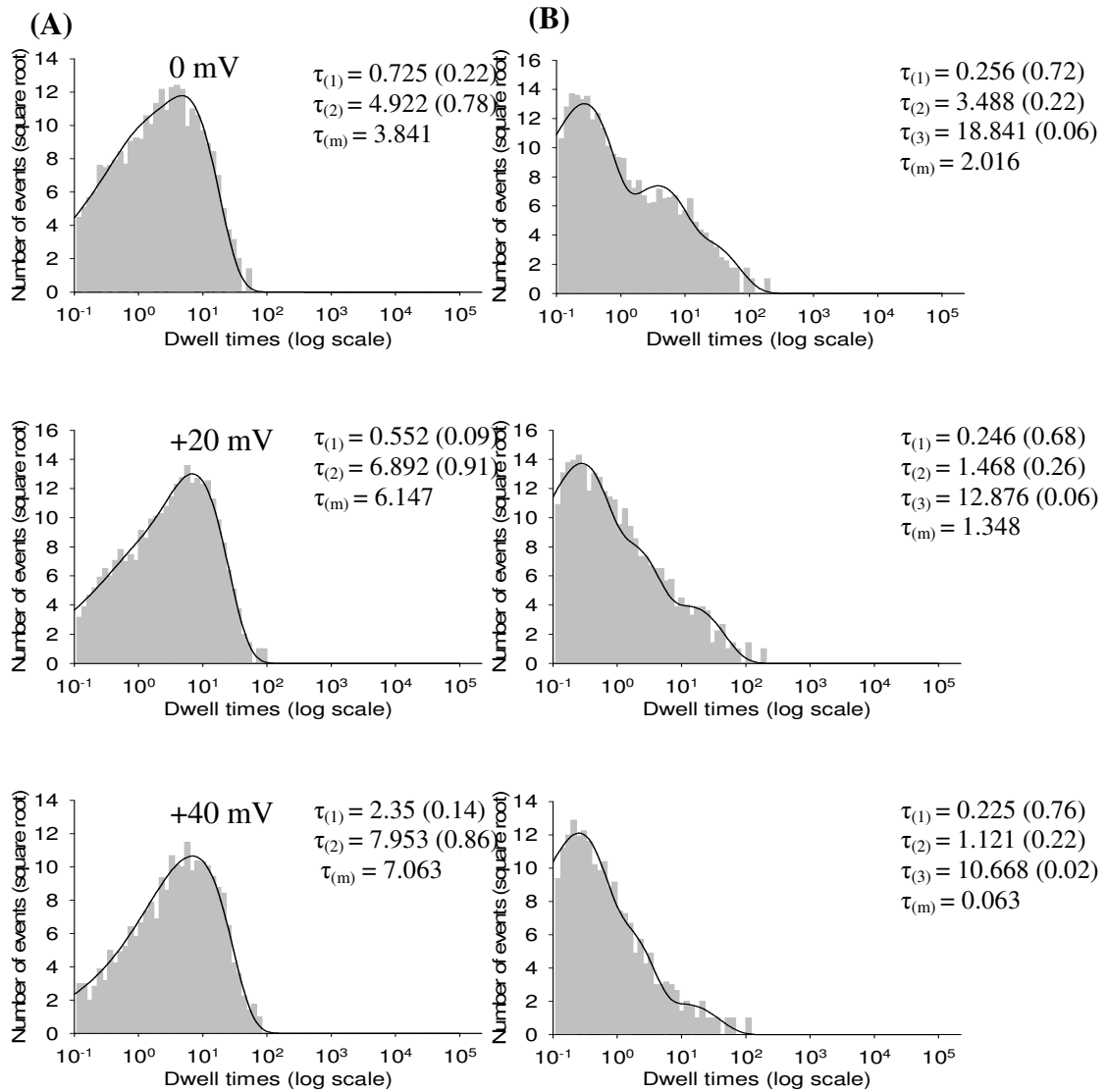


Figure 3.11 Effect of membrane potential on BK_{Ca} channel kinetics. **(A)** Open time constants and **(B)** Closed time constants. The time constants (in ms) for each are numbered with 1 being the fastest and 2 to 3 being the slowest. The proportion of the plot that that component makes up is in brackets. $\tau_{(m)}$ is the mean time constant for closed components and the corrected mean time constant for open components. Recordings were made in the presence of $10 \mu M [Ca^{2+}]_i$, $[K^+]_i = 140 \text{ mM}$, $[K^+]_o = 6 \text{ mM}$.

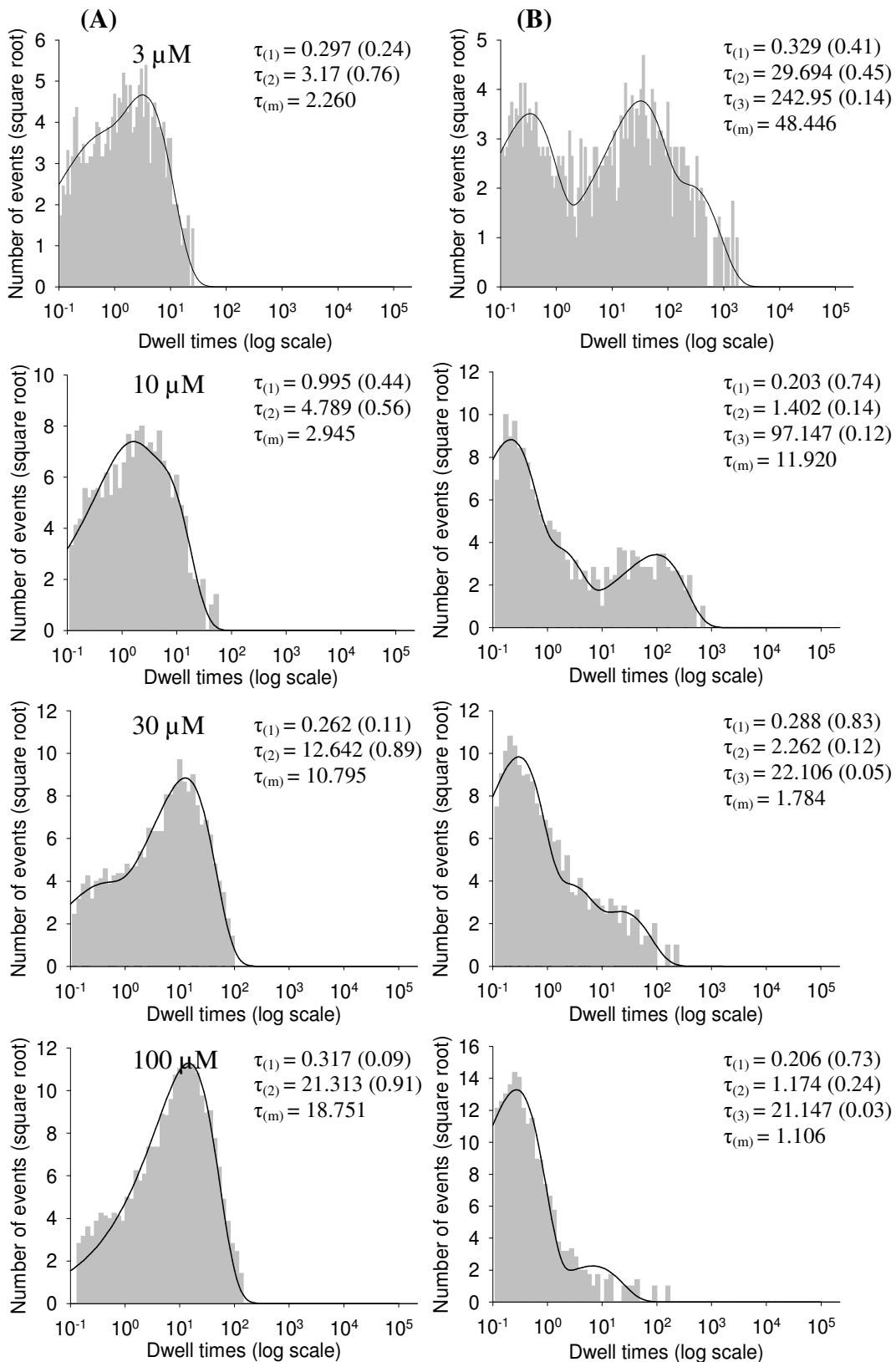


Figure 3.12 Effect of $[\text{Ca}^{2+}]_i$ on BK_{Ca} channel kinetics. **(A)** Open time constants and **(B)** Closed time constants. The time constants (in ms) for each are numbered with 1 being the fastest and 2 to 3 being the slowest. The proportion of the plot made up by that component is in brackets. $\tau_{(m)}$ is the mean time constant for closed components and the corrected mean time constant for open components. Recordings were made at a membrane potential of 0 mV. $[\text{K}^+]_i = 140$ mM. $[\text{K}^+]_o = 6$ mM.

3.4 Modulation of BK_{Ca} channels by 1,2 dioctanoyl-*sn*-glycerol

3.4.1 The effect of 1, 2-dioctanoyl-*sn*-glycerol on the activity of single BK_{Ca} channels

Next I looked at the effects of DOG on BK_{Ca} single channel activity. DOG is an active analogue of DAG and so is often used as a PKC activator. However, it has been reported that DOG may actually affect some ion channels directly (He et al, 2000; Rainbow et al, 2005), and so the effects of DOG on single channel BK_{Ca} currents in inside-out excised patches were investigated to see whether this might also be the case with BK_{Ca} channels. The minimum concentration of DOG required to activate PKC has not been reported, however, most groups report using micromolar concentrations of DOG when studying its effects.. The effects of two different concentrations of DOG, 1 μ M & 10 μ M, were investigated at a membrane potential of 0 mV.

10 μ M DOG starts to have an effect on the channel within 60 seconds of the compound reaching the bath. This is revealed by a $37.7 \pm 12.7\%$ decrease in the P_{open} of the channel, from 0.61 ± 0.07 to 0.36 ± 0.08 ($n = 5$; $P = < 0.05$, Student paired t test), 30-75 seconds after the compound reaches the patch. This inhibitory effect then increases with time until the channel is almost completely blocked after 5 min. P_{open} is seen to be drastically reduced by $83.1 \pm 0.5\%$ of control, from 0.61 ± 0.07 to 0.11 ± 0.04 after this time ($P = < 0.01$, Student's paired t test; figure 3.13A). The effect of 1 μ M DOG on the BK_{Ca} channel is much less pronounced. There appears to be a small decrease in P_{open} of $6.9 \pm 0.1\%$ at this first time-point from 0.77 ± 0.06 to 0.72 ± 0.06 ($n = 4$; $P = > 0.05$, Student's paired t test). After 300 seconds application there was a $34.1 \pm 1.5\%$ decrease in the P_{open} of the channel from 0.77 ± 0.06 to 0.51 ± 0.07 ($P = < 0.05$, Student's paired t

test ; figure 3.13B). Neither 1 μM nor 10 μM DOG had a significant effect on the current amplitude of the channel (figure 3.14). The effect of DOG on the Popen of single BKCa channels was stable at 5 minutes and was not seen to fall any further after this point. An appropriate experiment for the future would be to use an inactive analogue of DAG to show that this has no effect on BK_{Ca} single channel activity.

3.4.2 The effect of 1,2-dioctanoyl-sn-glycerol on BK_{Ca} channel kinetics

10 μM DOG decreases the slowest time constant of the open state with time whilst causing the slow time constant to increase markedly. After 300 seconds application, an additional closed state was required to accurately describe channel behaviour (figure 3.15). This is consistent with the effects of a channel blocker. Again, the effect of 1 μM DOG is less obvious. There is little difference in the slowest open time constant within the first 30 seconds of application, although an increase in the slowest closed time constant can be seen. After 300 seconds there is a more obvious decrease in the second open time constant and a further decrease in the slowest closed time constant (figure 3.16).

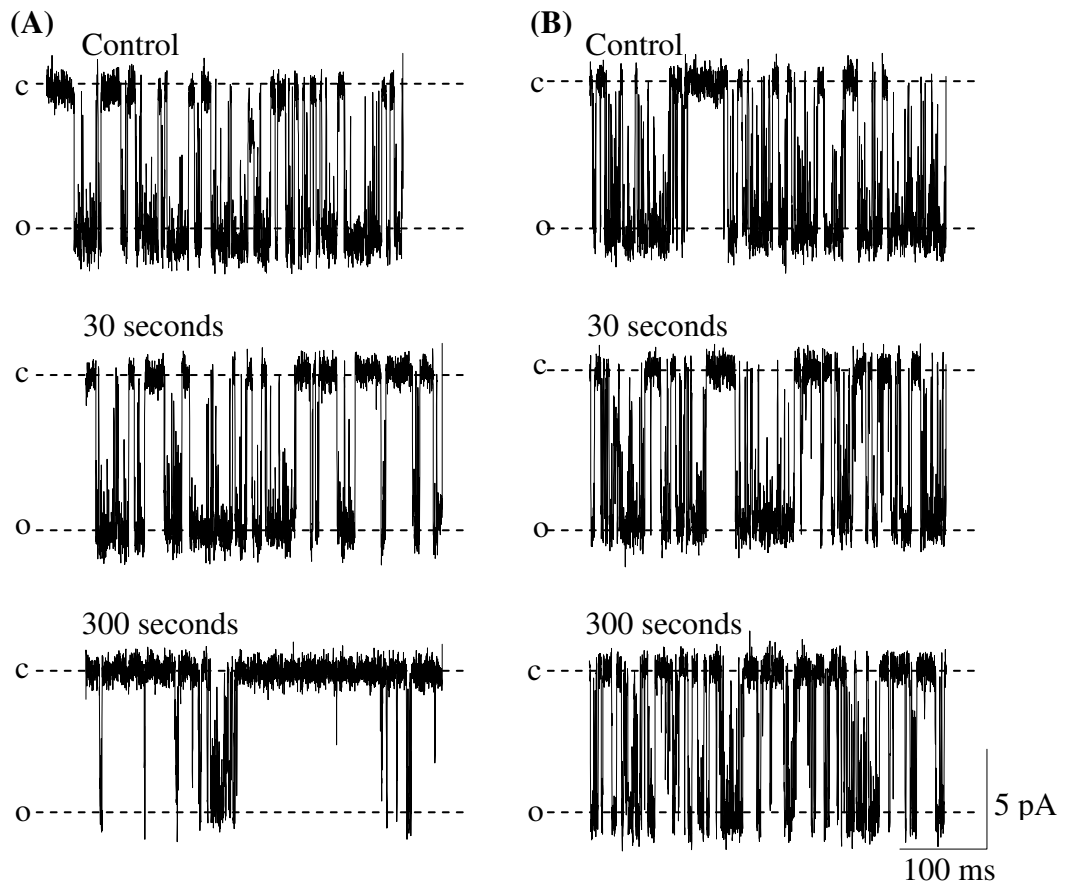


Figure 3.13 Effect of DOG on BK_{Ca} single channel activity. Example traces showing the effect of (A) $10 \mu\text{M}$ DOG and (B) $1 \mu\text{M}$ DOG on BK_{Ca} single channel activity. The time shown indicates how long the patch was in the presence of the compound, and does not include the length of time taken for the compound to reach the bath. The open (o) and closed (c) states of the channel are indicated. Recordings were made at a membrane potential of 0 mV in the presence of $10 \mu\text{M}$ $[\text{Ca}^{2+}]_i$. $[\text{K}^+]_i = 140 \text{ mM}$. $[\text{K}^+]_o = 6 \text{ mM}$.

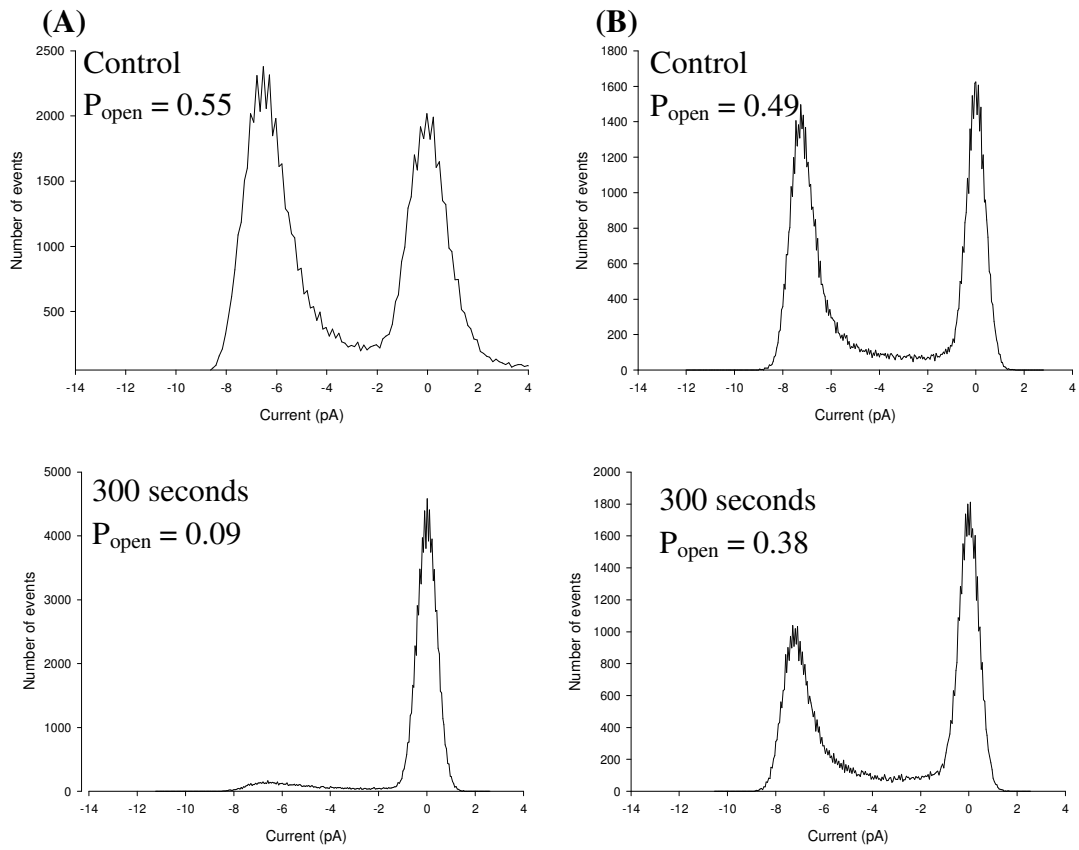


Figure 3.14 Effect of DOG on BK_{Ca} single channel amplitude. Amplitude histograms showing the effect of (A) $10 \mu M$ DOG, and (B) $1 \mu M$ DOG, on BK_{Ca} single channel amplitude. Recordings were made at a membrane potential of $0 mV$ in the presence of $10 \mu M [Ca^{2+}]_i$. $[K^+]_i = 140 mM$. $[K^+]_o = 6 mM$.

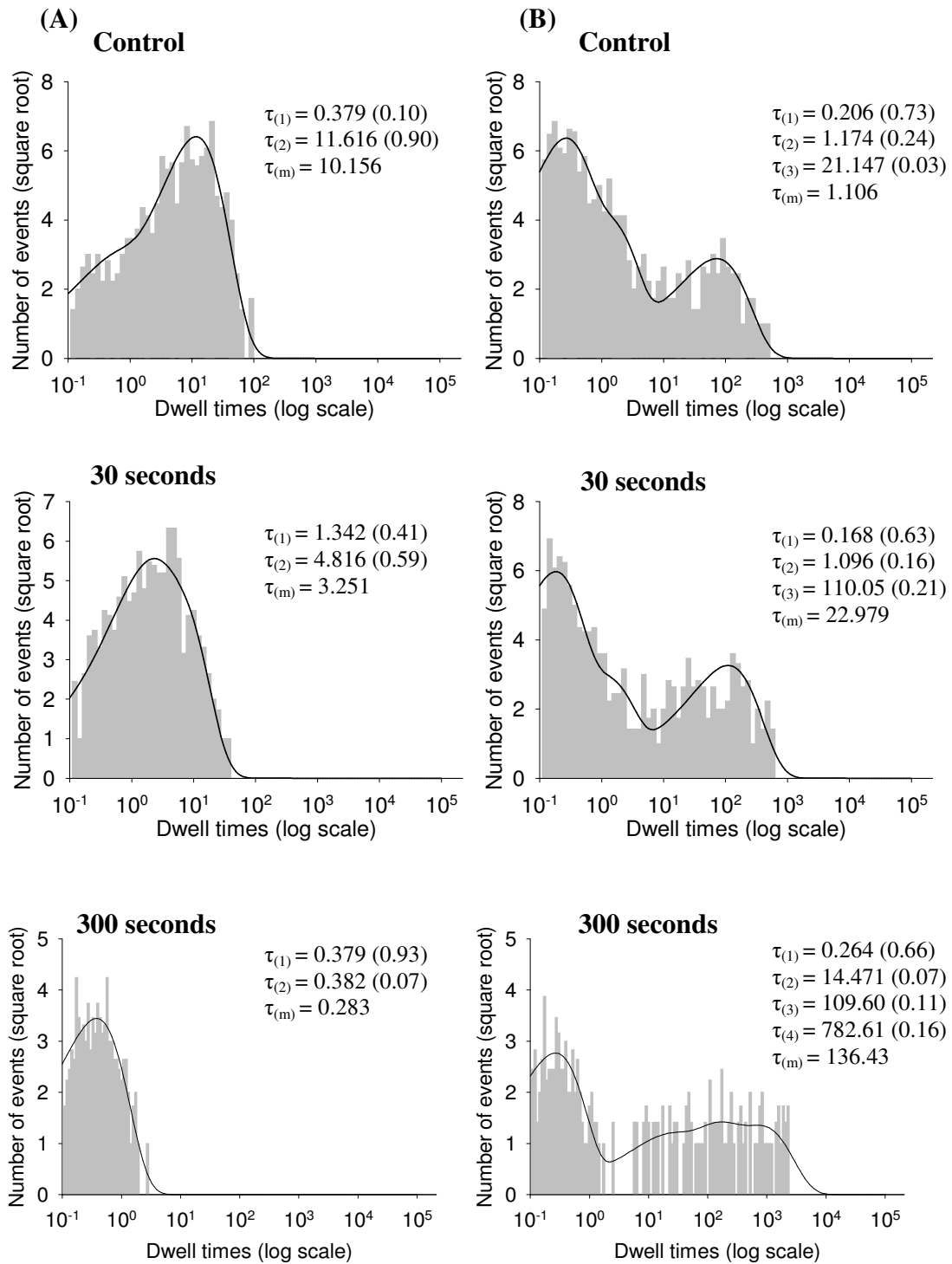


Figure 3.15 Effect of the application of $10 \mu\text{M}$ DOG on the kinetics of the BK_{Ca} channel. **(A)** Open time constants and **(B)** Closed time constants. The time constants (in ms) for each are numbered with 1 being the fastest and 2 to 3 being the slowest. The proportion of the plot that that component makes up is in brackets. $\tau_{(m)}$ is the mean time constant for closed components and the corrected mean time constant for open components. Recordings were made at a membrane potential of 0 mV in the presence of $10 \mu\text{M}$ $[\text{Ca}^{2+}]_i$, $[\text{K}^+]_i = 140 \text{ mM}$, $[\text{K}^+]_o = 6 \text{ mM}$.

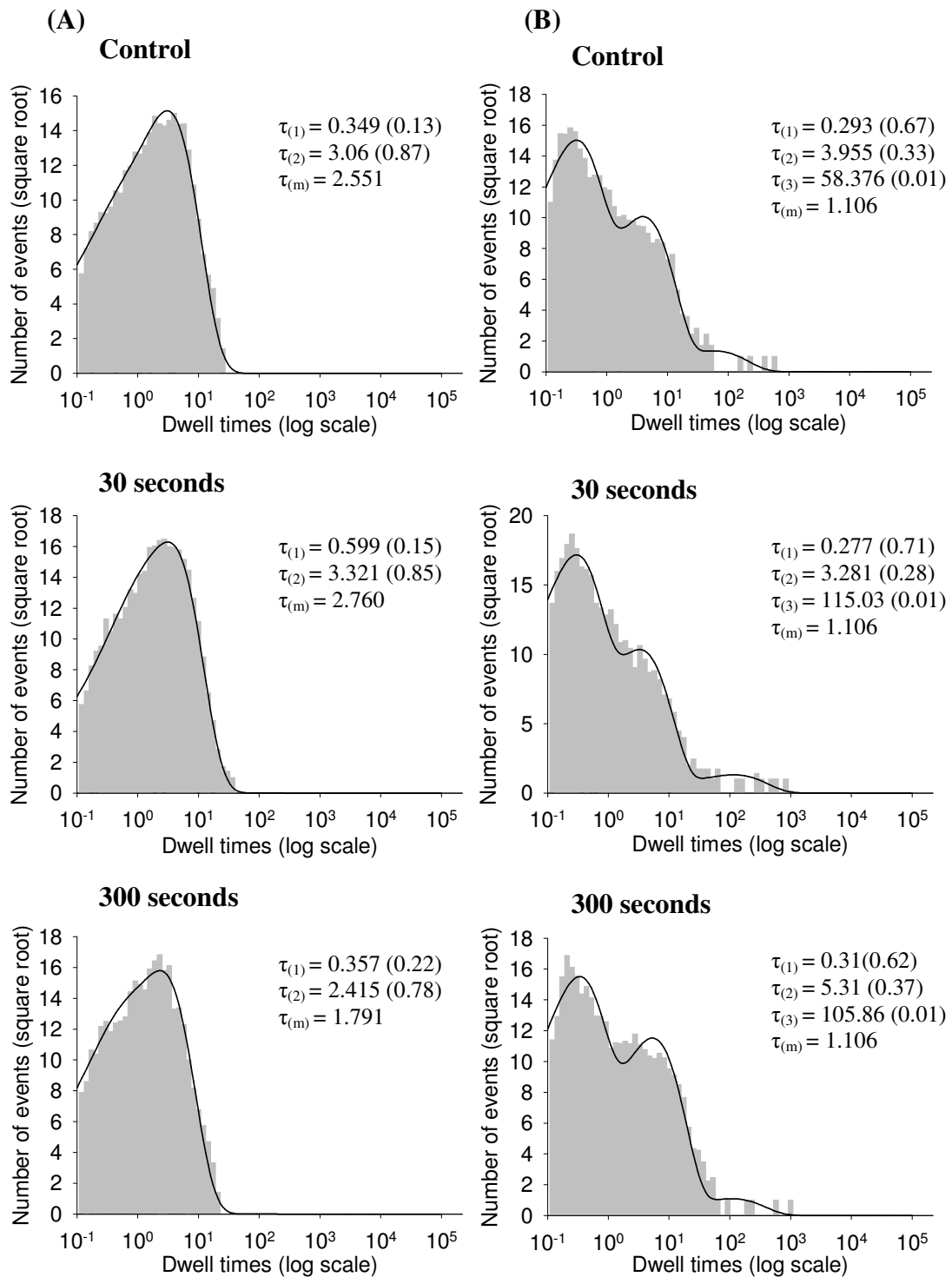


Figure 3.16 Effect of the application of $1 \mu\text{M}$ DOG on the kinetics of the BK_{Ca} channel. **(A)** Open time constants and **(B)** Closed time constants. The time constants (in ms) for each are numbered with 1 being the fastest and 2 to 3 being the slowest. The proportion of the plot that that component makes up is in brackets. $\tau_{(m)}$ is the mean time constant for closed components and the corrected mean time constant for open components. Recordings were made at a membrane potential of 0 mV in the presence of $10 \mu\text{M}$ $[\text{Ca}^{2+}]_i$, $[\text{K}^+]_i = 140 \text{ mM}$, $[\text{K}^+]_o = 6 \text{ mM}$.

3.5 Discussion

3.5.1 Recording BK_{Ca} single channel currents

BK_{Ca} single channel events were observed in rat mesenteric artery smooth muscle cells. These channels could be identified by their dependence on both $[Ca^{2+}]_i$ and membrane potential, and also by their large single channel conductance of 189.4 ± 12.0 pS, calculated as the slope conductance at 0 mV. Subconductance states of the channel were present but were rarely observed and did not affect the analysis of BK_{Ca} channel activity. The existence of subconductance states of the channel has been reported previously (Mistry & Garland, 1998; Nimigean & Magleby, 1999). It is thought that association of the β -subunit with the α -subunit may inhibit entry into subconductance states. This was shown by Nimigean and Magleby (Nimigean & Magleby, 1999) who transfected HEK 293 cells with either the α -subunit alone, or both α - and β -subunits. A comparison of the total time spent in various conductance states in the presence and absence of the β -subunit revealed that co-expression of both α - and β -subunits almost abolished entry into the subconductance state. This may explain why I rarely observed BK_{Ca} channel subconductance states.

3.5.2 The effect of Ca²⁺ and voltage on BK_{Ca} single channel activity

Depolarization increased the activity of BK_{Ca} channels at all $[Ca^{2+}]_i$. Increasing the $[Ca^{2+}]_i$ caused the channel to activate at more hyperpolarized membrane potentials, which was confirmed by a negative shift in the $V_{1/2}$ values obtained on fitting a Boltzmann equation (equation 2; section 2.5.1) to the data. The possible large shift in $V_{1/2}$ value between 3 μ M and 10 μ M $[Ca^{2+}]_i$ is interesting as estimates of local $[Ca^{2+}]$ during Ca²⁺ sparks are thought to be of this range (Zhuge *et al*, 2002). However,

plotting $V_{1/2}$ against $\log [Ca^{2+}]_i$ gave a fairly linear graph, and this is more in agreement with other reports in the literature (Jackson & Blair, 1998; Lippiat *et al*, 2003). Maximal P_{open} of the BK_{Ca} channel in the presence of $1 \mu M [Ca^{2+}]_i$ was not observed as membrane potentials of $+80$ mV or above generally made the patches very unstable. The $V_{1/2}$ obtained for this $[Ca^{2+}]_i$ is therefore unlikely to be accurate.

Concentration-response curves for $[Ca^{2+}]_i$ at different membrane potentials showed that depolarization of the cell membrane led to a decrease in the K_d for Ca^{2+} . This suggests that lower $[Ca^{2+}]_i$ was required to half-maximally activate the channel at more depolarized membrane potentials. Data showing the effect of $[Ca^{2+}]_i$ at 0 mV was plotted and the Hill equation was fitted to this in order to estimate the number of Ca^{2+} ions that bound to the BK_{Ca} channel. This membrane potential was chosen as it lay on the slopes of the fitted Boltzmann curves and increasing $[Ca^{2+}]_i$ had quite a large effect at this potential as no plateaus had been reached at any $[Ca^{2+}]_i$. The Hill coefficient of 3.2 suggests co-operative binding of four Ca^{2+} ions in order to maximally activate the channel. As mentioned previously, this could mean that one Ca^{2+} binds to each α -subunit of the BK_{Ca} channel. Hill coefficients ranging from two to five are typically observed for BK_{Ca} channels in a wide range of different muscle preparations indicating highly cooperative activation (Barrett *et al*, 1982; Golowasch *et al*, 1986; McManus & Magleby, 1991; Jahromi *et al*, 2008). Niu and Magleby (Niu & Magleby, 2002) demonstrated that cooperativity in BK_{Ca} channel activation relied largely on the functionality of the Ca^{2+} -bowl region, shown by a gradual increase in the Hill coefficient and a gradual decrease in the $[Ca^{2+}]_i$ required for half-maximal activation, as the number of functional Ca^{2+} -bowls was increased from 0 to 4 . The BK_{Ca} channel could open regardless of whether 0 , 1 , 2 , 3 or 4 Ca^{2+} -bowls were functional, however,

an increase in $[Ca^{2+}]_i$ was required for channel activation as the number of functional Ca^{2+} -bowls was decreased due to a reduction in Ca^{2+} sensitivity.

3.5.3 The effect of Ca^{2+} and voltage on BK_{Ca} single channel kinetics

Analysis of BK_{Ca} channel kinetics was limited to patches that contained only a single active BK_{Ca} channel. Channel activity could be accurately described by two open states and three closed states. This is in agreement with previous studies on BK_{Ca} channels from canine colon smooth muscle cells, the NT2-N neuronal cell line, and the cholinergic presynaptic nerve terminal (Kapicka *et al*, 1994; Chapman *et al*, 2007; Sun *et al*, 1999). However studies performed by Magleby and colleagues suggest that the channel may actually have as many as 3-4 open states and 4-8 closed states (McManus & Magleby 1988; Rothberg & Magleby 2000; Moss & Magleby 2001). It may be that recording for greater lengths of time would allow more of these states to be identified. Changes in both $[Ca^{2+}]_i$ and membrane potential were found to have an effect on BK_{Ca} channel gating, with increases in $[Ca^{2+}]_i$ and membrane depolarization leading to an increase in the duration of the slowest open state and a decrease in the duration of the slowest closed state.

3.5.4 The effect of 1, 2-dioctanoyl-*sn*-glycerol on BK_{Ca} single channel activity

The PKC activator, DOG, has been reported to affect channel function of a variety of different ion channels via a PKC-independent pathway, including Kv channels (He *et al*, 2000; Rainbow *et al*, 2005). I therefore decided to investigate whether DOG could

have a direct effect on BK_{Ca} single channel activity. DOG was found to affect BK_{Ca} single channel activity in a concentration dependent manner. 10 μ M DOG was found to cause an approximate 35% decrease in P_{open} within 75 sec of the compound reaching the patch. This inhibitory effect increased to approximately 84% after the patch had been exposed to this 10 μ M DOG solution for 5 min. The application of 1 μ M DOG decreased P_{open} by only 34% after 5 minutes. Many of the openings in the presence of DOG were very brief and an accurate determination of the current amplitude was difficult.

10 μ M DOG caused a decrease in the mean open time constant and an increase in the mean closed time that progressed with time following the application of DOG. As expected for a blocker, it was necessary to add an additional closed state to fit the closed time distributions in the presence of DOG. However, if silent BK_{Ca} channels do exist in arterial smooth muscle cells, then this extra closed state would be required even if the long-lived closed state was rare. In order to confirm whether or not DOG can effect BK_{Ca} channels directly, it would be necessary to repeat any DOG experiments in the presence of PKC-IP.

4 MODULATION OF VOLTAGE PULSE- INDUCED BK_{Ca} CURRENTS

4.1 Recording of BK_{Ca} whole-cell currents

Whole-cell BK_{Ca} currents were recorded in the presence of physiological [Ca²⁺]_i (100 nM) and with the same elevated [Ca²⁺]_o level of 2 mM that was used in the inside-out excised patch experiments. This high [Ca²⁺]_o was used in these whole-cell experiments in order to facilitate Ca²⁺ influx which is likely to be important for the replenishment of intracellular Ca²⁺ stores. In general, cells were held at a membrane potential of -20 mV in order to inactivate K_v currents, and BK_{Ca} whole-cell currents were induced by pulsing to +60 mV (figure 4.1). Current traces from 20 sweeps were averaged in order to reduce the effect of fluctuations in current. Currents recorded in this manner were completely blocked by the specific BK blocker penitrem A (100 nM; Knaus *et al*, 1994) as well as low concentrations of tetraethylammonium (TEA; 1 mM; figure 4.2). TEA is a quaternary ammonium cation that is known to block the pore of a variety of K⁺ channels. However, at this concentration it has been found to block BK_{Ca} alone (Langton *et al*, 1991). This suggests that the conditions used have suitably isolated BK_{Ca} channel currents for recording.

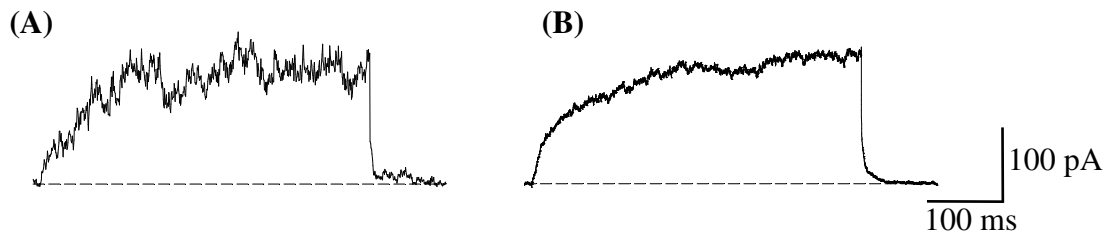


Figure 4.1 *BK_{Ca} control currents.* Example traces of *BK_{Ca}* control currents induced by voltage pulses from -20 to +60 mV. (A) A single sweep. (B) Average of 20 sweeps. 10 μ M ryanodine was included in the patch pipette.

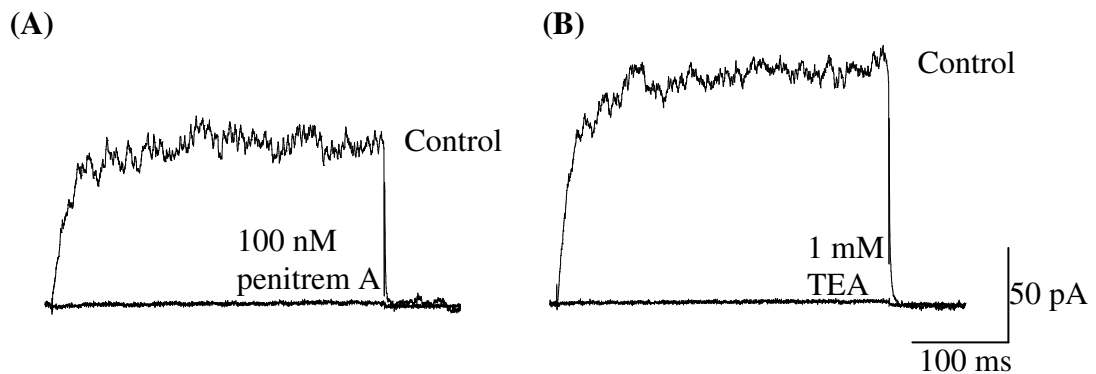


Figure 4.2 *Effect of *BK_{Ca}* channel blockers on whole-cell current induced by voltage pulses from -20 to +60 mV.* Example traces showing the effect of (A) 100 nM penitrem A and (B) 1 mM TEA on *BK_{Ca}* whole-cell current. 10 μ M ryanodine was included in the patch pipette.

4.1.1 Ryanodine reduces fluctuations in BK_{Ca} whole-cell current caused by the presence of STOCs

It was found that BK_{Ca} whole-cell current recordings could look rather noisy due to the presence of large STOCs when pulsing to highly depolarised potentials (e.g. +60 mV). In order to remove these STOCs and to allow the measurement of BK_{Ca} whole-cell current alone, 10 µM ryanodine was included in the patch pipette. Ryanodine acts on RyRs of the SR and, at this concentration, causes the release of Ca²⁺, and so leads to the depletion of intracellular stores (Wagner-Mann *et al*, 1992). This is believed to be due to ryanodine locking RyR in the open state (Iino, 1990b). Including ryanodine in this manner therefore caused an initial increase in STOCs as Ca²⁺ was released from the SR before greatly reducing STOC activity (figure 5.5). This concentration of ryanodine did not abolish STOC activity completely and so a small number of STOCs were still present, especially when pulsing to membrane potentials such as +60 mV that greatly depolarised the cell (figure 4.3). A higher ryanodine concentration of 50 µM is thought to be enough to actually inhibit the release of Ca²⁺ from the SR, however, concentrations as high as this appeared to have an adverse reaction on the health of the cell and it proved difficult to obtain an acceptable recording, so this concentration could not be tested. A concentration of 10 µM ryanodine was therefore routinely included in the patch pipette in order to reduce the appearance of STOCs. The average of 20 sweeps was also taken in order to reduce any other fluctuation in current and so give a more reliable picture of changes in BK whole-cell current (figure 4.3).

4.1.2 The effects of membrane potential and $[Ca^{2+}]_i$ on BK_{Ca} whole-cell current

I also investigated the effect of membrane potential in association with various free $[Ca^{2+}]_i$ to see what effect this had on whole-cell BK_{Ca} current. This was done in order to maximize BK_{Ca} whole-cell current whilst at the same time ensuring that the conditions did not have an adverse effect on the health of the cells. Cells were held at a membrane potential of -65 mV but quickly depolarized to -20 mV for a minimum of 5 seconds in order to inactivate Kv channels. BK_{Ca} currents were induced by depolarizing voltage steps from this holding membrane potential to potentials between -10 and +80 mV (see figure 2.3A). BK_{Ca} channels are voltage-dependent and so depolarizing the membrane potential leads to an increase in BK_{Ca} whole-cell current (figure 4.4). At physiological membrane potentials that the cell is likely to be subjected to *in vivo*, $[Ca^{2+}]_i$ has no significant effect on BK_{Ca} current ($n = \geq 4$; $P = >0.05$, one-way ANOVA with Bonferroni's test). At 20 nM $[Ca^{2+}]_i$, there appears to be a linear relationship between Ca^{2+} and voltage, whereas an increase in $[Ca^{2+}]_i$ to 100 and 300 nM sees a greater increase in BK_{Ca} activity at more depolarized potentials (figure 4.5). This is likely to be because the open probability of the channel is very low in the presence of 20 nM $[Ca^{2+}]_i$, even at highly depolarized membrane potentials. If the Boltzmann equation could be fit to the P_{open} values obtained in the presence of 20 nM $[Ca^{2+}]_i$, it is likely that these potentials would be before the slope of the curve, and so there are only small increases in P_{open} with membrane depolarization within this region. Increases in whole-cell BK_{Ca} current at this $[Ca^{2+}]_i$ are still likely to be due to the combined effect of increases in both P_{open} and single channel current amplitude, but the single channel current amplitude is perhaps largely responsible. The small tail currents obtained in the presence of 20 nM $[Ca^{2+}]_i$ are consistent with a low channel open probability. At 100

nM and 300 nM $[Ca^{2+}]_i$, there is a greater increase at depolarized potentials when compared to 20 nM $[Ca^{2+}]_i$. BK_{Ca} current density becomes significantly different between 20 nM and 300 nM $[Ca^{2+}]_i$ at +50 mV, and between 20 nM and 100 nM at +60 mV ($n = \geq 4$; $P = < 0.05$, one-way ANOVA with Bonferroni's test). The difference in BK_{Ca} current density at +50 mV was also significantly different between 100 nM and 300 nM $[Ca^{2+}]_i$ ($n = \geq 4$; $P = < 0.05$, one-way ANOVA with Bonferroni's test) but not at more depolarized membrane potentials. This slight difference between 100 nM and 300 nM $[Ca^{2+}]_i$ can also be seen when comparing BK_{Ca} tail current density (figure 4.6), although it does not appear to be significant. Exponentials were only fitted to tail currents at more depolarized potentials in the presence of 100 nM and 300 nM $[Ca^{2+}]_i$, as tail currents below 20 mV, and all those in the presence of 20 nM $[Ca^{2+}]_i$ were too small to fit accurately. This is probably due to a very low P_{open} under those particular conditions. Unfortunately tail currents could not be normalized to give a more accurate indication of the P_{open} of the BK_{Ca} channel as a plateau was not reached and so the maximal P_{open} of the channel is unlikely to have been achieved. The differences in BK_{Ca} whole-cell current between 20 nM $[Ca^{2+}]_i$ and the physiological $[Ca^{2+}]_i$ of 100 and 300 nM are therefore likely to be due to an increase in the P_{open} of the channel as $[Ca^{2+}]_i$ is increased.

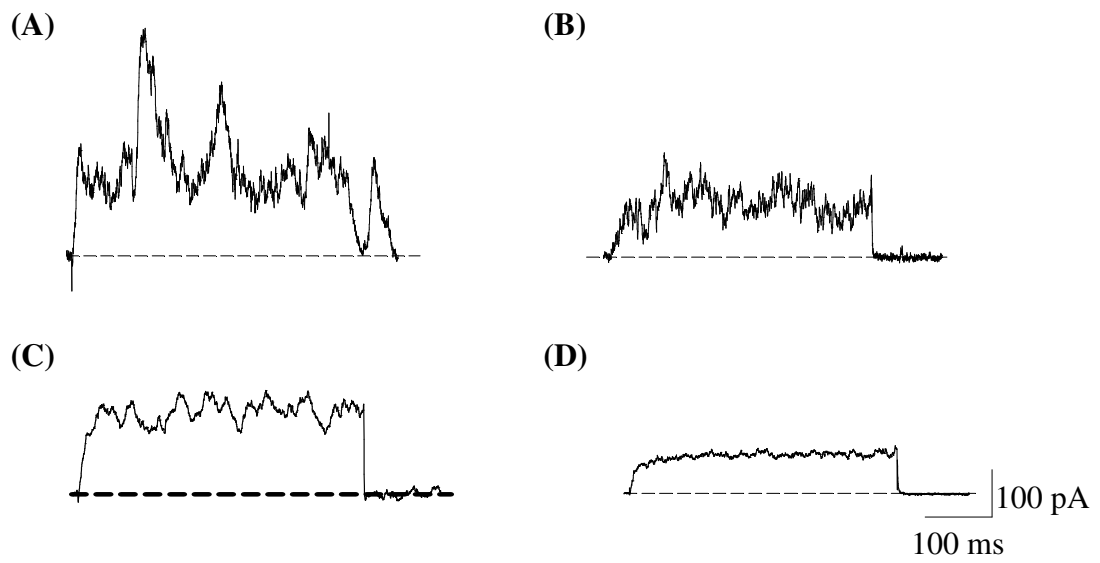


Figure 4.3 The effect of ryanodine on BK_{Ca} whole-cell current induced by voltage pulses from -20 to $+60$ mV. Example traces of a single sweep showing BK_{Ca} whole-cell current (A) in the absence of ryanodine and (B) after the inclusion of $10 \mu\text{M}$ ryanodine in the patch pipette. Example traces showing BK_{Ca} whole-cell current (C) in the absence of ryanodine (average of sweeps) and (D) after the inclusion of $10 \mu\text{M}$ ryanodine in the patch pipette (average of 20 sweeps).

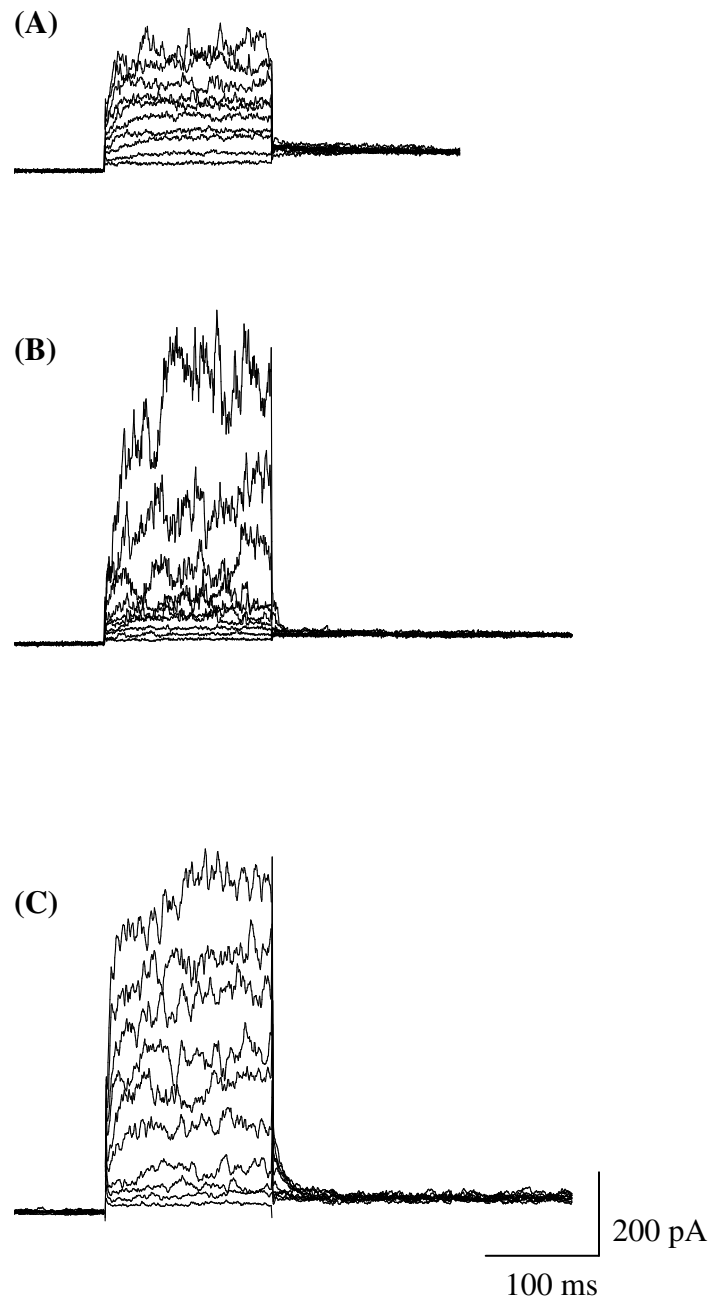


Figure 4.4 Effect of $[Ca^{2+}]_i$ on BK_{Ca} whole-cell current induced by voltage steps from -10 to $+80$ mV. Example traces showing the effect of depolarizing voltage steps in the presence of (A) 20 nM free $[Ca^{2+}]_i$, (B) 100 nM free $[Ca^{2+}]_i$, and (C) 300 nM free $[Ca^{2+}]_i$. Current traces were not averaged. 10 μ M ryanodine was included in the pipette.

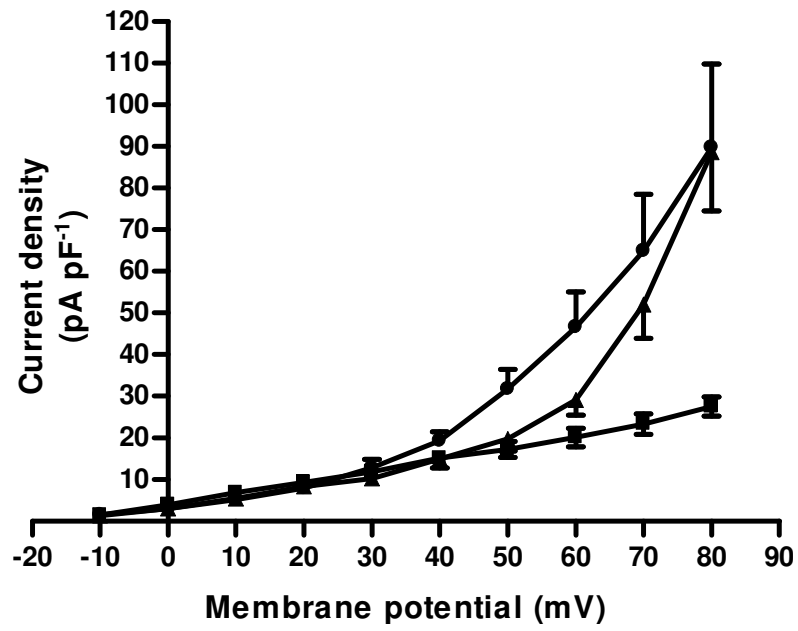


Figure 4.5 Current-voltage plot showing effect of $[Ca^{2+}]_i$ and voltage on BK_{Ca} whole-cell current. $[Ca^{2+}]_i$ concentrations are 20 nM (■), 100 nM (▲) and 300 nM (●). Error bars show SEM.

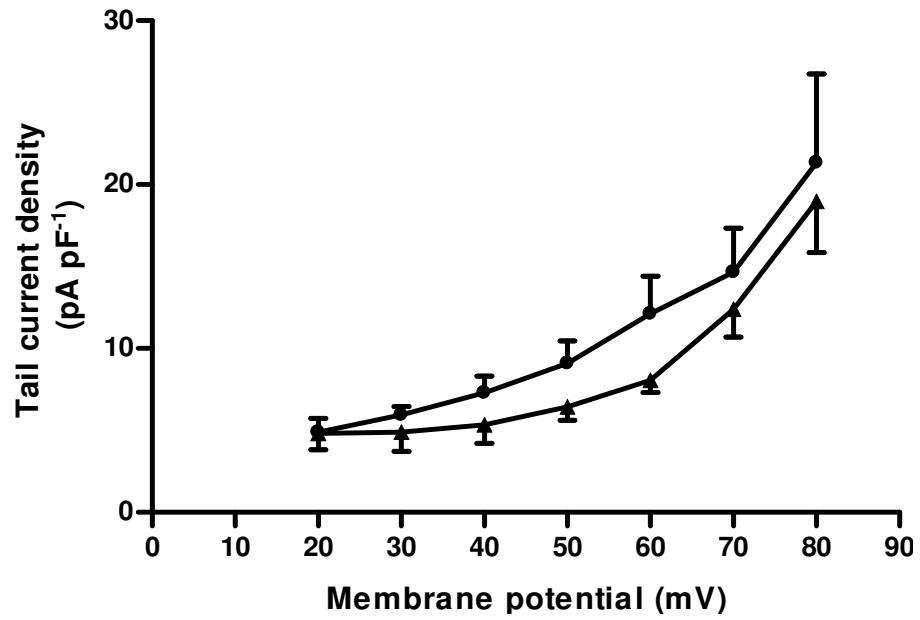


Figure 4.6 Tail current plot showing effect of $[Ca^{2+}]_i$ and membrane potential on BK_{Ca} tail currents, indicating the effect of these conditions on P_{open} . $[Ca^{2+}]_i$ concentrations are 100 nM (▲) and 300 nM (●). Error bars show SEM.

4.1.3 The effects of ET-1 on whole-cell BK_{Ca} current

ET-1 is known to be a potent vasoconstrictor that partially exerts its effect through the inhibition of K⁺ channels leading to depolarization of the membrane. Both ET_A and ET_B receptors are thought to be present in vascular smooth muscle, however ET-1 is believed to exert its primarily vasoconstrictory effect through the ET_A receptor. This receptor is coupled to the G_{α_{q/11}} G-protein and therefore leads to activation of PLC and the production of IP₃ and DAG, which in turn leads to Ca²⁺ release from the SR and the activation of PKC respectively. I therefore decided to explore the effect of ET-1 on BK_{Ca} whole-cell current, to see whether it may partially exert its effect through the inhibition of BK_{Ca} channels. ET-1 has been found to be effective at concentrations as low as 0.3 nM (Jones et al, 1998), however, the concentration of 10 nM ET-1 is most often used as this is the concentration found to be maximally effective. After consulting the literature in this way, and also discussing the matter with lab colleagues who were looking at the effect of this substance on Kv channels on isolated smooth muscle cells from the same tissue, a concentration of 10 nM ET-1 was chosen to ensure that any effects of ET-1 on BK_{Ca} channels could be clearly observed. Control BK_{Ca} currents were induced by pulsing from -20 to +60 mV. 10 nM ET-1 was then applied extracellularly and its effect was monitored by repeating the same depolarizing pulses every 3 min. ET-1 took approximately 9 min to have its full effect suggesting that it works through an intracellular signalling pathway involving enzyme activation such as PKC. 10 nM endothelin-1 reduced BK whole-cell current by 41.2 ± 4.8%, from 36 ± 9 pA pF⁻¹ to 20 ± 5 pA pF⁻¹ (n = 4; P = <0.01; figure 4.7). When the cell isolation procedure yielded a great number of healthy cells, almost all cells tested responded to treatment with 10 nM ET-1. There was no change in whole-cell current induced by voltage pulses within this timeframe under control conditions.

4.1.4 The effects of PKC activation on BK_{Ca} whole-cell current

ET-1 exerts its effect through the activation of PKC and DOG is an active analogue of DAG, an endogenous compound that is known to stimulate PKC activity. The effect of DOG on BK_{Ca} whole-cell current was therefore investigated to see whether activation of PKC in this manner could inhibit BK_{Ca} activity in these smooth muscle cells, and this could perhaps partly explain the effects of ET-1 on these channels. DOG reduced BK_{Ca} whole-cell current, induced by depolarizing pulses from 0 mV to +80 mV, from 17 ± 6 pA pF⁻¹ to 10 ± 6 pA pF⁻¹; a reduction in current of 46.1 ± 4.7 %, after approximately 9 min application ($n = 4$; $P = <0.01$; Student's paired t test; figure 4.8). It is interesting to note that the timecourses of ET-1 and DOG are similar, perhaps suggesting that they have their effects by a similar mechanism such as PKC activation. Previous work in our laboratory has shown that DOG inhibits Kv current by dramatically increasing the apparent rate of Kv channel inactivation (Rainbow *et al*, 2005) but DOG did not appear to have a similar effect on BK_{Ca} channel inactivation in these cells. This study on the effect of DOG on Kv current carried out by lab colleagues revealed that the effect of DOG on these channels was PKC-independent, and my results showing the effect of DOG on BK_{Ca} single channel activity suggest that DOG could also have a direct effect on BK_{Ca} channels. However, these results demonstrating the effect of DOG on whole-cell BK_{Ca} current are very different to the effects seen in excised patches (section 3.4.1). The apparent small effect of 10 μ M DOG on BK_{Ca} whole-cell current amplitude compared to the large decrease seen in excised patches could reflect differences in access to the inhibitory site in intact cells and excised patches or, if DOG acted as an open channel blocker, may reflect the low P_{open} seen in the whole-cell experiments (sections 3.4.1 and 4.1.2). However, it may also be that DOG does not affect BK_{Ca} channels directly in the intact rat mesenteric artery smooth muscle cell due to a higher

affinity for other proteins, such as those involved in cell signalling pathways. The similar timecourses seen for ET-1 and DOG suggest that this may be possible. Experiments to determine the effect of DOG in the presence of a PKC inhibitor peptide were attempted but unfortunately they could not be completed successfully due to the adverse effect that pre-incubation with a PKC inhibitor had on the health of the cells. These experiments may have helped to determine whether DOG is able to act on BK_{Ca} channels directly in the intact smooth muscle cell (a decrease in pulse-induced whole-cell current of approximately 80-85% in the presence of the inhibitor peptide, similar to that seen in excised patches, would suggest that this is possible) and so it was very disappointing that these experiments did not work.

4.1.5 The effects of ET-1 is inhibited by pre-incubation of the cells with PKC-IP

Since the ET-1 receptor, ET_A, found in rat mesenteric artery smooth muscle cells is known to be linked to Gq (Bouallegue *et al*, 2007), I examined the role of PKC in producing the effect of ET-1 on BK_{Ca} current. This was done by examining the effect of PKC inhibitor peptide 20-28 (PKC-IP), a pseudosubstrate of PKC, on the ET-1 induced inhibition. In order to carry out these experiments, a TAT-linked form of this PKC inhibitor was utilised. TAT (transacting activator of transcription) is a cell penetrating protein that provides an efficient mechanism for transporting non-membrane-permeable compounds (in this case, PKC-IP) across the cell membrane into the cytoplasm. Once the complex is inside the cell, the bond between TAT and PKC-IP is broken, and PKC-IP is released into the cytoplasm. This transport system was found to be very effective, as lower concentrations of PKC-IP were required to achieve the same effect seen with the myristoylated form of PKC-IP (100 nM compared to 50 μ M, respectively). The cells were incubated with the TAT-PKC-IP complex at room temperature for a minimum of 10 min beforehand and then the TAT-PKC-IP solution was washed off the cells before commencing the experiment. The protocol was the same as before, with 20 sweeps from -20 mV to +60 mV, to measure control current and this was repeated every 3 min after the application of 10 nM ET-1 to monitor the effect of the compound. 10 μ M ryanodine was included in the pipette to reduce STOC activity. In the presence of PKC-IP, 10 nM ET-1 had no significant effect on BK_{Ca} whole-cell current (figure 4.7). The difference in the effects of ET-1 in the presence and absence of PKC-IP was significant ($n = 4$; $P = <0.01$; one-way ANOVA with Bonferroni's test). The effect of ET-1 in the presence of PKC-IP was tested on healthy cells only after it was shown that a high proportion of cells isolated that day had responded successfully to ET-1

treatment in the absence of PKC-IP. All cells in the bath were replaced in between experiments.

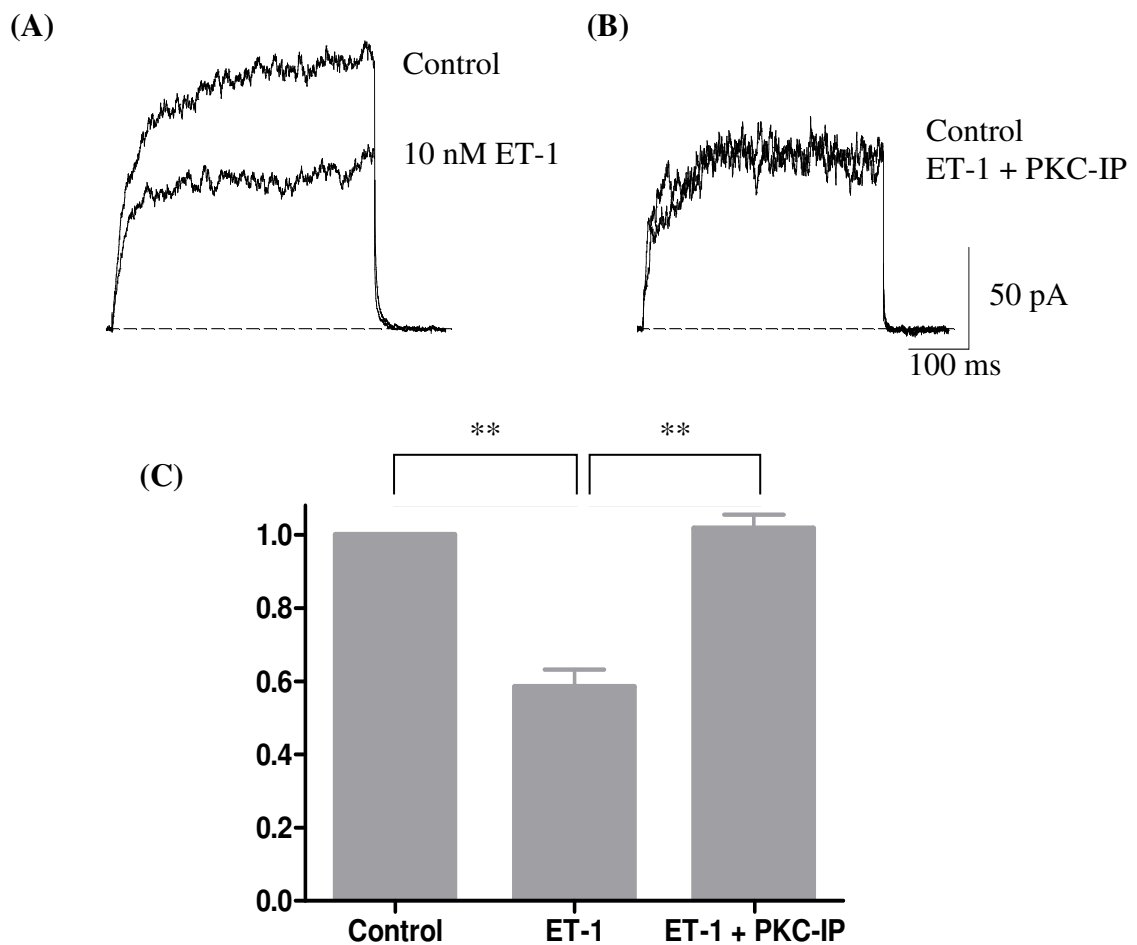
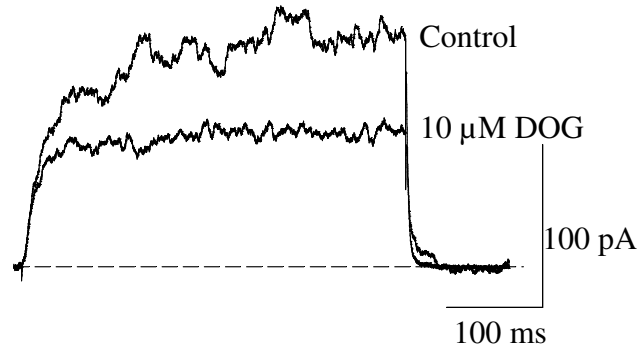


Figure 4.7 Inhibition of BK_{Ca} whole-cell current by 10 nM ET-1 induced by voltage pulses from -20 to +60mV. Example traces showing the effect of 10 nM ET-1 on BK_{Ca} whole-cell current (A) in the absence of PKC-IP, and (B) after 10 min pre-incubation with 100 nM TAT-linked PKC-IP. Both traces show the BK_{Ca} control current and also the BK_{Ca} current after 9 min application of 10 nM ET-1. Average of 20 sweeps with 10 μ M ryanodine included in the patch pipette. (C) Current recorded in the presence of ET-1 was normalised against the control current to show the percentage of control BK_{Ca} whole-cell current seen after 9 min application of 10 nM ET-1 in the absence of PKC-IP (ET-1), and after 10 min pre-incubation with 100 nM TAT-linked PKC-IP (ET-1 + PKC-IP). Error bars show SEM.

(A)



**

(B)

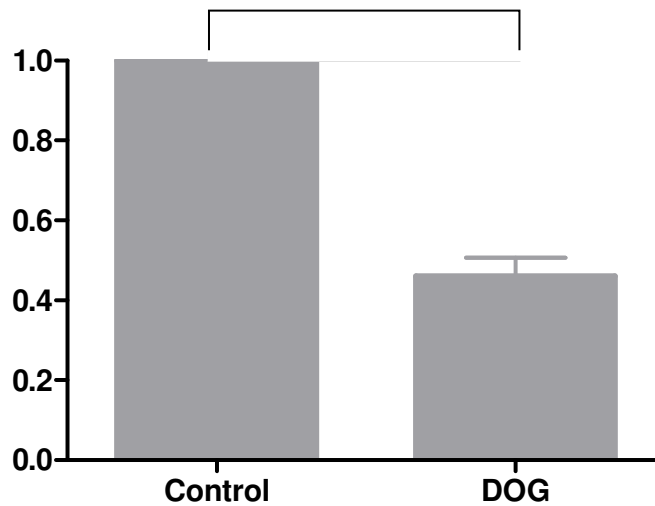


Figure 4.8 Effect of 1,2-dioctanoyl-*sn*-glycerol on BK_{Ca} whole-cell current induced by voltage pulses from 0 to +80mV. (A) Example trace showing BK_{Ca} current under control conditions and after 9 min application of 10 μM DOG. Average of 20 sweeps. (B) Current recorded in the presence of 10 μM DOG was normalised against the control current to show the percentage of control BK_{Ca} whole-cell current seen after 9 min application of 10 μM DOG. Error bars show SEM. Currents were recorded in the presence of 10 μM ryanodine.

4.1.6 The effects of Ang II on BK_{Ca} whole-cell current

A second endogenous vasoconstrictor, Ang II, is also known to cause vasoconstriction of smooth muscle through inhibition of K⁺ channels and so I decided to investigate whether this effect could be due to a reduction in BK_{Ca} current in these cells. After consultation of the available literature and with colleagues, 100 nM Ang II was chosen as a suitable concentration to elicit an effect. Control BK_{Ca} currents were induced by pulsing from -20 to +60 mV and then 100 nM Ang II was applied extracellularly and its effect monitored by repeating the same depolarizing pulses every 3 min. After 9 min application, this concentration was seen to reduce control BK_{Ca} whole-cell current from 23 ± 7 pA pF⁻¹ to 14 ± 5 pA pF⁻¹, by an average of $39.7 \pm 6.0\%$, (n = 5; P = <0.01; Student's paired *t* test; figure 4.9).

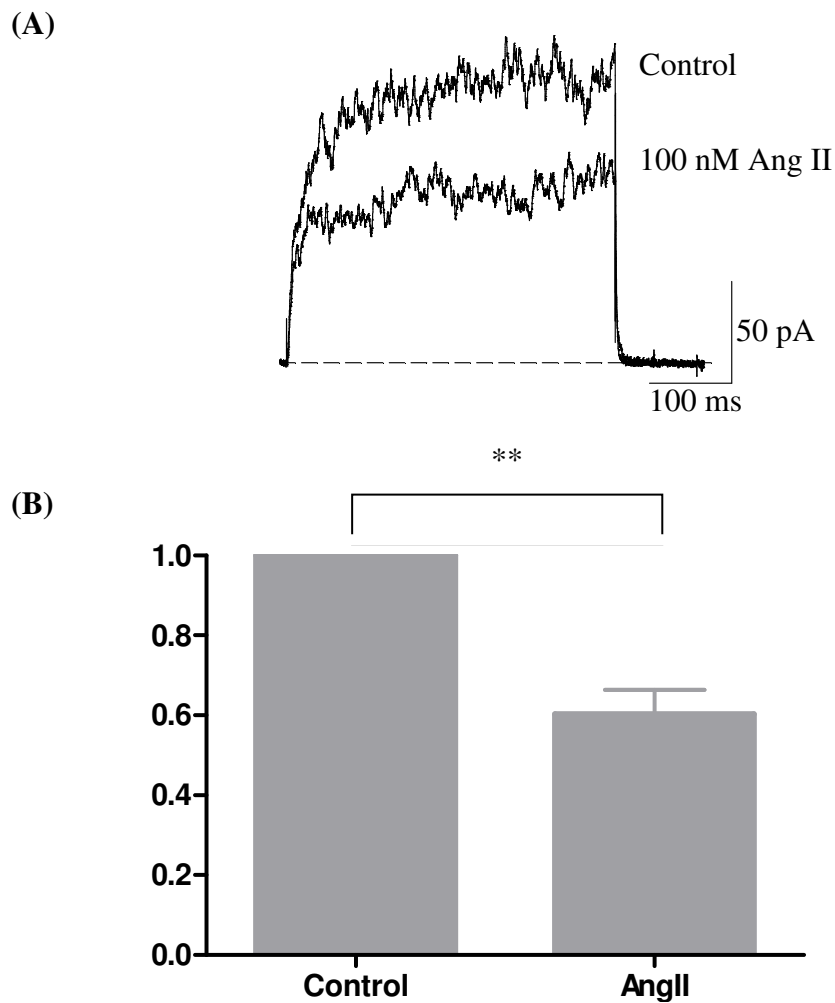


Figure 4.9 Effect of 100 nM Ang II on BK_{Ca} whole-cell current induced by voltage pulses from -20 to +60mV. (A) Example trace showing control BK_{Ca} current and BK_{Ca} current after 9 min application of 100 nM Ang II. Currents were recorded in the presence of 10 μ M ryanodine and the trace shows the average of 20 sweeps. (B) Current recorded in the presence of 100 nM Ang II was normalised against the control current to show the percentage of control BK_{Ca} whole-cell current seen after 9 min application of 100 nM Ang II. Error bars show SEM.

4.2 Discussion

4.2.1 Recording of BK_{Ca} whole-cell currents

BK_{Ca} whole-cell currents were observed in rat mesenteric artery smooth muscle. These currents were induced by voltage pulses from -20 to +60 mV and could then be inhibited by the external application of either 100 nM penitrem A or 1 mM TEA. The effects of these inhibitors on BK_{Ca} channels and the concentrations required to achieve inhibition are covered in great detail in the literature (Langton *et al*, 1991; Mistry & Garland, 1998; Dimitropoulou *et al*, 2002; Barlow & White, 1998). Generally, these inhibitors largely abolish BK_{Ca} current at the concentrations used. The purpose of these initial experiments was therefore not to discover their effect on these channels, but rather to determine the conditions necessary to successfully isolate BK_{Ca} channel currents from other K⁺ channel currents for the purpose of these recordings.

4.2.2 Ryanodine reduces fluctuations in BK_{Ca} whole-cell current caused by the presence of STOCs

After separating BK_{Ca} current from other K⁺ current, there was still the further complication of the presence of STOCs in whole-cell recordings. STOCs make the traces quite noisy and difficult to analyse, and their presence also makes it difficult to determine whether BK_{Ca} channels are affected by compounds such as ET-1 or Ang II, or whether the effects are actually on Ca²⁺ spark amplitude or frequency, leading to an apparent decrease in BK_{Ca} whole-cell current. The application of 10 μM ryanodine should lead to the “dumping” of intracellular stores, therefore minimizing this local Ca²⁺ release from the SR (Iino, 1990b; Nelson *et al*, 1995; White & McGeown, 2000). However, as mentioned, the inclusion of 10 μM ryanodine in the patch pipette did not

completely abolish STOCs, though the amplitude and frequency was greatly reduced. The reasons for this are unclear but the STOCs did not decrease any further over time after the recording of these currents had begun. It is therefore unlikely that the presence of the remaining STOCs was due to ryanodine requiring longer to exert its maximal effect. It may be that a concentration of 10 μM does not empty the SR completely, and that mechanisms exist for the remaining Ca^{2+} to continue to be released as sparks. Another possible explanation is that the depletion of Ca^{2+} stores by ryanodine leads to Ca^{2+} influx through store-operated channels (SOCs) which then serves to replenish the SR. This may start a cycle of simultaneous Ca^{2+} store depletion by ryanodine and replenishment by SOCs, with the ryanodine-induced Ca^{2+} release still able to generate STOCs due to the co-localization of RyRs with BK_{Ca} . It may have been better to use a greater concentration of ryanodine, as 50 μM ryanodine is known to actually inhibit the release of Ca^{2+} from the SR, rather than dump Ca^{2+} from the stores. However, at a concentration of 50 μM , ryanodine appeared to have an adverse effect on the health of the cells and so it was necessary to continue with the lower ryanodine concentration. It may have been possible to reduce STOCs further using a combination of caffeine and ryanodine, however, 10 mM caffeine tended to have an adverse effect on the health of the cells and 1 mM caffeine increased STOC activity without rundown over a period of minutes, Caffeine is therefore perhaps unsuitable to use for the purpose of reducing STOCs even in combination with ryanodine. Thapsigargin or cyclopiazonic acid may perhaps be more suitable for this purpose and could be used in future experiments. It is important to note, however, that although STOCs were not abolished completely, they were greatly reduced to a permissible level and the remaining STOCs were unlikely to affect the analysis of BK_{Ca} whole-cell current.

4.2.3 The effects of membrane potential and $[Ca^{2+}]_i$ on BK_{Ca} whole-cell current

BK_{Ca} whole-cell current was shown to be dependent upon membrane depolarization. For each $[Ca^{2+}]_i$, depolarization of the membrane potential as a series of 10 mV steps led to an increase in the mean steady-state current measured at the end of a 150 ms pulse. This results from an increase in both the P_{open} of BK_{Ca} channels and also an increase in the single channel current amplitude. Tail current amplitudes were measured by extrapolating the exponential fits to each tail current to the end of the test pulse. For all currents in the presence of 20 nM $[Ca^{2+}]_i$ and for currents activated by the more hyperpolarized potentials in the presence of 100 nM or 300 nM $[Ca^{2+}]_i$, tail currents were too small to be accurately analysed due to the low P_{open} of the channel under these conditions. Even at the highest $[Ca^{2+}]_i$ of 300 nM, tail current amplitudes were still increasing following a test pulse to +80 mV. This indicates that under these conditions that activation of whole-cell BK_{Ca} currents was submaximal, as expected from examining the relation between $[Ca^{2+}]_i$ and voltage in inside-out patches. Tail currents were therefore plotted as current density, normalized to the membrane capacitance of the cell. Because of the relatively low P_{open} of the BK_{Ca} channels under these conditions a plot of the activation curve from tail current analysis could not be obtained.

At 20 nM $[Ca^{2+}]_i$, the relationship between membrane potential and current density is rather shallow and probably reflects the very low P_{open} under these conditions. Increased $[Ca^{2+}]_i$ to 100 or 300 nM, causes a steeper increase in current with depolarization, although at membrane potentials more negative than +20 mV, there is no significant difference in BK_{Ca} current density between the $[Ca^{2+}]_i$ tested ($n \geq 4$; $P > 0.05$, one-way ANOVA with Bonferroni's test). At very depolarized membrane

potentials, it would be expected that BK_{Ca} channels would have a higher P_{open} at 300 nM [Ca²⁺]_i than at 100 nM [Ca²⁺]_i, especially as these two [Ca²⁺]_i are at the opposite ends of the physiological Ca²⁺ range in these cells. It is possible that had the membrane potential been depolarized further, above +80 mV, then the current density between these two [Ca²⁺]_i would begin to show more of a divergence. Comparing this data with those from the tail current analysis suggests that there is little difference in P_{open} between 100 nM and 300 nM [Ca²⁺]_i at these membrane potentials. Depolarization of the membrane potential to voltages more positive than +80 mV may show that increased [Ca²⁺]_i has a more significant effect on the P_{open} of BK_{Ca} channels.

4.2.4 The effects of ET-1 on BK_{Ca} whole-cell current

ET-1 is a very potent vasoconstrictor that is derived from the endothelium (Yanagisawa *et al*, 1988). Application of 10 nM ET-1 reduced BK_{Ca} whole-cell current in rat mesenteric artery smooth muscle cells by approximately 41%, and this inhibition of BK_{Ca} current has also been seen in a variety of other smooth muscle cells by a PKC-dependent mechanism (Betts & Kozlowski, 2000; Salamanca & Khalil, 2005; Hu *et al*, 1991). I therefore decided to investigate the effect of ET-1 in the presence of the TAT-linked PKC-IP 20-28 and discovered that the inhibition of BK_{Ca} whole-cell current caused by ET-1 was completely inhibited after 10 min pre-incubation of the cells with TAT-linked PKC-IP 20-28. This suggests that the effect of ET-1 on BK_{Ca} whole-cell current is mediated entirely by a PKC-dependent pathway in rat mesenteric artery smooth muscle cells. The effect of ET-1 has also been reported to be mediated by PKC inhibitors in a variety of other smooth muscle types (Breuiller-Fouché *et al*, 1998; Cain *et al*, 2002; Shin *et al*, 2002). The depletion of SR Ca²⁺ by ryanodine also suggests that

this PKC effect is due to inhibition of the channel and not secondary to an effect on Ca^{2+} release from the SR. This does not exclude an additional effect of PKC on Ca^{2+} release from stores.

4.2.5 The effects of 1, 2-dioctanoyl-*sn*-glycerol on BK_{Ca} whole-cell currents

ET-1 exerts its effect through the activation of PKC and DOG is an analogue of the PKC activator DAG, stimulating the translocation of PKC to the plasma membrane (Capogrossi *et al*, 1990). I therefore decided to investigate the effect of DOG to see whether the activation of PKC in this manner could modulate BK_{Ca} whole-cell current. Application of DOG reduced BK_{Ca} whole-cell current by approximately 46%, indicating that PKC plays a role in the regulation of BK_{Ca} channel activity. However, DOG has been reported to block some channels via a PKC-independent mechanism (He *et al*, 2000; Rainbow *et al*, 2005). An attempt was made to investigate the effect of DOG on whole-cell BK_{Ca} channels in the presence of PKC-IP, but unfortunately pre-incubating the cells with PKC-IP often made it very difficult to maintain viable whole-cell recordings for long enough. Application of DOG did, however, inhibit BK_{Ca} channel activity in excised patches, indicating that DOG may block BK_{Ca} channels directly (section 3.4).

4.2.6 The effects of Ang II on BK_{Ca} whole-cell current

100 nM Ang II, a second endogenous vasoconstrictor, had a similar effect on BK_{Ca} channels as ET-1, with a 39% decrease in steady-state current. This effect is likely to be

via the Ang II receptor, AT₁, as this is the predominant isoform of the Ang II receptor in the control of the vasculature where it is found almost exclusively in the smooth muscle (Sadoshima, 1998). Furthermore, Ang II induced inhibition of K_v currents in this preparation is blocked by losartan, and AT₁ receptor antagonist (Hayabuchi *et al*, 2001b). The actions of Ang II are complicated as they may involve many different signalling pathways, which may be either PKC-dependent or PKC-independent (Minami *et al*, 1995). This PKC-independent mechanism may be an inhibition of PKA as has been reported to be the case in the Ang II inhibition of both K_v and K_{ATP} channels in rat arterial smooth muscle (Hayabuchi *et al*, 2001b; Hayabuchi *et al*, 2001a).

5 MODULATION OF SPONTANEOUS TRANSIENT OUTWARD CURRENTS

STOCs were recorded in rat isolated mesenteric artery smooth muscle cells. Due to their transient nature, STOCs need to be detected and so a reliable detection method must be used. For the purpose of this thesis, STOCs were detected using the transient detection method of an in-house software programme, as described in section 2.5.3. The standard deviation of the baseline just before each STOC was calculated and STOCs were excluded if this figure was above 2 pA. A high standard deviation is indicative of a noisy baseline and tended to be caused by the activation of STOCs in quick succession. This area just before a STOC is used as the baseline from which to measure STOC amplitude, and so a noisy baseline makes it difficult to measure the amplitude of the STOC accurately. 1 min segments under the varying experimental conditions were used for analysis purposes. The STOCs recorded within this timeframe were identified and each STOC was written to file as a 512 bit record (as described in section 2.5.3). after which they could be analysed and the properties of STOCs under the various conditions could be compared,

5.1 Analysis of STOCs

STOC simulations were developed by Dr N. W. Davies (University of Leicester).

STOCs (s) were simulated according to the following equation:

$$s = a.(1-\exp(-t/\tau_a))^3.\exp(-t/\tau_i) \quad (\text{Equation 4})$$

$$\tau_a = \tau_{act} \pm s.d.$$

$$\tau_i = \tau_{inact} \pm s.d.$$

$$a = \max.(Rnd^{5.1} + Rnd^{0.85} - Rnd^{1.3})$$

$$gap = -\tau_i.Ln(Rnd)$$

where t is time in ms; a is STOC amplitude in pA obtained by multiplying a maximum amplitude (max) by the random function shown (Rnd is a random number between 0 and 1) to give a peak amplitude distribution similar to that recorded from smooth muscle cells; τ_a and τ_i were varied from a base value, τ_{act} and τ_{inact} within standard deviations of 0.5 ms (s.d. may have been more than one standard deviation away from the mean); gap is the time between successive STOCs. A number of fitted tau values from recorded STOCs and the standard deviation of these fits were used to generate the Gaussian distribution used in the simulation. This gave a distribution of tau values similar to those of recorded STOCs. Values for τ_{act} and τ_{inact} of 2.0 and 6.0 ms gave simulated STOCs similar in time duration to STOCs measured in experiments. Gaussian noise of 1.8 pA, which was the value measured from background recorded data, was added to the simulated data. The simulated data was analysed in the same way as recorded STOCs.

A control STOCs data file was simulated using the method described above. These STOCs were then reduced in amplitude by exactly 50% and placed onto the same baseline to create a 50% STOC amplitude data file. Analysis of the data files revealed a 51% decrease in the mean amplitude of STOCs from 31.7 ± 1.1 pA in the control file to 15.3 ± 0.5 pA in the 50% STOC amplitude file (figure 5.1). There was also an apparent decrease in STOC frequency, indicated by an increase in the exponential fit to the gap frequency histogram from 110.0 ms in the control file to 230.5 ms in the 50% STOC amplitude file. It is likely that the decrease in STOC amplitude reduced the number of STOCs that could be detected above the noise of the trace and so reduced the apparent frequency of STOCs.

5.2 Recording of STOCs

5.2.1 STOCs in mesenteric artery smooth muscle cells are due to activation of BK_{Ca} channels

Spontaneous transient outward currents were recorded in single rat mesenteric artery smooth muscle cells held at a membrane potential of 0mV. Under control recording conditions 100 nM [Ca²⁺]_i was present in the pipette and the [K⁺] was 140 mM inside and 6 mM outside, and STOCs were almost always seen in healthy cells that were isolated during a “good” cell dispersion. These currents were found to be completely inhibited 2-3 minutes after continuous application of the specific BK_{Ca} channel blocker penitrem A (concentration of 100 nM; Knaus *et al*, 1994; figure 5.2). No STOCs were present in the one minute analysis file after this application of penitrem A. The potassium channel blocker TEA also blocked STOCs at low concentrations (1mM) that are known to block BK_{Ca} specifically (Langton *et al*, 1991; figure 5.2). This data suggests that STOCs are due to the opening of BK_{Ca} channels alone.

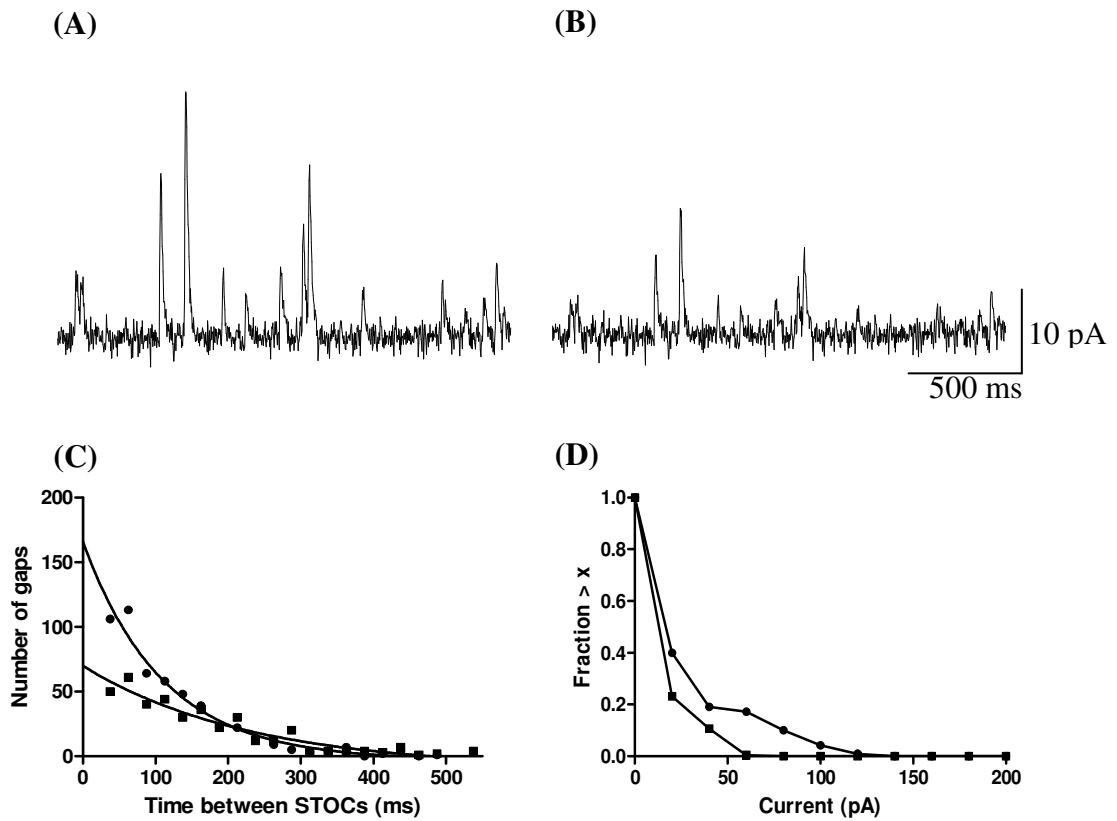


Figure 5.1 Use of in-house software to analyse simulated STOCs. (A) Control example trace. (B) Trace (A) after the amplitude of the STOCs had been reduced by 50% and then placed onto the original baseline. (C) Histogram showing the effect that a 50% reduction in amplitude had on STOC frequency. (D) Histogram showing the normalized distribution of STOC amplitudes. ● = control amplitude, ■ = 50% amplitude.

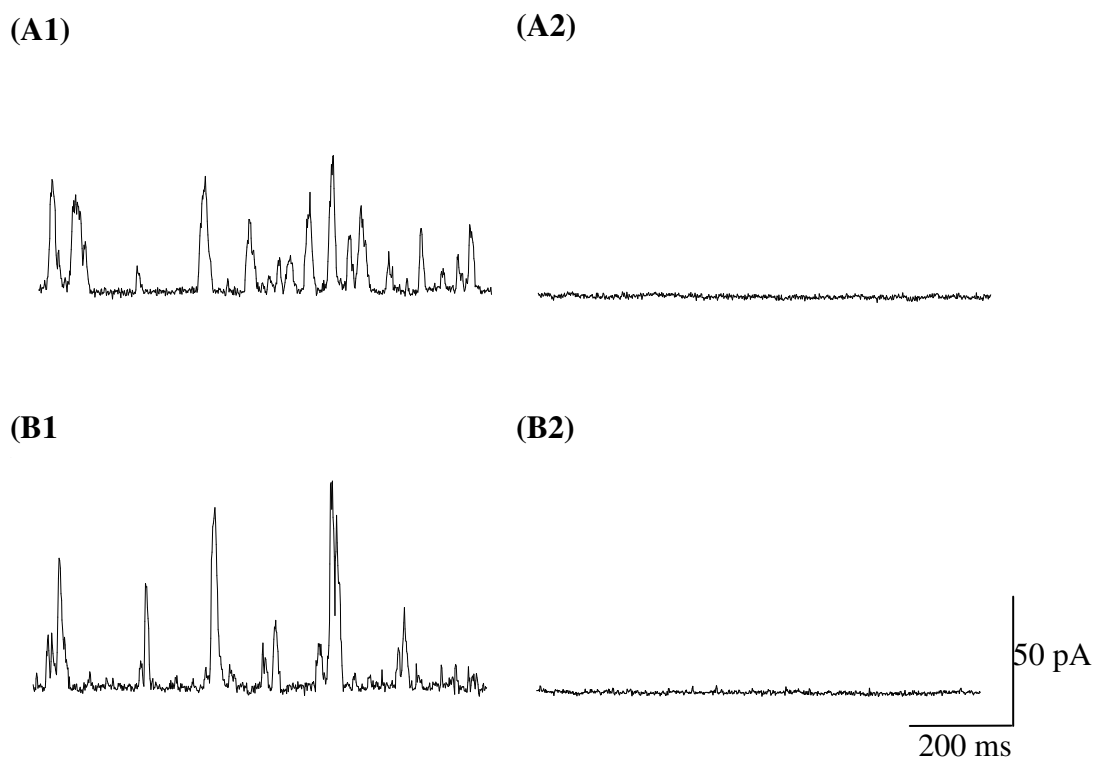


Figure 5.2 The effect of BK_{Ca} channel blockers on STOCs. Example traces showing the effect of (A) 100 nM penitrem A, and (B) 1 mM TEA, on STOCs. Control traces are shown on the left and the effect of the appropriate compound after 3 min application is shown at the right. Cells were held at a membrane potential of 0 mV. $[Ca^{2+}]_i = 100$ nM; $[K^+]_i = 140$ mM; $[K^+]_o = 6$ mM.

5.2.2 The effect of Ca²⁺ buffering on STOC activity

STOCs are activated by increases in [Ca²⁺]_i and so it stands to reason that buffering [Ca²⁺] more tightly would decrease STOC activity. The effect of the strength of Ca²⁺ chelation on STOCs was briefly investigated with different EGTA concentrations of 1 mM and 10 mM. The amount of Ca²⁺ added was altered so that the free [Ca²⁺] in both intracellular solutions was buffered at 100 nM as described in section 2.3.3. The tighter Ca²⁺ buffering provided by 10 mM EGTA drastically reduced the amplitude and frequency of STOCs, almost abolishing STOCs completely (n = ≥3; figure 5.3). An exponential could not be fitted to the gap frequency histogram for 10 mM EGTA as the slope of the graph was too shallow (figure 5.4). This suggests that STOCs are activated by changes in local [Ca²⁺]_i and that the higher EGTA concentration buffers Ca²⁺ too quickly and tightly for these changes to be sensed by BK_{Ca} channels. This is interesting as EGTA is thought to be quite a slow Ca²⁺ chelator, and suggests that RyRs and BK_{Ca} channels are located far enough apart for chelation to take place before BK_{Ca} channels can be activated. These results are inconsistent with reports suggesting that RyR and BK_{Ca} channels are found within 1 μM of each other (Wallner *et al*, 1999; Devine *et al*, 1972; Bennett, 1996). Proximity is therefore perhaps not the reason for the strength of this chelation

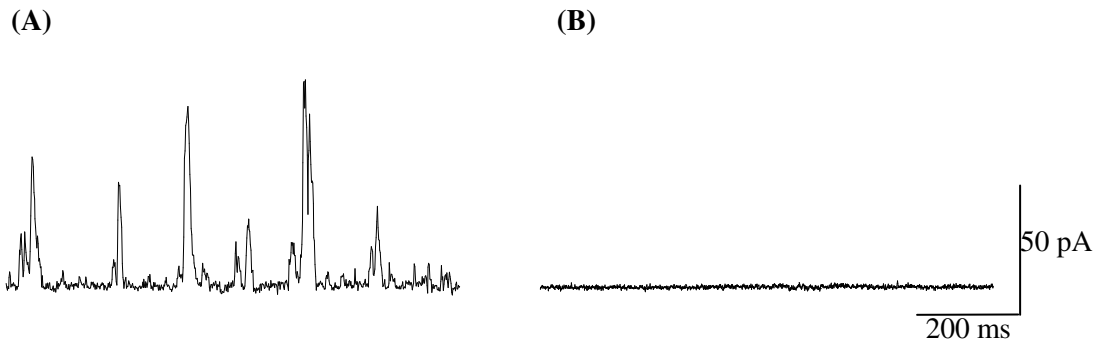


Figure 5.3 The effect of EGTA on STOCs. Example traces showing the effect of (A) 1 mM EGTA, and (B) 10 mM EGTA on STOCs. Cells were held at a membrane potential of 0 mV. $[Ca^{2+}]_i = 100$ nM; $[K^+]_i = 140$ mM; $[K^+]_o = 6$ mM. STOCs were analysed for 1 min.

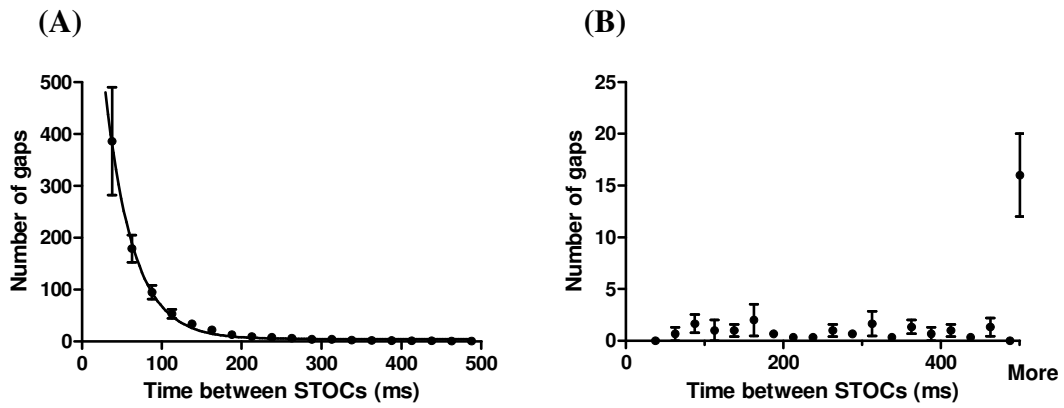


Figure 5.4 The effect of EGTA on the frequency of STOCs. Histograms showing STOC frequency in the presence of (A) 1 mM EGTA, and (B) 10 mM EGTA.

5.2.3 Ca²⁺-release is from the SR

As changes in [Ca²⁺]_i were found to be the trigger for STOC activation, the role of the SR Ca²⁺ store in activating BK_{Ca} channels was investigated. Ryanodine and caffeine are two compounds known to cause Ca²⁺ release from the SR (Wagner-Mann *et al*, 1992; Ganitkevich & Isenberg, 1992), and so the effect of their application on STOC activity was investigated.

As mentioned previously, the inclusion of 10 μM ryanodine in the intracellular solution contained in the pipette is thought to cause the SR to “dump” its store of calcium by forcing the channel to remain in an open state. It appears to cause an initial large increase in BK_{Ca} channel activity and STOCs, but then activity is diminished and STOCs look to be almost completely blocked within 5 minutes of gaining whole-cell access (figure 5.5). As ryanodine was included in the patch pipette, it is likely that it had already begun to take effect when recording was started; hence the large amount of STOC activity seen at the very start of the trace. As Ca²⁺ was continuously released, Ca²⁺ stores were depleted and the amount of Ca²⁺ released from the SR is likely to have decreased over time, leading to a large decrease in STOCs. The application of 10 μM ryanodine also had an effect on STOC decay, decreasing the mean time constant of the decay, τ , from 7.75 ± 0.64 ms as calculated at the beginning of the trace, to 2.09 ± 0.11 ms ($n = \approx 30$ STOCs from a minimum of 3 cells;), as calculated from the few remaining STOCs after a recording time of at least 3 min ($P = < 0.01$; Student paired t test; figure 5.5). This effect on the mean time constant of STOC decay was not simply due to a smaller mean STOC amplitude as the time constant of control STOCs of varying amplitudes were not found to be affected.

The effect of caffeine on Ca^{2+} release is known to be concentration dependent, therefore the effects of the external application of two different caffeine concentrations, 1 mM and 10 mM, on STOC activity were investigated. The application of 10 mM caffeine had a similar effect on STOCs as 10 μM ryanodine. There appeared to be a large initial increase in STOC activity as 10 mM caffeine was applied, which then quickly decreased until STOCs were almost completely abolished (figure 5.6). However, this effect occurred on a much quicker timescale with 10 mM caffeine application. The removal of caffeine from the extracellular solution allowed STOCs to eventually return as intracellular Ca^{2+} stores were replenished. Application of a lower concentration of caffeine (1 mM) did not have the same effect. The initial dramatic increase in STOC activity was not seen, and instead there was a smaller but longer term increase in the frequency of STOCs (figure 5.7). The application of this lower concentration (1 mM) of caffeine also seemed to have an effect on the time constant of STOC decay, increasing it from 7.28 ± 0.45 ms under control to conditions to 13.72 ± 2.33 ms after application ($n = 30$ STOCs from a minimum of 3 cells; $P = <0.05$; Student paired t test; figure 5.7).

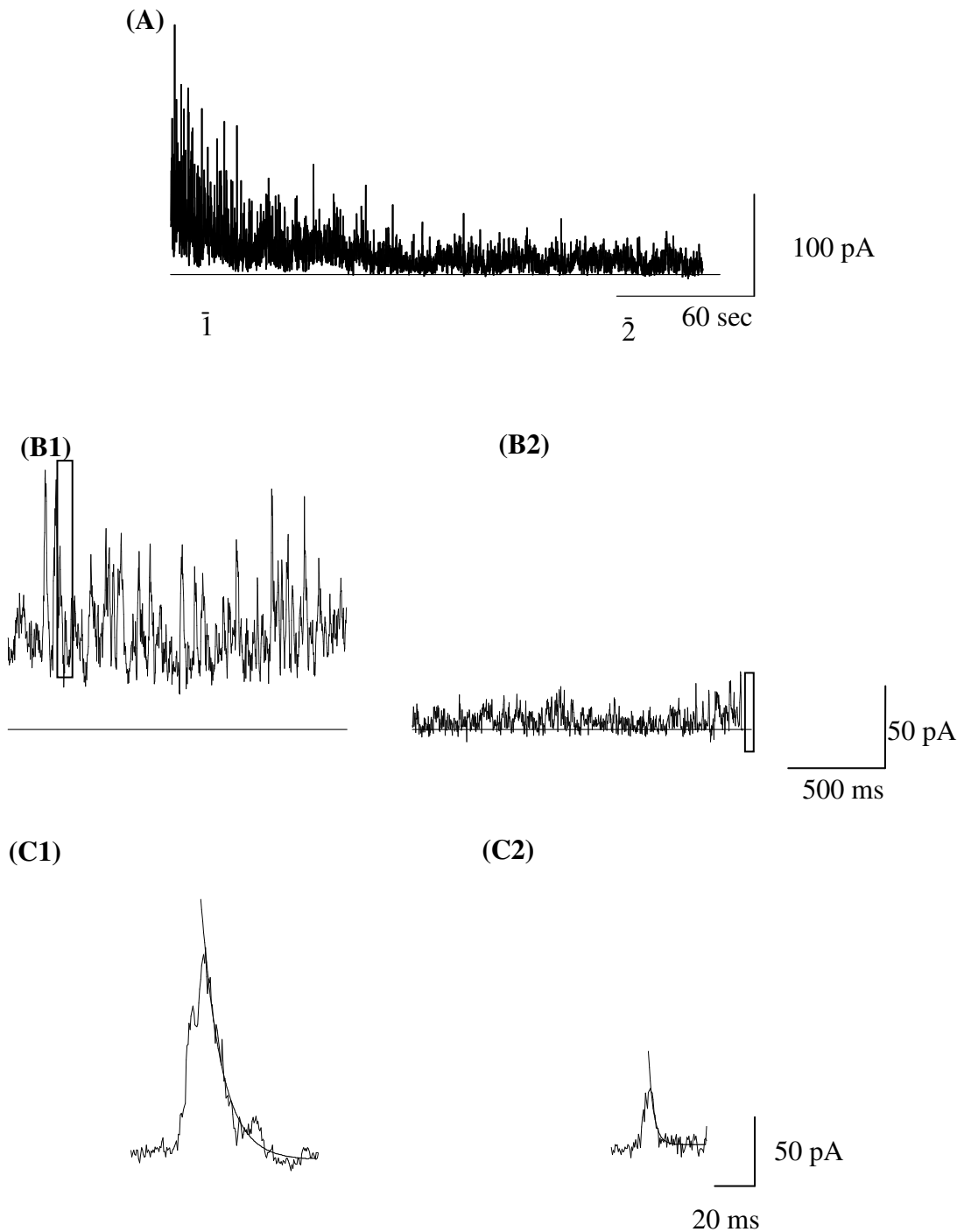


Figure 5.5 Example traces showing the effect of the inclusion of $10 \mu\text{M}$ ryanodine in the patch pipette on STOCs. (A) Compressed trace showing the effect of $10 \mu\text{M}$ ryanodine. Ryanodine will have already begun to diffuse into the cell at the beginning of the trace. The recording was started within approximately 45 seconds of gaining access to the cell. (B) Traces-up showing a close-up of the corresponding regions numbered in (A). The baseline of the trace is shown. (C) Traces showing the decay of the particular STOC highlighted in traces B1 and 2. $\tau = 8.26 \text{ ms}$ and 2.48 ms for STOCs at the beginning and end of the trace, respectively. Cells were held at a membrane potential of 0 mV . $[\text{Ca}^{2+}]_i = 100 \text{ nM}$; $[\text{K}^+]_i = 140 \text{ mM}$; $[\text{K}^+]_o = 6 \text{ mM}$.

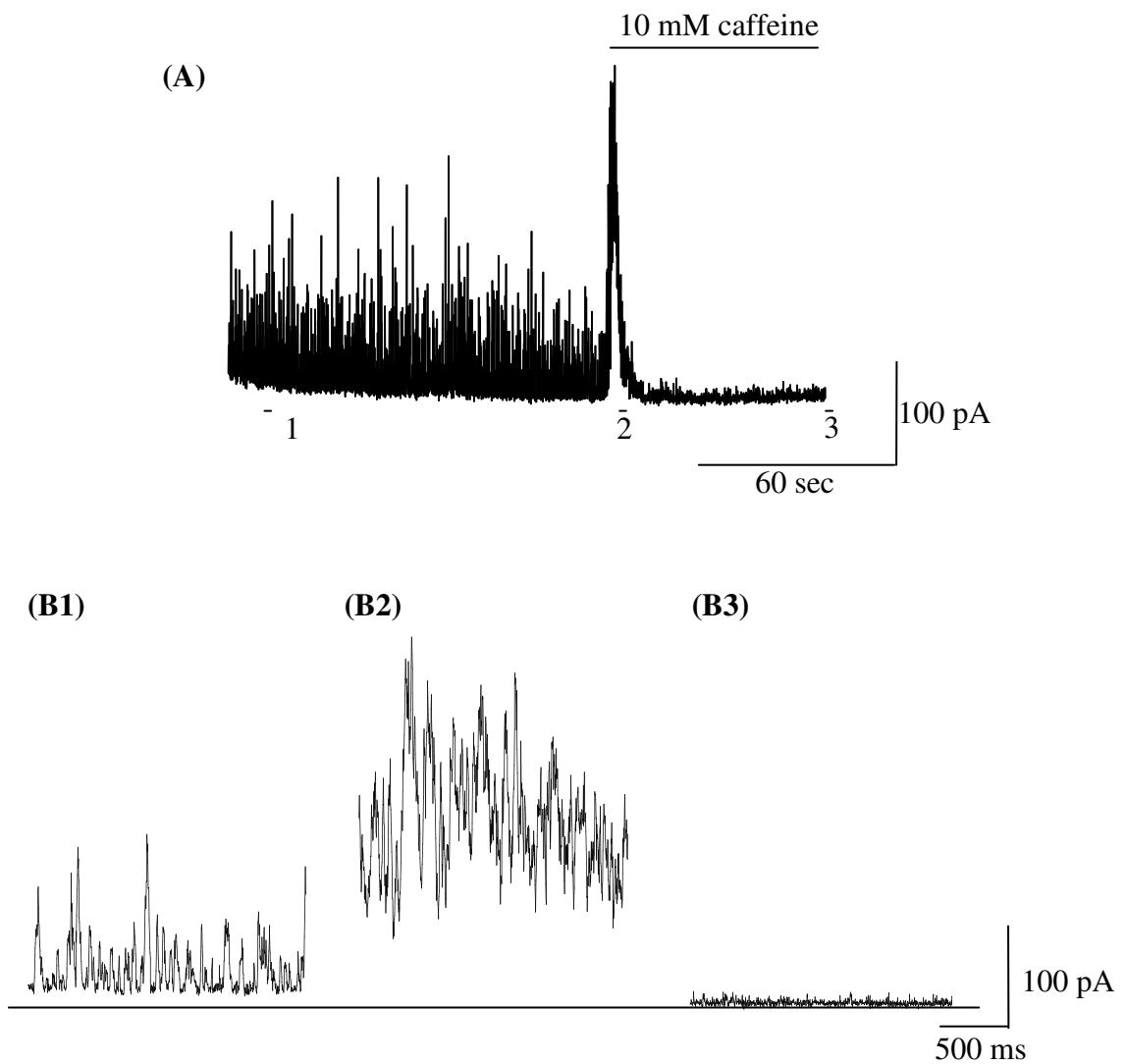


Figure 5.6 The effect of 10 mM caffeine on STOCs. (A) Compressed trace showing the effect of 10 mM caffeine on STOC activity. (B) Traces showing a close-up of the corresponding regions numbered in (A). Cells were held at a membrane potential of 0 mV. $[Ca^{2+}]_i = 100$ nM; $[K^+]_i = 140$ mM; $[K^+]_o = 6$ mM.

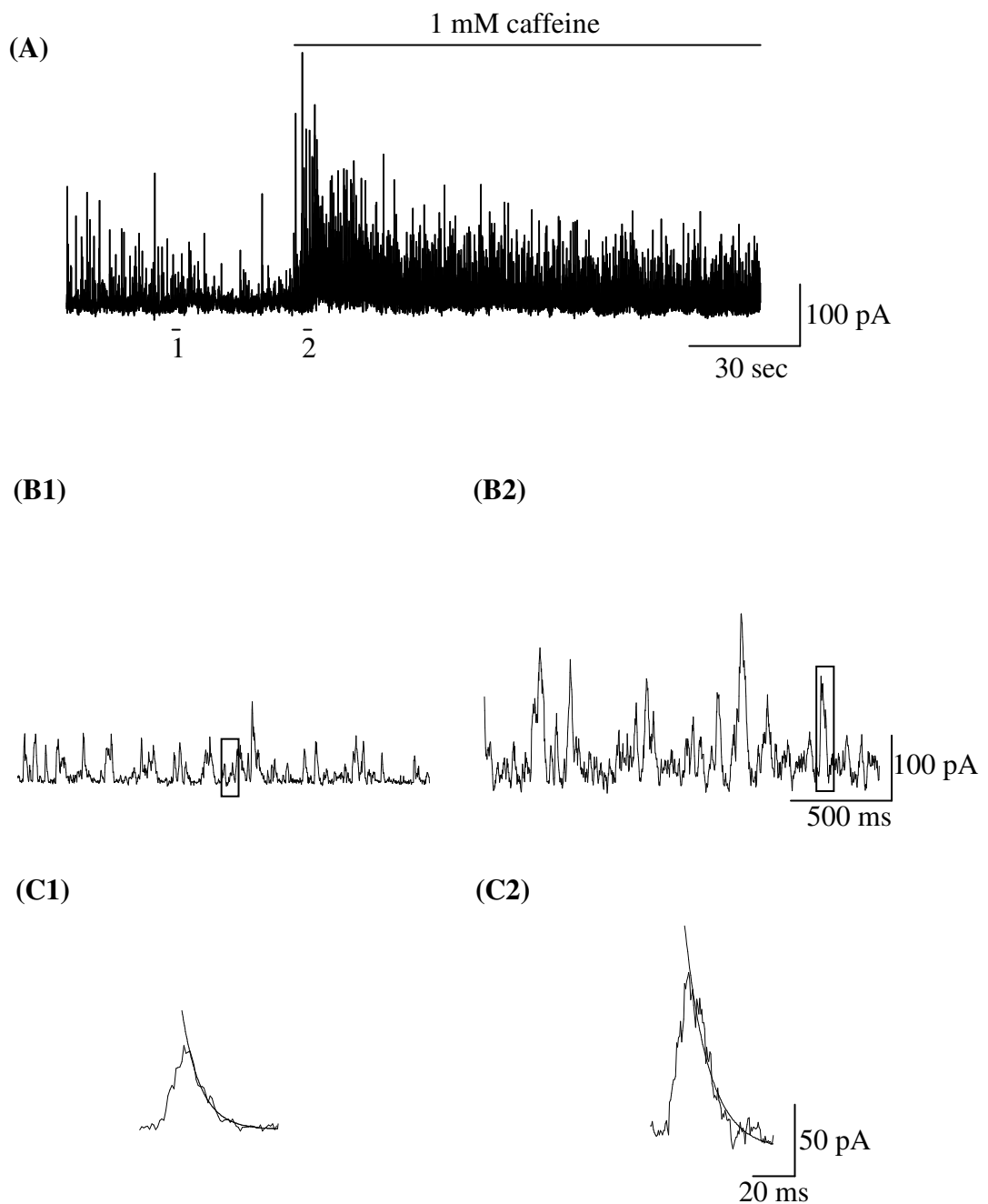


Figure 5.7 The effect of 1 mM caffeine on STOCs. (A) Compressed trace showing the effect of 1 mM caffeine on STOC activity. (B) Traces showing a close-up of the corresponding regions numbered in (A). (C) Traces showing the decay of the particular STOC highlighted in traces B1 and 2. $\tau = 7.32$ ms and 10.71 ms for control STOCs and STOCs after application with ET-1, respectively. Cells were held at a membrane potential of 0 mV. $[Ca^{2+}]_i = 100$ nM; $[K^+]_i = 140$ mM; $[K^+]_o = 6$ mM.

5.2.4 The effect of membrane potential on STOC activity

Having briefly investigated the role of SR Ca^{2+} stores in STOC activation, the effects of BK_{Ca} channel characteristics were then examined. A defining characteristic of BK_{Ca} channels is their ability to be modulated by both membrane potential and $[\text{Ca}^{2+}]_i$. I therefore decided to examine the effects of membrane potential on STOC activity. Table 5.1 shows the mean amplitude of STOCs recorded at different membrane potentials. Depolarization of the membrane potential significantly increased the mean amplitude of STOCs under all conditions, except for between -20 and -40 mV in the presence of 300 nM $[\text{Ca}^{2+}]_i$. This information shows that membrane depolarization increases the mean amplitude of STOCs ($n = 5$; $P = < 0.05$, one-way ANOVA with Bonferroni's test). Comparing this data to the amplitude data from single BK_{Ca} channel recordings suggests that this increase in STOC amplitude caused by membrane depolarization may largely be due to an increase in the single channel current, as the mean single channel current increases by a factor of ~ 3 between -40 and 0 mV compared to an increase in mean STOC amplitude by a factor of ~ 4 between these same potentials. The slightly larger increase in mean STOC amplitude may be due to a small increase in the amplitude of Ca^{2+} sparks. As was suggested by Perez, Ca^{2+} spark amplitude and the resultant STOC amplitude are believed to be related (Perez *et al*, 1999). In the presence of 100 nM $[\text{Ca}^{2+}]_i$, hyperpolarization of the cell membrane caused an increase in the fitted time constant of the gap frequency histogram from 36.59 ± 6.13 ms at 0 mV to 52.44 ± 14.15 ms at -20 mV, and 123.96 ± 11.34 ms at -40 mV ($n = 5$; figures 5.8 & 5.10). Hyperpolarization of the cell membrane from either 0 or -20 mV to -40 mV significantly decreased STOC frequency ($P = < 0.05$; one-way ANOVA with Bonferroni's test). Voltage was also seen to have an effect on the decay of STOCs, with hyperpolarization causing a decrease in the time constant at all $[\text{Ca}^{2+}]_i$. At 100 nM

$[Ca^{2+}]_i$, the time constant of STOC decay decrease from 8.21 ± 0.38 ms at 0 mV to 6.64 ± 0.24 ms and 4.31 ± 0.28 ms at -20 mV and -40 mV respectively ($n = \geq 30$ STOCs from a minimum of 3 cells; $P = <0.01$, one-way ANOVA with Bonferroni's test). Voltage was found to have no effect on the activation slope of STOCs (figure 5.11). This was compared to the activation of simulated STOCs where the rise time of the slope was altered in order to change tau activation and so demonstrate how a change in STOC activation would affect the plot of slope against maximum amplitude. Alteration of the rise time of simulated STOCs was found to affect the slope of the graph in very different manner to that of voltage (figure 5.12).

5.2.5 The effect of $[Ca^{2+}]_i$ on STOC activity

STOC amplitude and frequency also exhibit some dependence upon the $[Ca^{2+}]_i$. At physiological $[Ca^{2+}]_i$ of 100 and 300 nM the gap frequency histograms for STOCs observed at a membrane potential of 0 mV were fitted with time constants of 36.59 ± 6.13 ms and 32.06 ± 3.41 ms respectively. In the presence of 20 nM $[Ca^{2+}]_i$ the fitted time constant of the gap frequency histogram was 62.16 ± 5.73 ms at a membrane potential of 0 mV indicating a decrease in frequency. This increase in the fitted time constant at 20 nM $[Ca^{2+}]_i$ was found to be significant ($n = \geq 3$; $P = <0.05$, one-way ANOVA with Bonferroni's test). STOC amplitude does not appear to be greatly affected at lower $[Ca^{2+}]_i$ of between 20 and 100 nM, but an increase was seen between these $[Ca^{2+}]_i$ and 300 nM $[Ca^{2+}]_i$, particularly at 0 mV where the increase was found to be significant ($n \geq 4$; $P = < 0.01$, Student's unpaired t test; table 5.1). $[Ca^{2+}]_i$ was found to have no significant effect on either the time constant of STOC decay ($n = \geq 30$

STOCs from a minimum of 3 cells; $P = >0.05$, Student's paired t test; table 5.1; figure 5.9) or the slope of STOC activation (figure 5.13).

	20 nM $[Ca^{2+}]_i$		100 nM $[Ca^{2+}]_i$		300 nM $[Ca^{2+}]_i$	
	Mean amp (pA)	Decay (ms)	Mean amp (pA)	Decay (ms)	Mean amp (pA)	Decay (ms)
0 mV	36.8±0.6	8.21±0.33	39.8 ± 0.4	8.21±0.38	59.8 ± 1.2	8.93±0.26
-20 mV	21.6±0.4	6.47±0.25	26.2 ± 0.3	6.64±0.24	29.8 ± 0.6	7.11±0.29
-40 mV	9.9±0.2	4.61±0.21	9.2 ± 0.1	4.31±0.28	13.9 ± 0.2	4.94±0.34

Table 5.1 Table showing the mean amplitude and the mean time constant of the decay of STOCs under the appropriate recording conditions. Amplitude is expressed as mean amplitude in pA ± SEM; decay is expressed as mean time constant in ms ± SEM ($n \geq 3$).

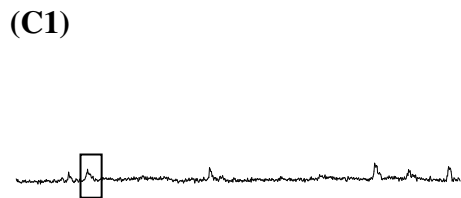
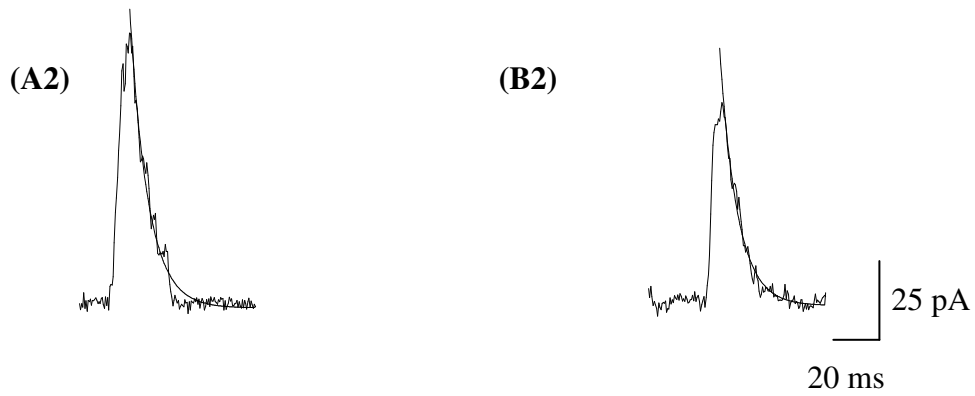
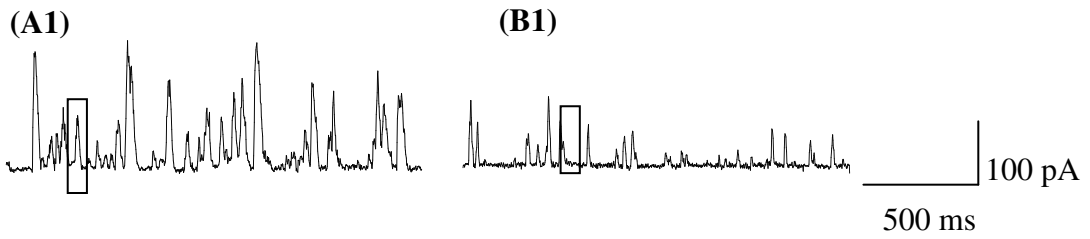
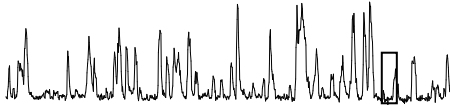
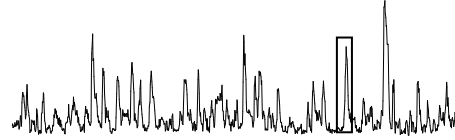


Figure 5.8 Effect of membrane potential on STOC activity. (A), (B), and (C) are traces recorded at 0 mV, -20 mV and -40 mV respectively. Traces numbered (1) show an example trace of STOCs recorded at the appropriate voltage. Traces numbered (2) show the highlighted STOC in (1) with an exponential fitted to the decay. $\tau = 7.91$ ms, 6.81 ms and 4.27 ms for STOCs recorded at 0 mV, -20 mV and -40 mV, respectively. All STOCs were recorded from cells with 100 nM $[Ca^{2+}]$ present in the patch pipette.

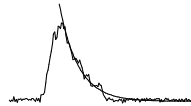
(A1)



(B1)



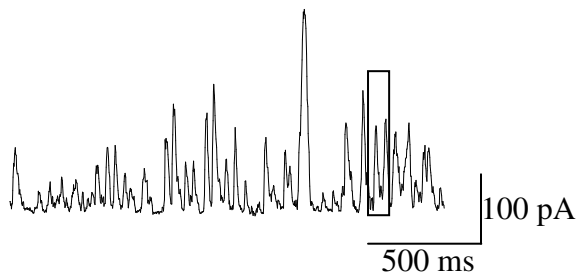
(A2)



(B2)



(C1)



(C2)

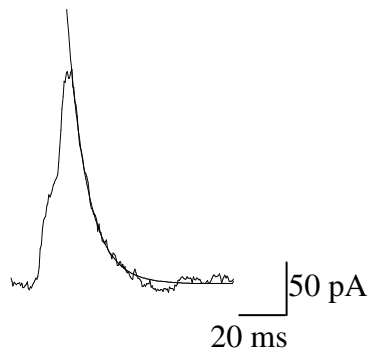


Figure 5.9 Effect of $[Ca^{2+}]_i$ on STOC activity. (A), (B), and (C) are traces recorded in the presence of 20 nM, 100 nM and 300 nM $[Ca^{2+}]_i$ respectively. Traces numbered (1) show an example trace of STOCs recorded with the appropriate $[Ca^{2+}]_i$. Traces numbered (2) show the highlighted STOC in (1) with an exponential fitted to the decay. $\tau = 8.36$ ms, 8.01 ms and 8.83 ms for STOCs in the presence of 20 nM, 100 nM and 300 nM, respectively. All STOCs were recorded from cells held at a membrane potential of 0 mV. $[Ca^{2+}]_i = 100$ nM; $[K^+]_i = 140$ mM; $[K^+]_o = 6$ mM.

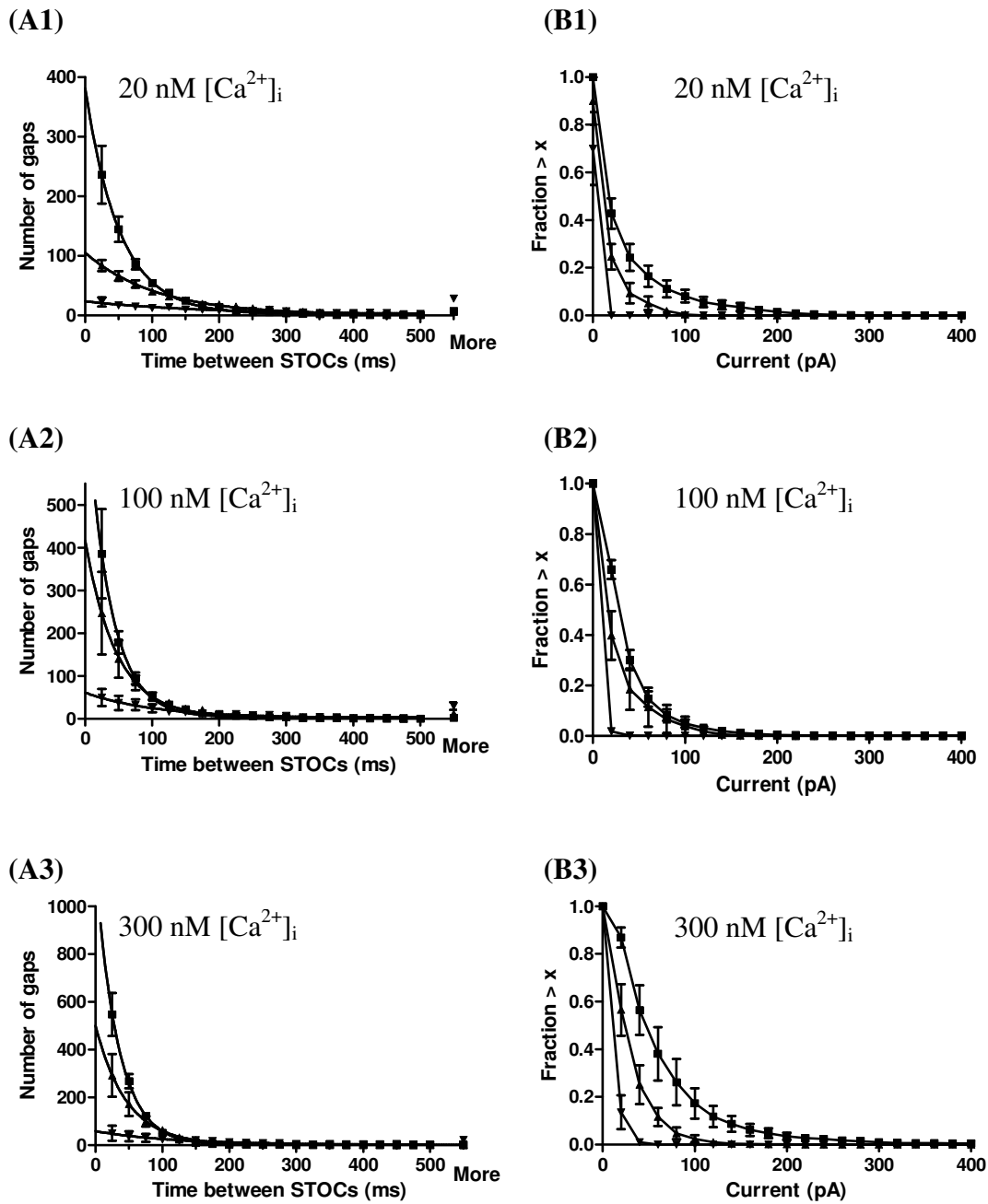


Figure 5.10 Effect of $[Ca^{2+}]_i$ and membrane potential on the frequency and amplitude of STOCs. Histograms showing (A) the collated frequency of STOCs, and (B) the normalized amplitude of STOCs from all collated recordings, showing the proportion of STOCs above a given amplitude. For all data, membrane potentials were at 0 mV (■), -20 mV (▲) and -40 mV (▼). $[Ca^{2+}]_i$ was as shown. STOCs were analysed for 1 min under each condition.

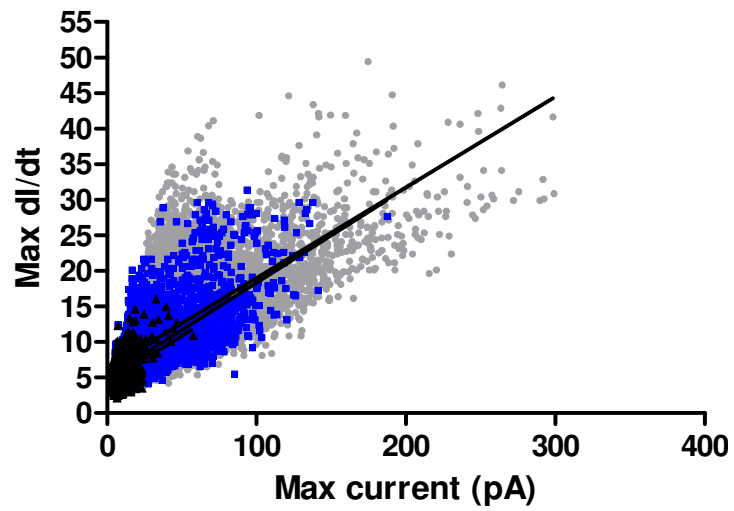


Figure 5.11 Graph showing the effect of membrane potential on the slope of STOC activation. -40 mV = black, -20 mV = blue, and 0 mV = grey.

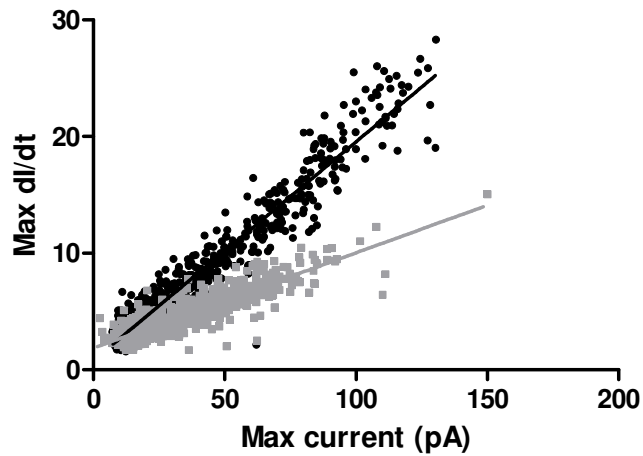


Figure 5.12 Graph showing the effect of an increase in STOC rise time on the activation slope of simulated STOCs. 2 ms rise time = black and 5 ms rise time = grey.

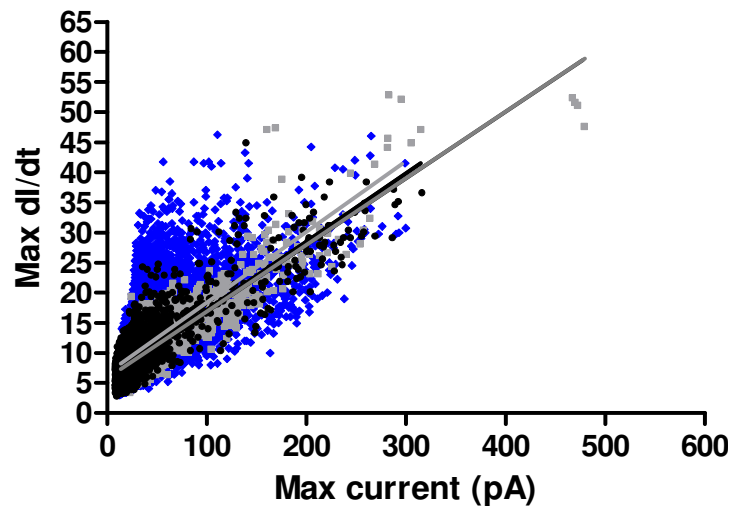


Figure 5.13 Graph showing the effect of $[Ca^{2+}]_i$ on the slope of STOC activation. 20 nM = black, 100 nM = blue, and 300 nM = grey.

5.2.6 The effects of vasoconstrictors on STOCs

Endogenous vasoconstrictors such as ET-1 and Ang II have been shown to affect both Ca^{2+} release from the SR and BK_{Ca} channel activity (Bonev *et al*, 1997; Porter *et al*, 1998). It is therefore logical to presume that they may regulate STOC activity in some way.

ET-1 reduced STOC amplitude from a mean of 43.4 ± 6.9 pA to 23.3 ± 3.7 pA ($n = 5$), a reduction of $46 \pm 5\%$ ($P = < 0.01$; Student paired t test; figures 5.14 & 5.15). This effect was independent of STOC amplitude; it did not remove any particular size class of STOCs. Application of 10 nM ET-1 also reduced STOC frequency, as indicated by an increase in the frequency histogram time constant from 59.75 ± 7.72 ms to 552.02 ± 181.36 ms ($n = 5$; figures 5.14 & 5.15). Background noise was similar for control and ET-1 experiments and so it is unlikely that a larger proportion of small STOCs went unresolved due to a larger background noise. This does therefore not explain the reduction in frequency. In order to test whether this apparent decrease in frequency was due to the reduction of STOC amplitude or whether ET-1 perhaps had an effect elsewhere, TEA was used as a control. TEA blocks the pore of the BK_{Ca} channel and should therefore have no effect on Ca^{2+} sparks. A concentration of 0.2 mM TEA was found to decrease BK_{Ca} whole-cell current by approximately 54%, a similar extent to the inhibition of BK_{Ca} caused by application of 10 nM ET-1. This concentration of TEA was therefore applied to STOCs to investigate its effect on STOC frequency. 0.2 mM TEA decreased STOC amplitude by 51% and increased the STOC frequency time constant from 49.21 ± 11.69 to 95.54 ± 21.17 ms ($n = 3$; $P = < 0.05$, Student's paired t test; figures 5.16 & 5.17). 0.2 mM TEA did not affect the rise time of the STOC activation slope in comparison with simulated STOCs. Although the effect of TEA on

STOC frequency appears to be smaller than the effect of ET-1, the difference was not found to be significant, possibly because of a large variance in the effect of ET-1 on frequency between cells ($P = >0.05$; Student unpaired t test). It is unfortunate that ET-1 cannot therefore be said to have an effect on Ca^{2+} spark activity as the data certainly suggests that this is the case. Fitting an exponential to the decay of the STOC showed that there was no significant difference after application of 10 nM ET-1, with τ values of 6.34 ± 0.14 ms and 5.78 ± 0.40 ms in the absence and presence of 10 nM ET-1 respectively ($n = \approx 50$ STOCs from 5 cells; $P = > 0.05$; Student paired t test; figure 5.14). The slope of STOC activation did not appear to be affected by application of ET-1 (figure 5.18).

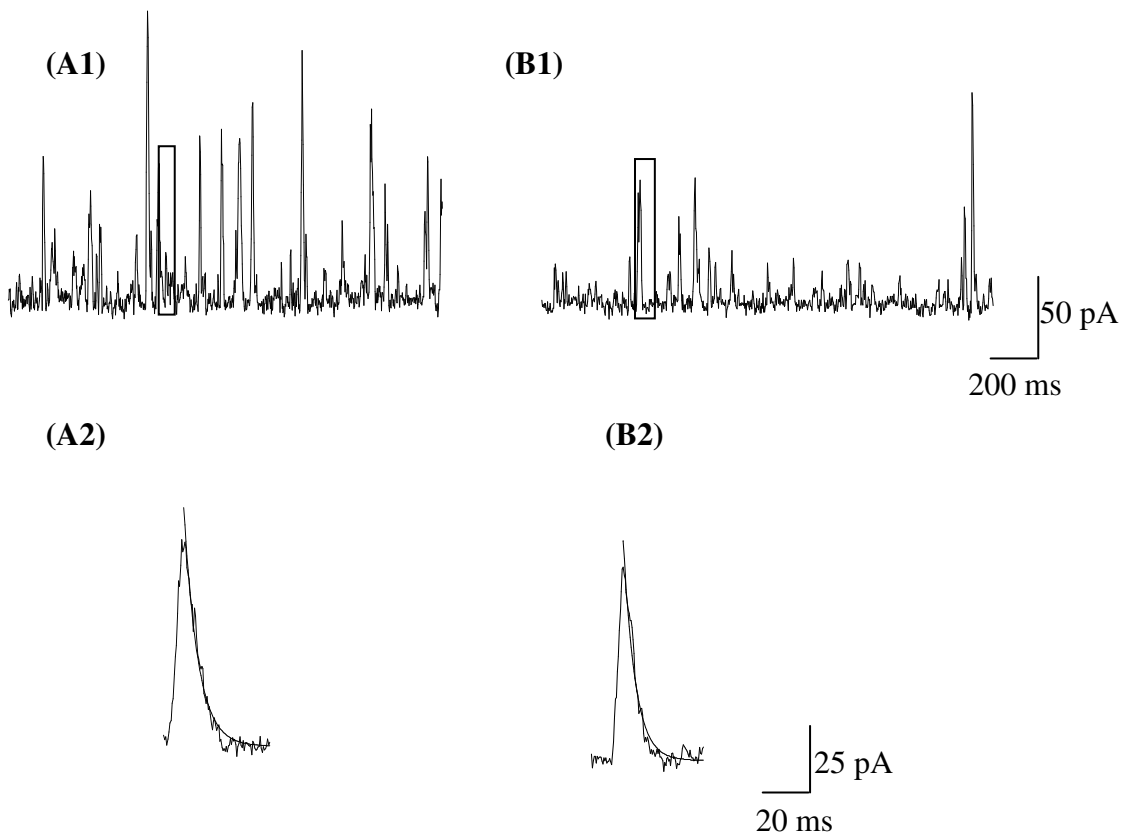


Figure 5.14 Effect of ET-1 on STOCs. (A) and (B) are traces recorded under control conditions and in the presence of 10 nM ET-1 respectively. Traces numbered (1) show an example trace of STOCs recorded. Traces numbered (2) show the highlighted STOC in (1) with an exponential fitted to the decay. $\tau = 6.16$ ms and 6.06 ms for control STOCs and STOCs after application with ET-1, respectively. Cells were held at a membrane potential of 0 mV. $[Ca^{2+}]_i = 100$ nM; $[K^+]_i = 140$ mM; $[K^+]_o = 6$ mM.

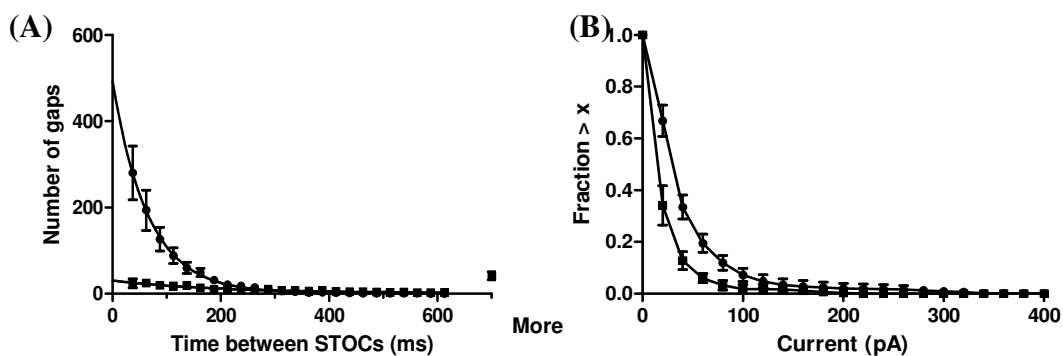


Figure 5.15 The effect of ET-1 on STOC frequency and amplitude. Histograms showing the effect of application of 10 nM ET-1 on (A) the frequency, and (B) the amplitude of STOCs. STOCs were analysed for 1 min.

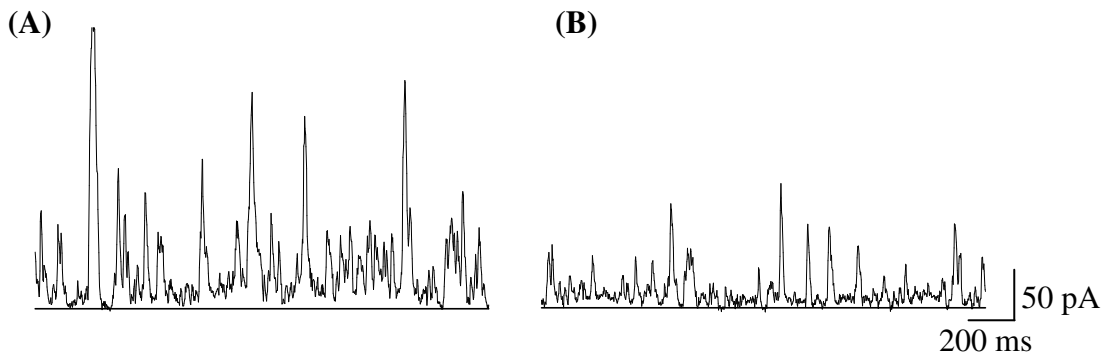


Figure 5.16 Effect of TEA on STOCs. Example traces recorded (A) under control conditions and, (B) in the presence of 0.2 mM TEA. Cells were held at a membrane potential of 0 mV with 100 nM $[Ca^{2+}]_i$ present in the patch pipette.

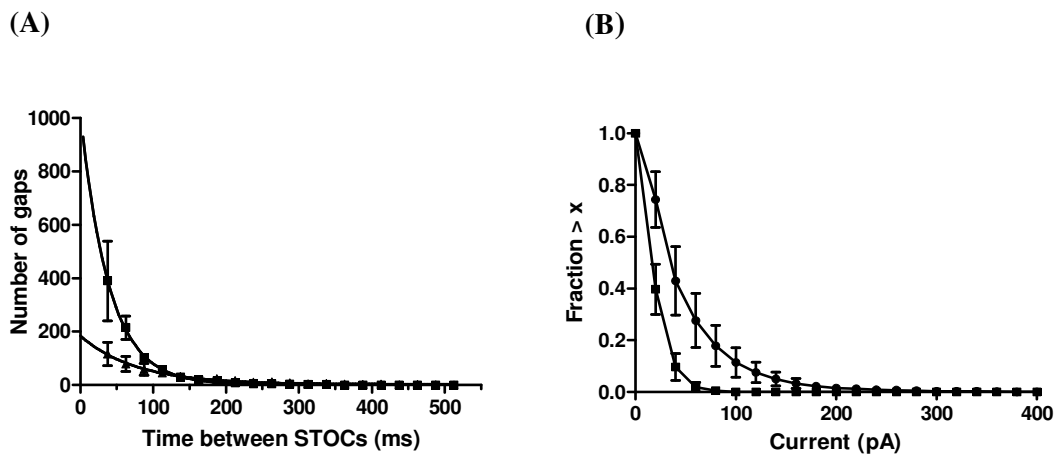


Figure 5.17 Effect of TEA on STOCs. Histograms showing the effect of application of 0.2 mM TEA on (A) the frequency, and (B) the amplitude of STOCs. Cells were held at a membrane potential of 0 mV. $[Ca^{2+}]_i = 100$ nM; $[K^+]_i = 140$ mM; $[K^+]_o = 6$ mM. STOCs were analysed for 1 min.

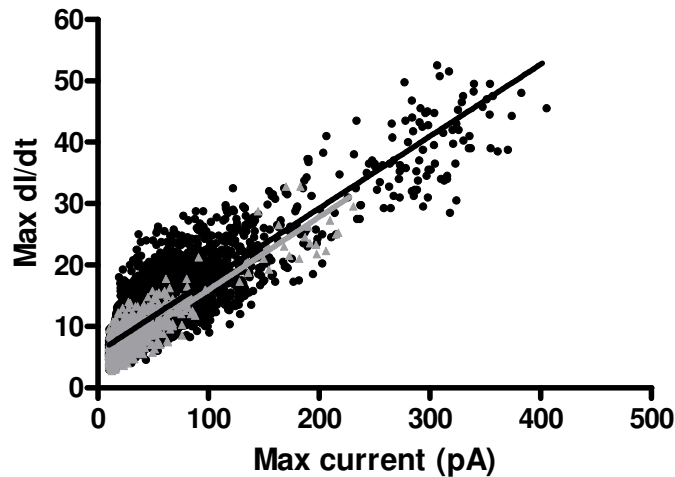


Figure 5.18 Graph showing the effect of application of 10 nM ET-1 on the slope of STOC activation. Control = black and ET-1 = grey.

Ang II also had an effect on STOC amplitude but much smaller in comparison to ET-1 as it only reduced mean STOC amplitude by $26 \pm 6\%$, from 50.0 ± 10.1 pA to 36.2 ± 5.8 pA ($n = 3$; $P = <0.05$; Student paired t test; figures 5.19 & 5.20). This effect was independent of STOC amplitude; it did not remove any particular size class of STOCs. The fitted time constant of the gap frequency histogram was increased from 43.18 ± 0.77 ms to 177.26 ± 25.55 ms suggesting that Ang II also had an effect on STOC frequency ($n = 3$; figures 5.19 & 5.20). Comparison of this decrease in frequency with that of 0.2 mM TEA showed that this decrease in frequency was statistically significant and so Ang II may have a modulatory effect on Ca^{2+} spark frequency ($P = <0.05$; Student's unpaired t test). However, Ang II reduced STOC amplitude to a much lesser degree than TEA and so it is perhaps not appropriate to make this comparison, even though the frequency data was found to be statistically significant despite the smaller effect on STOC amplitude. Fitting an exponential to the decay of the STOC gave mean time constants of 6.98 ± 0.28 ms and 6.85 ± 0.26 ms in the absence and presence of 100 nM Ang II respectively ($n = 30$ STOCs from 3 cells). This small decrease in the time

constant of STOC decay was not found to be significant ($P = >0.05$; Student's paired t test). A comparison of the slope of STOC activation in the absence and presence of 100 nM Ang II also showed that this was not affected (figure 5.21).

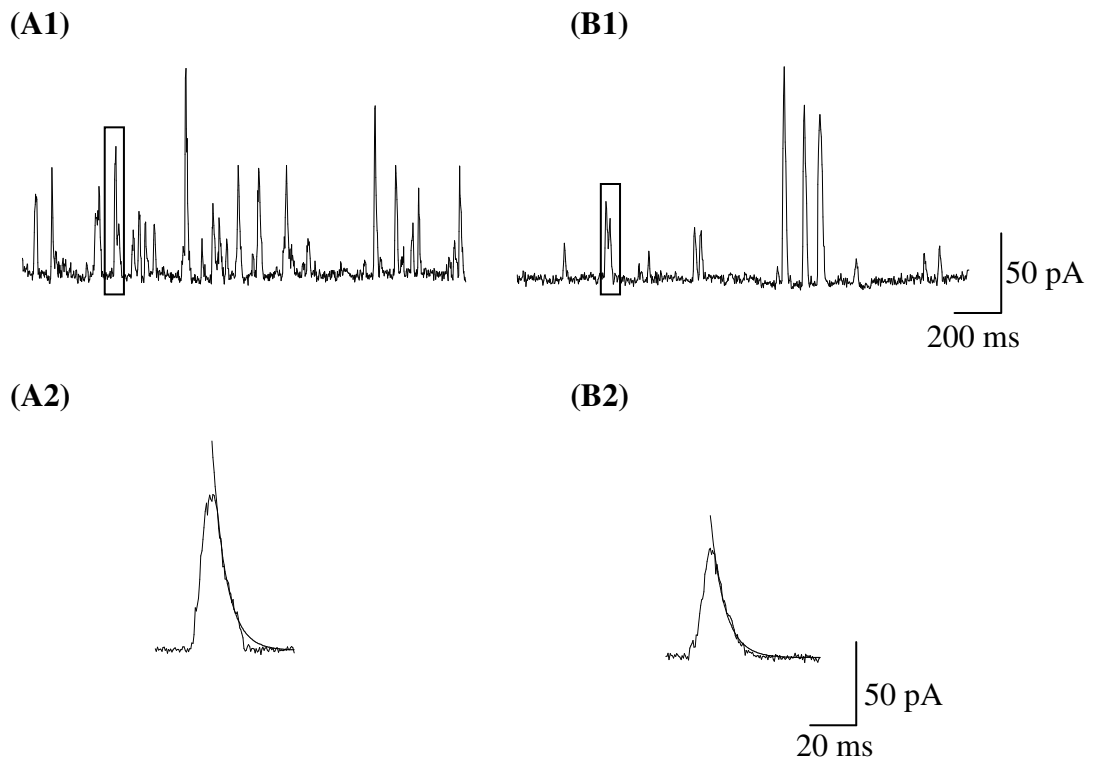


Figure 5.19 Effect of Ang II on STOCs. (A) and (B) are traces recorded under control conditions and in the presence of 100 nM Ang II respectively. Traces numbered (1) show an example trace of STOCs recorded. Traces numbered (2) show the highlighted STOC in (1) with an exponential fitted to the decay. $\tau = 6.81$ ms and 6.97 ms for control STOCs and STOCs after application with Ang II, respectively. All STOCs were recorded from cells held at a membrane potential of 0 mV with 100 nM $[Ca^{2+}]$ present in the patch pipette.

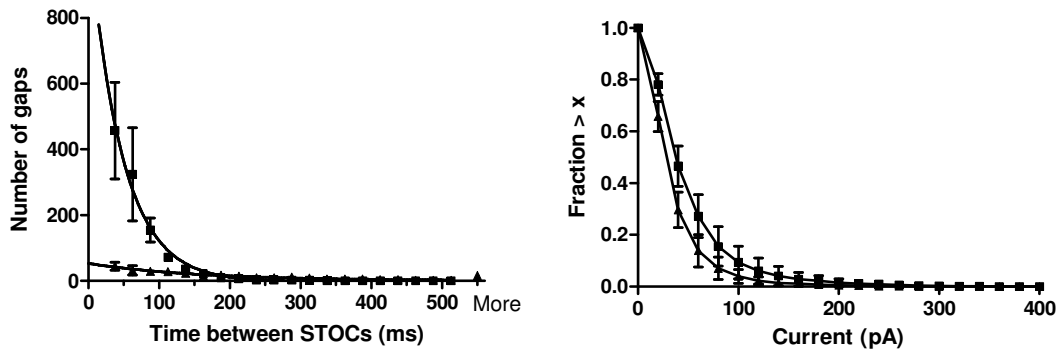


Figure 5.20 Effect of Ang II on STOCs. Histograms showing the effect of application of 100 nM Ang II on (A) the frequency, and (B) the amplitude of STOCs. Cells were held at a membrane potential of 0 mV. $[Ca^{2+}]_i = 100$ nM; $[K^+]_i = 140$ mM; $[K^+]_o = 6$ mM. STOCs were analysed for 1 min.

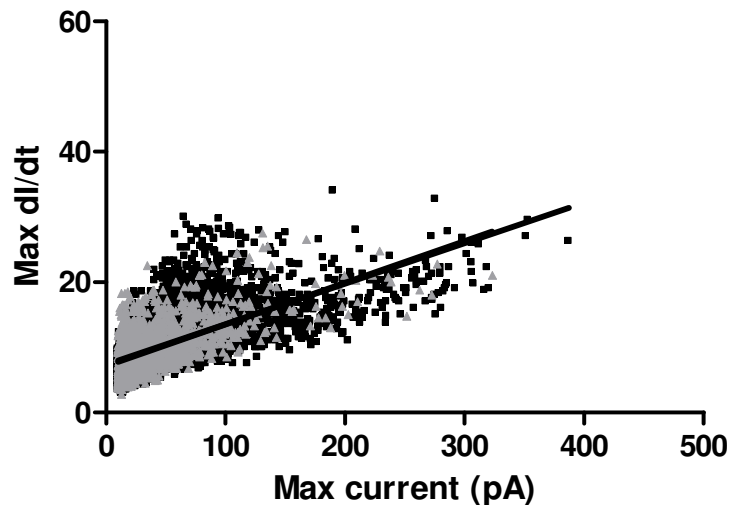


Figure 5.21 Graph showing the effect of application of 100 nM Ang II on the slope of STOC activation. Control = black and Ang II = grey.

5.3 Discussion

STOCs were observed when holding cells at constant physiological membrane potentials between 0 and -40 mV. As mentioned previously, the transient nature of STOCs means that a method for their detection is required. For the purpose of this thesis STOCs were detected using an in-house software programme (section 2.5.3).

5.3.1 Analysis of STOCs

Analysis of the simulated STOC files using the transient detection method described previously (section 2.5.3) revealed that a decrease in the amplitude of STOCs alone can also reduce the number of STOCs detected and so reduce the apparent frequency of STOCs. Analysis of STOCs simulated at 50% of the control amplitude resulted in a mean amplitude of approximately 49% of the original, as expected, but there was also an apparent decrease in frequency, indicated by an increase in the exponential fit to the gap frequency histogram from 110.0 ms to 230.5 ms. This decrease in frequency is likely to be caused by a number of STOCs going undetected above the noise of the trace.

5.3.2 STOCs in mesenteric artery smooth muscle cells are due to activation of BK_{Ca} channels

Application of either 100 nM penitrem A or 1 mM TEA largely abolished STOCs in isolated rat mesenteric artery smooth muscle cells, indicating that these currents are due to the activation of BK_{Ca} channels alone in this cell type. Many other groups have also reported the inhibition of STOCs upon application of BK_{Ca} channel blockers (Benham

& Bolton, 1986; Bolton & Lim, 1989; Bychkov *et al*, 1997; Borisova *et al*, 2007), indicating that the occurrence of STOCs is due to the activation of BK_{Ca} channels.

5.3.3 The effect of Ca²⁺ buffering on STOC activity

The tighter Ca²⁺ buffering provided by 10 mM EGTA drastically reduced the amplitude and frequency of STOCs. This suggests that STOCs are activated by changes in local [Ca²⁺]_i and the higher EGTA concentration limits these local concentration changes so limiting the activation of BK_{Ca} channels (Benham & Bolton, 1986). Ca²⁺ sparks are believed to increase the local [Ca²⁺]_i to a level of around 10 μM (Zhuge *et al*, 2002). In the presence of 1 mM EGTA it is quite likely that there are only a small number of EGTA molecules in this region, causing saturation of EGTA and still allowing the activation of BK_{Ca} channels by Ca²⁺ sparks. At 0 mV, and in the presence of 1 mM EGTA, nearly all healthy cells exhibited STOC activity. When the EGTA concentration is increased to 10 mM, the EGTA molecules are less likely to become saturated and so are able to buffer the release of Ca²⁺ from the SR much more effectively, reducing the probability of STOC activation under these conditions. It might be expected that reducing the EGTA concentration to 0.1 mM would cause STOC activity to increase further, however, Benham & Bolton (1986) did not report an increase in either the amplitude or frequency of STOCs when they reduced the EGTA concentration from 0.77 to 0.07 mM in isolated rabbit jejuna smooth muscle cells. However, they did report an increase in the number of cells exhibiting STOCs in the presence of reduced EGTA. It should be noted that they performed their experiments at a membrane potential of -40 mV where fewer cells exhibit STOCs under control

conditions and so increases in the number of cells exhibiting STOC can be more easily observed.

STOCs recorded from vascular smooth muscle cells using the perforated patch technique display quite a large amount of STOC activity, closer to that seen in whole-cell recordings buffered with 1 mM EGTA than with 10 mM (Liu *et al*, 2004; Hayoz *et al*, 2007). This technique gives an idea of how the intact vascular smooth muscle cell acts because the intracellular milieu remains intact.

5.3.4 Ca²⁺-release is from the SR

The activity of STOCs could be modulated by including ryanodine and caffeine in the extracellular solution. Both of these compounds are known to cause the release of Ca²⁺ from the SR with the concentrations used. As mentioned previously, ryanodine at a concentration of 10 μM is known to cause Ca²⁺ store depletion by holding the RyR in the open conformation (Wagner-Mann *et al*, 1992). The initial release of Ca²⁺ caused an increase in STOC activity in the first instance, which was seen as soon as a recording was started, but then STOCs were greatly reduced as the Ca²⁺ store became empty. Caffeine also affects Ca²⁺ release probably by increasing the sensitivity of RyRs to Ca²⁺ (Ganitkevich & Isenberg, 1992). 10 mM caffeine quickly depletes Ca²⁺ stores and, as was seen after the application of 10 μM ryanodine, this resulted in large initial increase in STOC activity before STOCs were then reduced. Contrary to the effect of ryanodine however, store depletion by caffeine occurred much faster and led to the complete inhibition of STOCs. Application of 1 mM caffeine also appeared to increase Ca²⁺ release but the initial release was to a lesser extent than that of 10 mM caffeine. This was indicated by an increase in STOC activity but in a different manner to that caused

by 10 mM caffeine. The initial increase in STOC activity was much smaller than that seen in the presence of 10 mM caffeine, but this increase could be sustained rather than quickly leading to a reduction in STOCs. Ca^{2+} release is therefore likely to have been stimulated but not to the extent where stores were depleted within the timeframe of these experiments. Application of caffeine in this manner suggests that CICR is able to occur through the RyRs present in rat mesenteric arterial smooth muscle cells.

5.3.5 The effect of membrane potential on STOC activity

I have shown that hyperpolarization of the cell membrane decreases both the frequency and amplitude of STOCs in rat mesenteric artery smooth muscle cells. At all $[\text{Ca}^{2+}]_i$, hyperpolarization of the cell membrane led to a decrease in the frequency of STOCs. In the presence of 100 nM $[\text{Ca}^{2+}]_i$, the mean fitted decay of the gap frequency histogram increased from 36.59 ± 6.13 ms at 0 mV to 52.44 ± 14.15 ms and 123.96 ± 11.34 ms at -20 and -40 mV respectively, indicating a decrease in the frequency of STOCs, especially when the membrane is hyperpolarized to -40 mV ($n = 5$). These decreases in frequency, in the presence of either 100 or 300 nM $[\text{Ca}^{2+}]_i$, were significant when hyperpolarizing the membrane potential to -40 mV ($P = <0.05$; one-way ANOVA with Bonferroni's test). This decrease in frequency with hyperpolarization is likely to be due mostly to a decrease in BK_{Ca} channel activity, with the P_{open} of the channel decreasing with membrane hyperpolarization due to the voltage-dependence of BK_{Ca} the channel. This means that at hyperpolarized membrane potentials it is possible that some smaller STOCs may go undetected as they cannot be resolved above the noise. As the membrane potential depolarizes, the P_{open} of these channels increases, increasing the amplitude of some of the STOCs so that they can now be detected. Membrane

depolarisation may also cause the single channel amplitude to increase and this may lead to undetected STOCs increasing in size so that they may then be detected. This would show as an apparent increase in STOC frequency upon analysis but would be due to the increased activity of BK_{Ca} channels rather than any effect on Ca²⁺ spark frequency. Testing of the transient detection method did reveal that some STOCs may not be detected when the amplitude of STOCs was decreased by a set figure of 50%, as the decay of the frequency histogram increased. In some smooth muscle types, depolarization may lead to an increase in Ca²⁺ spark activity, due possibly to the activation of VDCCs increasing Ca²⁺ influx that can then go on to activate RyRs to induce Ca²⁺ release by a CICR mechanism (Burdyga *et al*, 1995; Kamishima & McCarron, 1997). This increase in RyR activity may then increase STOC activity due to the close proximity of RyRs to BK_{Ca} channels. Using only electrophysiological methods it is difficult to separate the effect of membrane potential on BK_{Ca} channels from any effect that membrane potential may have on Ca²⁺ sparks. In addition to the effect on BK_{Ca} channel activation, an increase in Ca²⁺ spark frequency following depolarization may contribute to the increase in STOC frequency.

An increase in STOC amplitude upon cell membrane depolarization was also seen across all [Ca²⁺]_i, and this may be due to a number of factors. Depolarization leads to an increase in both the P_{open} and single channel current of BK_{Ca} channels. This will therefore increase STOC amplitude for a Ca²⁺ spark of fixed amplitude through a combination of an increase in the number of BK_{Ca} channels activated and also greater single channel current amplitude for those channels. It may also cause an increase in the frequency or amplitude of Ca²⁺ sparks (Jaggar *et al*, 1998b). It has been suggested that a large proportion (41%) of STOCs observed in smooth muscle cells isolated from cerebral arteries may occur without a detectable Ca²⁺ spark associated with it (Perez *et*

al, 1999). The mean amplitude of these particular STOCs was 16 pA compared to a mean amplitude of 33 pA in “spark-induced” STOCs (cells held at -40 mV). If “sparkless” STOCs such as these were actually to exist, then this could explain the small mean amplitude of STOCs that I recorded at -40 mV. As cell membrane potential was depolarized, Ca²⁺ spark frequency may have increased and a lower proportion of STOCs may have been activated without a detectable Ca²⁺ spark, leading to an increase in the mean amplitude of STOCs at these depolarized potentials. However, confocal microscopy is only able to scan a certain portion of the cell whereas STOCs are recorded from the whole of the cell membrane when recorded in the whole-cell patch configuration. Perez therefore concluded that these so-called sparkless STOCs were actually activated by small, brief Ca²⁺ sparks from areas of the cell that were not scanned. It is therefore unlikely that sparkless STOCs are the reason for the small mean STOC amplitude seen at -40 mV and so an increase in Ca²⁺ spark frequency was probably not the cause of the increase in amplitude that I observed. It may instead be that CICR increased the amplitude of the Ca²⁺ spark, and that this increase in the amount of Ca²⁺ release was instead the cause of the increase in STOC amplitude, as the larger Ca²⁺ spark amplitude would increase the local [Ca²⁺]_i to increase the P_{open} of BK_{Ca} channels. Perez (Perez *et al*, 1999) also reported that Ca²⁺ spark amplitudes and STOC amplitudes were related, and that there was a strong correlation between Ca²⁺ spark amplitude and the amplitude of the associated STOC. However, examination of the effect of membrane depolarization on Ca²⁺ spark amplitude revealed that an increase in membrane potential from -50 mV to -20 mV led to only a 30% increase in spark amplitude (Herrera *et al*, 2001). The increase in STOC amplitude is much greater and therefore is more likely to be due an increase in BK_{Ca} channel activity, partly through an increase in the P_{open} of the channel, and partly through an increase in the single channel

current. Membrane depolarization led to an increase in the time constant of STOC decay, from 4.31 ± 0.28 ms at -40 mV to 6.64 ± 0.24 ms and 8.21 ± 0.38 ms at -20 mV and 0 mV respectively in the presence of 100 nM $[Ca^{2+}]_i$. A similar increase in the time constant of STOC decay was also seen in the presence of 20 nM and 300 nM $[Ca^{2+}]_i$. This is concurrent with an effect on channel kinetics by changes in membrane potential. This alteration of kinetics could be due to an effect on the kinetics of either the BK_{Ca} channel alone, or of both RyR and BK_{Ca} channels. However, it has been reported that depolarization of the cell membrane has no effect on the decay of Ca^{2+} sparks in intact cerebral arteries (Jaggar *et al*, 1998b) and so any effect of membrane potential on STOC decay observed here is perhaps more likely to be due to altered BK_{Ca} channel kinetics. There are also a number of other factors that may also influence STOC decay tau besides an effect on BK_{Ca} kinetics. For example, the further the BK_{Ca} channels from the Ca^{2+} spark release site, the greater the level of Ca^{2+} diffusion and so tau is smaller. An increase in the rate of Ca^{2+} removal or reuptake by membrane proteins of the SR or plasma membrane will also decrease the decay time of the STOC. A change in the Ca^{2+} sensitivity of the BK_{Ca} channel may also affect the decay time of the STOC. An increase in Ca^{2+} sensitivity, such as that seen when a beta1 subunit associates with the alpha-subunit when compared to the alpha-subunit alone, would mean that the channels may still be activated by Ca^{2+} even after some Ca^{2+} diffusion has occurred. This may cause the STOC decay tau to be increased. Positive cooperativity between Ca^{2+} release sites may cause further Ca^{2+} release to occur which could cause further BK_{Ca} channels even once the STOC has started to decay. The decay may then occur at a slower rate and so the STOC decay tau would be increased.

Depolarization of the cell membrane potential had no effect on the rise time of STOC activation. It is possible that STOC activation is primarily governed by the characteristics of the Ca^{2+} spark.

5.3.6 The effect of $[\text{Ca}^{2+}]_i$ on STOC activity

STOCs also show a degree of dependence on $[\text{Ca}^{2+}]_i$, but from my data this does not appear to be to the same extent as that of voltage. Between the physiological $[\text{Ca}^{2+}]_i$ of 100 and 300 nM, there appears to be an increase in mean STOC amplitude, particularly at 0 mV where a 50% increase in mean amplitude from 39.8 ± 0.4 pA to 59.8 ± 1.2 pA was observed, but not in frequency. At a given voltage the frequency of STOCs was not significantly different between $[\text{Ca}^{2+}]_i$ of 100 and 300 nM, with decay values from the frequency histogram of 36.59 ± 6.13 ms, 52.44 ± 14.15 ms and 123.96 ± 11.34 ms at 0, -20 and -40 mV respectively in the presence of 100 nM $[\text{Ca}^{2+}]_i$ compared to values of 32.06 ± 3.41 ms, 46.03 ± 3.91 ms and 195.92 ± 54.25 ms at the same respective voltages in the presence of 300 nM $[\text{Ca}^{2+}]_i$ ($n = \geq 3$; $P = >0.05$; Student's unpaired t test). The increase in STOC amplitude at the higher $[\text{Ca}^{2+}]_i$ could perhaps be due to more BK_{Ca} channels at the periphery of the Ca^{2+} spark being activated, as the increase in $[\text{Ca}^{2+}]_i$ would have a larger effect on the P_{open} of BK_{Ca} channels situated further away from the source of the Ca^{2+} spark than those situated closest to the release site. The similar STOC frequencies suggest that $[\text{Ca}^{2+}]_i$ within the physiological range may not have any effect on Ca^{2+} spark frequency. This is in agreement with many reports describing the requirement of micromolar $[\text{Ca}^{2+}]_i$ to induce the release of Ca^{2+} through RyRs by a CICR mechanism (Fill; Copello, 2002). Also, with Ca^{2+} sparks increasing the local $[\text{Ca}^{2+}]_i$ to micromolar levels, it is possible that the increased global $[\text{Ca}^{2+}]_i$

would have a minimal effect on the local $[Ca^{2+}]_i$ in the area surrounding BK_{Ca} channels and RyRs. 20 nM $[Ca^{2+}]_i$ had very little effect on STOC amplitude when compared to 100 nM $[Ca^{2+}]_i$, perhaps suggesting that the P_{open} of BK_{Ca} is not significantly different between these two $[Ca^{2+}]_i$. The reduction in STOC frequency observed in the presence of 20 nM $[Ca^{2+}]_i$ may be due to a reduced SR load.

As was the case for membrane depolarization, an increase in $[Ca^{2+}]_i$ had no effect on the rise time of STOC activation. Again, this could be because STOC activation is primarily controlled by the Ca^{2+} spark. Also, $[Ca^{2+}]_i$ at the levels tested did not appear to have any significant effect on the decay of STOCs. This indicates that global $[Ca^{2+}]_i$ is perhaps unlikely to have a great effect on the P_{open} of BK_{Ca} channels when Ca^{2+} sparks have increased local $[Ca^{2+}]_i$ to a micromolar level, as there would not be a great difference in overall local $[Ca^{2+}]_i$ once a Ca^{2+} spark has been released. However, it is important to note that there are difficulties concerned with the analysis of all $[Ca^{2+}]_i$ data, as the effect of $[Ca^{2+}]_i$ on STOCs was only ever investigated in different cells, two $[Ca^{2+}]_i$ were not compared within the same cell. It might be expected that an increase in $[Ca^{2+}]_i$ from 100 to 300 nM would increase the Ca^{2+} load of SR stores, leading to an increase in Ca^{2+} spark frequency, but this was not observed. The wide variation in Ca^{2+} spark activity between cells due to a difference in the number of spark sites could affect this data to quite a great extent, which might explain why no difference in STOC frequency was observed at these $[Ca^{2+}]_i$. The ability to monitor both Ca^{2+} spark and STOC activity simultaneously would produce much more conclusive data when trying to separate the effects of $[Ca^{2+}]_i$ and membrane potential on Ca^{2+} sparks from those directly on BK_{Ca} channels.

It is possible that the increase in $[Ca^{2+}]_i$ from 100 to 300 nM reduces the buffering capacity of EGTA as one would expect that there would be less unbound EGTA

present. Both 100 and 300 nM $[Ca^{2+}]_i$ are within the “good buffering range” of EGTA, however concentrations of 10 μ M, the local $[Ca^{2+}]$ believed to be produced by a Ca^{2+} spark, is much higher. It is therefore unlikely that reduced buffering capacity is to blame for the increase in STOC activity seen in the presence of 300 nM $[Ca^{2+}]_i$.

5.3.7 Modulation of STOCs by ET-1 & Ang II

The external application of either of the known vasoconstrictive compounds, ET-1 and Ang II, was seen to have an effect on both the frequency and amplitude of STOCs.

10 nM ET-1 reduced mean STOC amplitude significantly from 43.4 ± 6.9 pA to 23.3 ± 3.7 pA ($n = 5$). It also reduced the frequency of STOCs, indicated by an increase in the fitted time constant of the gap frequency histogram from 59.75 ± 7.72 ms to 552.02 ± 181.36 ms. To determine whether this effect on frequency was due to an effect on BK_{Ca} channels alone or also on Ca^{2+} spark frequency, this data was compared to that of the application of 0.2 mM TEA. TEA is a compound known to block the pore of BK_{Ca} channels (Langton *et al*, 1991) and should therefore have no effect on Ca^{2+} spark frequency. Any effect of TEA on the frequency of STOCs should therefore be due to a decrease in STOC amplitude, reducing the number of STOCs that could be detected. This concentration of TEA decreased the mean amplitude of STOCs by approximately 51% and also increased the decay of the frequency histogram from 49.21 ± 11.69 ms to 95.54 ± 21.17 ms, indicating a decrease in STOC frequency ($n = 3$; $P = <0.05$; Student's paired t test). This effect of TEA on frequency was not found to be significantly different from that of ET-1 and so this suggests that the effect of ET-1 on frequency is due to a decrease in BK_{Ca} channel activity, not Ca^{2+} sparks. However, the variation in Ca^{2+} spark activity seen even under control conditions makes this difficult

to compare and it is possible that the large variance in the time constant of the gap frequency histogram is the reason why the effect of ET-1 on frequency was not found to be significantly different to that of 0.2 mM TEA. It is perhaps possible that the decrease in STOC amplitude seen is due to a reduction in the number of channels, caused by inactivation of BK_{Ca} channels as described by McManus & Magleby (1988). However, as STOCs are spontaneous events caused by the opening of a number of BK_{Ca} channels, and these currents were recorded over a period of minutes, it is unlikely that a large proportion of channels would remain silent over this length of time. It might be expected that the effect of long-lived closed states could be evened out during this length of time. Since it is impossible to know whether this is the cause it must be presumed that the effect was due to an ET-1 effect on STOCs. It is possible that ET-1 could perhaps increase the possibility of BK_{Ca} channels entering the long-lived closed state.

Application of ET-1 also decreased the time constant of STOC decay from 6.34 ± 0.19 ms to 5.78 ± 0.40 ms but this was not found to be significant. The effect of ET-1 on the activation slope of STOCs was also examined and plotting slope against maximum amplitude showed that this was not found to be affected. This was compared to the activation of simulated STOCs where the rise time of the slope could be altered to demonstrate how a change in STOC activation would affect the plot of slope against maximum amplitude. Comparison of STOC activation in this manner suggested that ET-1 is unlikely to have any effect on STOC activation. STOC activation is likely to be almost entirely dependent upon Ca²⁺ spark release, with spark activation determining STOC activation, and this data suggests that coupling between Ca²⁺ sparks and STOCs has not been affected by ET-1 in this way.

Considering all of this data together, the effects of ET-1 on STOCs appears to be largely due to an effect on BK_{Ca} channels rather than Ca²⁺ sparks, and yet BK_{Ca} channel kinetics do not appear to be significantly affected. It is therefore not clear exactly how ET-1 is having an effect. This data suggests that ET-1 may reduce the number of channels of BK_{Ca} channels present in the cell membrane, perhaps by removing channels or preventing channels from being inserted in the membrane during protein recycling, rather than the actual modulation of channel activity within the membrane (Nesti *et al*, 2004). It is perhaps possible that phosphorylation by protein kinases such as PKC could target the channel for removal from the membrane, or that this phosphorylation could prevent the channels from being inserted into the membrane. The data also suggests that ET-1 has an effect on Ca²⁺ spark frequency, however, this was not found to be statistically significant and so should not be considered.

Application of 100 nM Ang II decreased the mean amplitude of STOCs from 50.0 ± 10.1 pA to 36.2 ± 5.8 pA. It also decreased the frequency of STOCs, indicated by an increase in the decay of the gap frequency histogram from 43.18 ± 0.77 ms to 177.26 ± 25.55 ms. When this effect on STOC frequency was compared to that of TEA the decrease was found to be significant (n = 3; P = < 0.05; Student's paired *t* test). It is therefore possible that Ang II may modulate Ca²⁺ spark frequency.

Ang II was found to have no effect on STOC activation as the plot of the activation slope against maximum amplitude was not seen to be affected. There was also no significant decrease in STOC decay as the fitted time constants were 6.98 and 6.85 ms for control and Ang II respectively.

Ang II appears to have a significant effect on both the amplitude and frequency of STOCs suggesting that it exert its effects through modulation of both BK_{Ca} channels

and RyRs. The observed effect on STOC frequency suggests that it may also modulate Ca^{2+} spark frequency. The effects of Ang II on STOC amplitude are likely to be due to modulation of BK_{Ca} channels. However, this does not appear to be due to an alteration of BK_{Ca} single channel activity as neither STOC activation nor STOC decay was affected. The effects of Ang II may therefore be due to an alteration in the number of channels present in the cell membrane, as was hypothesized for ET-1.

ET-1 appears to have a greater effect on STOC amplitude than Ang II, despite these two compounds having a similar effect on BK_{Ca} whole cell current. These differences in the effects of ET-1 and Ang II are perhaps due to different signalling pathways being utilized by ET-1 and Ang II, with these two peptides perhaps relying on different PKC isoforms. Ang II has also been reported to inhibit Kv and K_{ATP} channels through a PKA-dependent mechanism (Hayabuchi *et al*, 2001a; Hayabuchi *et al*, 2001b). It is therefore possible that Ang II may also modulate BK_{Ca} channels through a similar PKA-dependent mechanism and this could partly explain the different effects of ET-1 and Ang II on STOCs. Inhibition of PKA could also be responsible for the additional reduction in Ca^{2+} spark frequency. Both PKC and PKA have been shown to modulate Ca^{2+} spark activity in some way. Bonev reported that activators of PKC, such as phorbol 12-myristate13-acetate (PMA) and DOG, decreased Ca^{2+} spark frequency by 72% and 60% respectively in cerebral arterial smooth muscle cells (Bonev *et al*, 1997). Activators of PKA, on the other hand, such as forskolin and cAMP, have been shown to increase Ca^{2+} spark frequency, and this is believed to be through relief of phospholamban inhibition of the SR Ca^{2+} -ATPase (Wellman *et al*, 2001). This effect could be reversed using PKA inhibitors.

6 DISCUSSION

In this thesis I have attempted to characterize the modulation of BK_{Ca} channel activity by Ca²⁺, ET-1 and Ang II using both inside-out excised patch and conventional whole-cell patch clamp techniques. The voltage- and Ca²⁺-dependence of single channel activity, STOCs and BK_{Ca} whole-cell currents have been investigated in turn, using near physiological [K⁺] in each case, in order to facilitate the comparison of results between the different recording methods used. The effects of ET-1 and Ang II on STOCs and BK_{Ca} whole-cell currents, and the effects of the PKC activator, DOG, on single channel activity and BK_{Ca} whole-cell current were also investigated. Additionally, the role of PKC in mediating the ET-1 induced inhibition of BK_{Ca} currents was investigated using a TAT-linked PKC inhibitor peptide. Some interesting questions were raised during the discussion of specific results in their appropriate chapters, and it is to be hoped that the comparison of BK_{Ca} currents observed via different methods may partly be able to answer these questions.

BK_{Ca} channels are believed to play an important role in the regulation of vascular tone. It is interesting however, that BK_{Ca} whole-cell current displayed low channel activity unless the membrane was held at depolarized potentials not usually observed *in vivo*. Whole-cell current also showed little difference in BK_{Ca} activity between 100 and 300 nM, probably because the P_{open} of the channel was very low at the membrane potentials tested, with these values being found at the very start of the Boltzmann curve, before the slope. Comparison with the data acquired from single channel recordings confirmed this, as even at [Ca²⁺]_i of 1 μM the P_{open} of BK_{Ca} channels was close to zero at physiological membrane potentials. This is in agreement with reports in the literature. Under resting physiological conditions of approximately 100 nM [Ca²⁺]_i and at

membrane potentials of 0 mV and below, the P_{open} of BK_{Ca} channels has been found to be extremely low (Singer & Walsh, 1987). Meera (Meera *et al.*, 1996) also reported that at $[\text{Ca}^{2+}]_i$ below 1 μM , BK_{Ca} are closed at all physiological membrane potentials. However, it is important to note that the density of BK_{Ca} channels is very high, and this, coupled with their large conductance, means that the activation of these channels can have a large effect on membrane potential.

STOCs, however, were seen to be very active at 0 mV, and so the local $[\text{Ca}^{2+}]_i$ must be increased greatly by Ca^{2+} sparks. Single channel data shows that BK_{Ca} activity increases greatly at $[\text{Ca}^{2+}]_i$ of between 3 and 10 μM . P_{open} of BK_{Ca} channels increases from around 0.12 to around 0.67 between these $[\text{Ca}^{2+}]_i$. This data is in agreement with Ca^{2+} imaging data that suggests that Ca^{2+} sparks increase local $[\text{Ca}^{2+}]_i$ to around 10 μM (Zhuge *et al.*, 2002). It has also been reported that at $[\text{Ca}^{2+}]_i$ of above 10 μM , channels are in the open state over a range of physiological potentials (Meera *et al.*, 1996). This suggests that the main mechanism of BK_{Ca} activation *in vivo* is through the activation of STOCs by Ca^{2+} sparks, and that this is perhaps where future studies should focus. However, understanding how BK_{Ca} whole cell current is modulated may aid our comprehension of STOC activity. Similarly, it is important to appreciate how BK_{Ca} single channels are modulated under certain conditions in order to truly understand how this may affect STOC activity. When considering the intact tissue, the activation of STOCs is likely to be filtered by neighbouring cells. When STOCs are activated in a number of cells, a large hyperpolarization of the tissue will occur and this will cause vasodilation of the blood vessel.

The study of BK_{Ca} whole-cell current can still prove to be useful as it provides a steady-state current, the alteration of which can be easily identified and analyzed. The transient nature of STOCs makes their analysis more difficult, especially as Ca^{2+} spark activity

can vary greatly due to a differing number of Ca^{2+} spark release sites between cells. Excised patches are also unsuitable for some experiments where it is important that intracellular signalling pathways remain intact. The recording of whole-cell currents can be useful in these cases. Comparison of the effects on whole-cell current and STOCs may also reveal how BK_{Ca} currents are modulated, and perhaps help to differentiate between effects on BK_{Ca} channels and those on Ca^{2+} sparks, as Ca^{2+} release was largely inhibited in my experiments when examining BK_{Ca} whole cell currents due to the presence of ryanodine in the patch pipette.

ET-1 and Ang II inhibited both BK_{Ca} whole-cell current and the frequency and amplitude of STOCs. It has been reported that this may be due to a PKC-dependent inhibition of Ca^{2+} sparks (Bonev *et al*, 1997). However, comparison with the effect of 0.2 mM TEA on STOCs suggested that the apparent effect on STOC frequency observed in my experiments may actually be due to the reduction in STOC amplitude in the case of ET-1. Ang II however, had a significant effect STOC frequency compared to TEA, and so it is possible that it may also have an effect on Ca^{2+} spark frequency. It has also been reported elsewhere that PKC may inhibit BK_{Ca} channels directly (Schubert *et al*, 1999); however, the analysis of the effect of ET-1 and Ang II on the activation and decay of the STOCs suggested that neither peptide had a significant effect on BK_{Ca} channel kinetics. If this is the case, how exactly does ET-1 exert its inhibitory effects? As suggested in section 5.3.7, it could be that the application of either ET-1 or Ang II leads to the removal of BK_{Ca} channels from the plasma membrane. It is thought that this could be induced by PKC-dependent cell signalling pathways that lead to a tyrosine phosphorylation-dependent suppression of current. It has been reported that tyrosine phosphorylation of Kv1.2 and Kir1.1 channels causes endocytosis of the channel protein (Nesti *et al*, 2004; Sterling *et al*, 2002; Zeng *et al*,

2002) so could this also provide a possible mechanism for ET-1- and Ang II-induced reduction of BK_{Ca} currents? Nesti (Nesti *et al*, 2004) showed that endocytosis of Kv1.2 channels occurred within 10 min stimulation of the cells by carbachol, the PKC activator phorbol 12-myristate 13-acetate (PMA), or the tyrosine phosphatase inhibitor pervanadate. This data suggests that ET-1 and Ang II could perhaps inhibit BK_{Ca} channels by this mechanism within the timeframe of my experiments (9 min). It is also possible that tyrosine phosphorylation may prevent the anchoring of the channel in the cell membrane, by destabilizing the interaction of the channel with the actin cytoskeleton, namely the actin-binding protein cortactin, as has been found to be the case with Kv1.2 channels (Hattan *et al*, 2002). This effect was seen to occur after 20 min treatment with carbachol and so it is not clear whether either ET-1 or Ang II could have an effect on BK_{Ca} channel cell surface expression via this mechanism within 9 min application as was the case for these experiments. Both endocytosis and destabilization of the actin cytoskeleton, as reported by these groups, occurred as a result of tyrosine phosphorylation of the K⁺ channel. However, it has so far been reported that tyrosine phosphorylation of the BK_{Ca} channel tends to lead to increased activation of the channel, although it has been seen to inhibit a wide variety of other K⁺ channels (reviewed by Davis *et al*, 2001). Tyrosine phosphorylation of BK_{Ca} channels has not been studied in depth, however, and it is perhaps possible that it could lead to disruption of BK_{Ca} cell surface expression by mechanisms not yet investigated.

It is also possible that ET-1 and Ang II modulate BK_{Ca} activity through the activation of Ca²⁺ sensitive enzymes. As mentioned previously, the amount of contractile force generated for any given [Ca²⁺] can be decreased by cGMP and increased by RhoA and Rho kinase pathways. These substances have also been shown to modulate ion channel activity. Since PKC isoforms have been found to activate RhoA, and ET-1 and Ang II

are known to activate PKC, it is perhaps possible that these vasoconstrictors also modulate BK_{Ca} activity in this way.

It is perhaps also possible that ET-1 and Ang II could have their effects by disrupting modulation of the α -subunit by its modulatory β partner. This would reduce the Ca²⁺ sensitivity of the BK_{Ca} channel and so could BK_{Ca} channel activity in this way. However, if this was the case, then it would perhaps be expected that STOC activity and/or decay may also be affected, which was not the case in these experiments.

The vasoconstrictors ET-1 and Ang II had varying effects on BK_{Ca} whole-cell current and STOCs. ET-1 inhibited whole-cell current and STOC amplitude to a similar extent (41% inhibition of BK_{Ca} whole-cell current compared to 46% inhibition of STOC amplitude. Ang II however had a much greater effect on BK_{Ca} whole-cell current than it did on STOCs (39% compared to 26% inhibition, respectively). This probably results from the different signalling pathways utilized by the two peptides and how they affect Ca²⁺ release. Ang II can affect PKA activation as well as modulate PKC activity. It may be that Ang II shows a greater dependency on PKA inhibition than PKC activation and the way in which these two combined mechanisms are utilized may lead to a lesser effect on BK_{Ca} activity in the presence of high local [Ca²⁺] that are observed through Ca²⁺ spark activation. Work within the lab on vasoconstrictor-induced inhibition of K_v channels in rat mesenteric artery smooth muscle cells has shown that ET-1 and Ang II activate different isoforms of PKC in order to exert their effects. This is also likely to explain the difference between ET-1 and Ang II-induced inhibition of BK_{Ca} channels.

The pre-incubation of rat mesenteric artery smooth muscle cells with TAT PKC-IP 20-28 prevented the inhibition of BK_{Ca} whole-cell current by ET-1 rather convincingly, suggesting that ET-1-induced inhibition of BK_{Ca} channels is mediated entirely by a

PKC-dependent mechanism. However, it has to be noted that some of the control BK_{Ca} currents in these experiments were smaller than expected. It is possible that this is due to continual problems with the cell isolation procedure leading to reduced cell surface expression of the channel, perhaps through disruption of the cytoskeleton. However, it is important to note that ET-1 was still seen to have its effect in the absence of PKC-IP in these cells and so cell signalling pathways within the cell do not appear to have been affected adversely.

I could not use DOG as a PKC activator because it inhibited BK_{Ca} single channel activity directly in inside-out excised patches. As was discussed briefly in section 3.4.2, it was necessary to add an additional closed state to fit the closed time distributions of single channel recordings in the presence of DOG. This suggests that DOG is a blocker of BK_{Ca} channels. This inhibitory effect was observed much quicker and had a much greater effect on BK_{Ca} activity in excised patches than it did on BK_{Ca} whole-cell current where intracellular signalling pathways remained intact. This may be because DOG is unable to access the inhibitory site *in vivo*, perhaps because DOG requires the channel to be open in order to bind. The P_{open} of the channel is very low in whole-cell current recordings and so it may be very difficult for the compound to gain access to the inhibitory site if this is the case. It may also be because DOG could have higher affinity for other intracellular molecules when signalling pathways remain intact than it does for the inhibitory site of the channel. It may therefore associate with these molecules in whole-cell experiments, activating pathways that lead to the inhibition of BK_{Ca} channels, but not to the same extent as direct inhibition of the channel. It would be interesting to see whether DOG could act directly on the BK_{Ca} channel in whole-cell experiments where association of the compound with PKC is prevented by pre-incubation of cells with a PKC-IP.

An interesting experiment would be to apply DOG and ET-1 at the same time to see if any additional effects could be seen. If the effects of ET-1 are largely through PKC and DOG activates PKC without having any other effect, then it might be expected that applying both ET-1 and DOG together would not have any greater effect. However, if much of the ET-1 effect is also due to the production of IP₃ and the resulting release of Ca²⁺, or indeed that DOG may act indirectly when PKC is already activated through the production of DAG by ET-1, then this combination of effects may result in an alteration of BK_{Ca} channel activation when compared to the separate results of these two compounds.

It is important to consider the data of McManus & Magleby (1988) when attempting to discuss much of the work in this thesis. As mentioned previously, they reported that BK_{Ca} channels can remain closed for periods of longer than 1 minute when recorded in cultured rat skeletal muscle. However, it is possible that cultured BK_{Ca} channels have different properties to those freshly isolated and so it is not possible to be sure whether this may also be the case for the arterial smooth muscle cells used for the experiments in this thesis. It could be that coincidental channel inactivation is the reason for the decrease in BK_{Ca} activity seen in the presence of ET-1 and Ang II. However, the fact that no reduction in current was seen when ET-1 was applied after pre-incubation with PKC-IP suggests that ET-1 does indeed have an effect on BK_{Ca} channel activity.

6.1 Future work

BK_{Ca} is the most predominant K⁺ channel in many different types of smooth muscle and it has such a large conductance that its regulation is likely to have a major effect on the membrane potential of the cell. It is therefore important to find out more about its properties and how it can be modulated by vasoactive compounds.

The inhibition of BK_{Ca} whole-cell current by ET-1 was prevented by pre-incubation of the cells with a PKC-IP. This suggests that the effect of ET-1 on BK_{Ca} channels is mediated entirely by a PKC-dependent pathway. I would have liked to investigate the effect of PKC inhibition on Ang II modulation of BK_{Ca} channels to see whether this is also dependent entirely on PKC signalling pathways or whether other PKC-independent signalling pathways, such as PKA inhibition, are also involved in Ang II inhibition of BK_{Ca} channels in these cells. It would be interesting to develop this work further by investigating which PKC isoforms are involved in both the ET-1- and Ang II-induced inhibition of BK_{Ca} channels by using isoform specific PKC inhibitors. As has been mentioned, work within the lab has shown that ET-1 and Ang II activate different PKC isoforms to exert effects on rat mesenteric artery smooth muscle cells. Similar work could be carried out to discover which PKC isoforms are involved in BK_{Ca} modulation by these peptides, and whether these are the same isoforms that are involved in the inhibition of Kv channels. It would also be interesting to carry out Ca²⁺-imaging and patch clamp experiments simultaneously so that the effects of ET-1 and Ang II on both Ca²⁺ spark and STOC activity could be monitored.

The actions of the PKC activator DOG were found to differ greatly between excised patches and whole-cell experiments. A PKC-IP could be used to see whether the lesser

effect seen whole-cell is due to a greater affinity for intracellular signalling proteins, or whether it is due to reduced access to the inhibitory site.

It is known that the α -subunit of the BK_{Ca} channel contains consensus sequences corresponding to possible binding sites for protein kinases such as PKA, PKG, and PKC suggesting that it may be possible for these protein kinases to phosphorylate the channel directly. I had hoped to investigate whether PKC may have a direct effect on BK_{Ca} channels as part of my thesis, by investigating whether the PKC catalytic subunit could modulate single channel activity in excised inside-out patches, but unfortunately this was not possible due to time constraints. However, it has been reported that this may indeed be the case. Schubert (Schubert *et al*, 1999) examined the effect of the PKC catalytic subunit on BK_{Ca} channels in rat tail artery and discovered that it did have a direct effect on the channel. It is therefore possible that PKC may also be able to directly modulate BK_{Ca} channel activity in smooth muscle cells isolated from the rat mesenteric artery.

Understanding how intracellular signalling pathways such as these modulate BK_{Ca} channel activity could lead to the development of drugs to lower blood pressure and treat conditions such as hypertension. It is therefore very important that work in this area continues.

REFERENCES

- Amedee T, Renaud JF, Jmari K, Lombet A, Mironneau J, Lazdunski M. (1986). The presence of Na⁺ channels in myometrial smooth muscle cells is revealed by specific neurotoxins. *Biochem Biophys Res Commun* **137**, 675-81.
- Barlow RS, White RE. (1998). Hydrogen peroxide relaxes porcine coronary arteries by stimulating BKCa channel activity. *Am J Physiol Heart Circ Physiol* **275**, H1283-H1289.
- Barman SA, Zhu S, White RE. (2004). PKC activates BKCa channels in rat pulmonary arterial smooth muscle via cGMP-dependent protein kinase. *Am J Physiol Lung Cell Mol Physiol* **286**, L1275-81.
- Barrett JN, Magleby KL, Pallotta BS. (1982). Properties of single calcium-activated potassium channels in cultured rat muscle. *J Physiol* **331**, 211-30.
- Bayguinov O, Hagen B, Bonev AD, Nelson MT, Sanders KM. (2000). Intracellular calcium events activated by ATP in murine colonic myocytes. *Am J Physiol Cell Physiol* **279**, C126-C135.
- Bayguinov O, Hagen B, Kenyon JL, Sanders KM. (2001). Coupling strength between localized ca(2+) transients and K(+) channels is regulated by protein kinase C. *Am J Physiol Cell Physiol* **281**, C1512-23.
- Bayliss WM. (1902). On the local reactions of the arterial wall to changes of internal pressure. *J Physiol* **28**, 220-231.

- Benham CD, Bolton TB. (1986). Spontaneous transient outward currents in single visceral and vascular smooth muscle cells of the rabbit. *J Physiol* **381**, 385-406.
- Bennett MR. (1996). Autonomic neuromuscular transmission at a varicosity. *Prog Neurobiol* **50**, 505-532.
- Berra-Romani R, Blaustein MP, Matteson DR. (2005). TTX-sensitive voltage-gated Na^+ channels are expressed in mesenteric artery smooth muscle cells. *Am J Physiol Heart Circ Physiol* **289**, H137-45.
- Betts LC, Kozlowski RZ. (2000). Electrophysiological effects of endothelin-1 and their relationship to contraction in rat renal arterial smooth muscle. *bjp* **130**, 787-796.
- Bezprozvanny I, Watras J, Ehrlich BE. (1991). Bell-shaped calcium-response curves of $ins(1,4,5)P_3$ - and calcium-gated channels from endoplasmic reticulum of cerebellum. *Nature* **351**, 751-4.
- Boittin FX, Coussin F, Macrez N, Mironneau C, Mironneau J. (1998). Inositol 1,4,5-trisphosphatase and ryanodine-sensitive Ca^{2+} release channel-dependent Ca^{2+} signalling in rat portal vein myocytes. *Cell Calcium* **23**, 303-314.
- Bolton TB, Lim SP. (1989). Properties of calcium stores and transient outward currents in single smooth muscle cells of rabbit intestine. *J Physiol* **409**, 385-401.
- Bolz SS, de Wit C, Pohl U. (1999). Endothelium-derived hyperpolarizing factor but not NO reduces smooth muscle Ca^{2+} during acetylcholine-induced dilation of microvessels. *Br J Pharmacol* **128**, 124-34.

Bolz SS, Vogel L, Sollinger D, Derwand R, de Wit C, Loirand G, et al. (2003). Nitric oxide-induced decrease in calcium sensitivity of resistance arteries is attributable to activation of the myosin light chain phosphatase and antagonized by the RhoA/Rho kinase pathway. *Circulation* **107**, 3081-7.

Bonev AD, Jaggar JH, Rubart M, Nelson MT. (1997). Activators of protein kinase C decrease Ca²⁺ spark frequency in smooth muscle cells from cerebral arteries. *Am J Physiol* **273**, C2090-5.

Borisova L, Shmygol A, Wray S, Burdyga T. (2007). Evidence that a Ca²⁺ sparks/STOCs coupling mechanism is responsible for the inhibitory effect of caffeine on electro-mechanical coupling in guinea pig ureteric smooth muscle. *Cell Calcium* **42**, 303-11.

Bouallegue A, Daou GB, Srivastava AK. (2007). Endothelin-1-induced signaling pathways in vascular smooth muscle cells. *Curr Vasc Pharmacol* **5**, 45-52.

Bradley KN, Craig JW, Muir TC, McCarron JG. (2004). The sarcoplasmic reticulum and sarcolemma together form a passive Ca²⁺ trap in colonic smooth muscle. *Cell Calcium* **36**, 29-41.

Bradley KN, Flynn ERM, Muir TC, McCarron JG. (2002). Ca²⁺ regulation in guinea-pig colonic smooth muscle: The role of the Na⁺-Ca²⁺ exchanger and the sarcoplasmic reticulum. *J Physiol (Lond)* **538**, 465-482.

Brayden JE. (1996). Potassium channels in vascular smooth muscle. *Clinical and Experimental Pharmacology and Physiology* **23**, 1069--1076.

Brenner R, Perez GJ, Bonev AD, Eckman DM, Kosek JC, Wiler SW, et al. (2000). Vasoregulation by the beta1 subunit of the calcium-activated potassium channel. *Nature* **407**, 870-6.

Breuiller-Fouché M, Tertrin-Clarya C, Héluva V, Fourniera T, Ferréa F. (1998). Role of protein kinase C in endothelin-1-induced contraction of human myometrium. *Biol Reprod* **59**, 153.

Burdyga TV, Taggart MJ, Wray S. (1995). Major difference between rat and guinea-pig ureter in the ability of agonists and caffeine to release Ca²⁺ and influence force. *J Physiol* **489**, 327-335.

Burnham MP, Johnson IT, Weston AH (2006). Reduced Ca²⁺-dependent activation of large-conductance Ca²⁺-activated K⁺ channels from arteries of Type 2 diabetic Zucker diabetic fatty rats. *Am J Physiol Heart Circ Physiol* **290** (4) H1520-7.

Bychkov R, Gollasch M, Ried C, Luft FC, Haller H. (1997). Regulation of spontaneous transient outward potassium currents in human coronary arteries. *Circulation* **95**, 503-10.

Cain AE, Tanner DM, Khalil RA. (2002). Endothelin-1--induced enhancement of coronary smooth muscle contraction via MAPK-dependent and MAPK-independent [Ca²⁺]_i sensitization pathways. *Hypertension* **39**, 543-9.

Capogrossi MC, Kaku T, Filburn CR, Pelto DJ, Hansford RG, Spurgeon HA, et al. (1990). Phorbol ester and dioctanoylglycerol stimulate membrane association of protein kinase C and have a negative inotropic effect mediated by changes in cytosolic Ca²⁺ in adult rat cardiac myocytes. *Circ Res* **66**, 1143-55.

Carl A, Lee HK, Sanders KM. (1996). Regulation of ion channels in smooth muscles by calcium. *Am J Physiol Cell Physiol* **271**, C9-C34.

Carrington WA, Lynch RM, Moore ED, Isenberg G, Fogarty KE, Fay FS. (1995). Superresolution three-dimensional images of fluorescence in cells with minimal light exposure. *Science* **268**, 1483-7.

Casteels R, Droogmans G. (1981). Exchange characteristics of the noradrenaline-sensitive calcium store in vascular smooth muscle cells or rabbit ear artery. *J Physiol* **317**, 263-79.

Chapman H, Piggot C, Andrews PW, Wann KT (2007). Characterisation of large-conductance calcium-activated potassium channels (BK_(Ca)) in human NT2-N cells. *Brain Res* **1129**, 15-25.

Cox DH, Aldrich RW. (2000). Role of the beta1 subunit in large-conductance Ca⁽²⁺⁾-activated K(+) channel gating energetics. mechanisms of enhanced ca(2+) sensitivity. *J Gen Physiol* **116**, 411-32.

Davis MJ, Hill MA. (1999). Signaling mechanisms underlying the vascular myogenic response. *Physiol Rev* **79**, 387-423.

Davis MJ, Wu X, Nurkiewicz TR, Kawasaki J, Gui P, Hill MA, et al. (2001). Regulation of ion channels by protein tyrosine phosphorylation. *Am J Physiol Heart Circ Physiol* **281**, H1835-H1862.

DeFelice LJ (1993). Molecular and biophysical view of the Ca channel: a hypothesis regarding oligomeric structure, channel clustering, and macroscopic current. *J Membr Biol*. **133**(3) 191-202.

Devine CE, Somlyo AV, Somlyo AP. (1972). Sarcoplasmic reticulum and excitation-contraction coupling in mammalian smooth muscles. *J Cell Biol* **52**, 690-718.

Dimitropoulou C, Han G, Miller AW, Molero M, Fuchs LC, White RE, et al. (2002). Potassium (BK(Ca)) currents are reduced in microvascular smooth muscle cells from insulin-resistant rats. *Am J Physiol Heart Circ Physiol* **282**, H908-17.

Earley S, Heppner TJ, Nelson MT, Brayden JE. (2005). TRPV4 forms a novel Ca²⁺ signalling complex with ryanodine receptors and BK_{Ca} channels. *Circ Res* **97**, 1270-9.

Fill M, Copello JA. (2002). Ryanodine receptor calcium release channels. *Physiol Rev* **82**, 893-922.

Finch EA, Turner TJ, Goldin SM. (1991). Calcium as a coagonist of inositol 1,4,5-trisphosphate-induced calcium release. *Science* **252**, 443-446.

Ganitkevich V, Isenberg G. (1990). Isolated guinea pig coronary smooth muscle cells. acetylcholine induces hyperpolarization due to sarcoplasmic reticulum calcium release activating potassium channels. *Circ Res* **67**, 525-8.

Ganitkevich VY, Isenberg G. (1992). Caffeine-induced release and reuptake of Ca²⁺ by Ca²⁺ stores in myocytes from guinea-pig urinary bladder. *J Physiol* **458**, 99-117.

Ghatta S, Nimmagadda D, Xu X, O'Rourke ST. (2006). Large-conductance, calcium-activated potassium channels: Structural and functional implications. *Pharmacol Ther* **110** (1), 103-16.

Golowasch J, Kirkwood A, Miller C. (1986). Allosteric effects of Mg²⁺ on the gating of Ca²⁺-activated K⁺ channels from mammalian skeletal muscle. *J Exp Biol* **124**, 5-13.

Gordienko DV, Bolton TB, Cannell MB (1998). Variability in spontaneous subcellular calcium release in guinea-pig ileum smooth muscle cells. *J Physiol*. **507** 707-20.

Gordienko DV, Bolton TB. (2002). Crosstalk between ryanodine receptors and IP(3) receptors as a factor shaping spontaneous ca(2+)-release events in rabbit portal vein myocytes. *J Physiol* **542**, 743-62.

Guerrero A, Fay FS, Singer JJ. (1994). Caffeine activates a ca(2+)-permeable, nonselective cation channel in smooth muscle cells. *J Gen Physiol* **104**, 375-94.

Hattan D, Nesti E, Cachero TG, Morielli AD. (2002). Tyrosine phosphorylation of Kv1.2 modulates its interaction with the actin-binding protein cortactin. *J Biol Chem* **277**, 38596-606.

Hayabuchi Y, Davies NW, Standen NB. (2001a). Angiotensin II inhibits rat arterial KATP channels by inhibiting steady-state protein kinase A activity and activating protein kinase Ce. *J Physiol* **530**, 193-205.

Hayabuchi Y, Standen NB, Davies NW. (2001b). Angiotensin II inhibits and alters kinetics of voltage-gated K⁺ channels of rat arterial smooth muscle. *Am J Physiol Heart Circ Physiol* **281**, H2480-H2489.

Hayoz S, Beny J-L, Bychkov R (2007). Intracellular cAMP: the "switch that triggers on "spontaneous transient outward currents" generation in freshly isolated myocytes from thoracic aorta. *Am J Physiol Cell Physiol*. **292**, C1502-09.

He J, Pi Y, Walker JW, Kamp TJ. (2000). Endothelin-1 and photoreleased diacylglycerol increase L-type Ca²⁺ current by activation of protein kinase C in rat ventricular myocytes. *J Physiol* **524**, 807-820.

Herrera GM, Heppner TJ, Nelson MT. (2001). Voltage dependence of the coupling of Ca²⁺ sparks to BKCa channels in urinary bladder smooth muscle. *Am J Physiol Cell Physiol* **280**, C481-C490.

Hill AJ, Hinton JM, Cheng H, Gao Z, Bates DO, Hancox JC, Langton PD, James AF. (2006). A TRPC-like non-selective cation current activated by α 1-adrenoceptors in rat mesenteric artery smooth muscle cells. *Cell Calcium* **40** (1), 29-40.

Hille B. (2001). *Ion channels of excitable membranes*. Sinauer Associates, Inc, .

Hogg RC, Wang Q, Helliwell RN, Large WA. (1993). Properties of spontaneous inward currents in rabbit pulmonary artery smooth muscle cells. *Pflügers Archiv European Journal of Physiology* **425**, 233-240.

- Hu S, Kima HS, Jenga AY. (1991). Dual action of endothelin-1 on the Ca^{2+} -activated K^+ channel in smooth muscle cells of porcine coronary artery. *Eur J Pharmacol* **194**, 31-36.
- Iino M. (1990a). Biphasic Ca^{2+} dependence of inositol 1,4,5-trisphosphate-induced Ca^{2+} release in smooth muscle cells of the guinea pig taenia caeci. *J Gen Physiol* **95**, 1103-22.
- Iino M. (1990b). Calcium release mechanisms in smooth muscle. *Jpn J Pharmacol* **54**, 345-54.
- Iino M, Endo M. (1992). Calcium-dependent immediate feedback control of inositol 1,4,5-trisphosphate-induced Ca^{2+} release. *Nature* **360**, 76-8.
- Jackson WF, Blair KL. (1998). Characterization and function of Ca^{2+} -activated K^+ channels in arteriolar muscle cells. *Am J Physiol* **274**, H27-34.
- Jaggari JH, Wellman GC, Heppner TJ, Porter VA, Perez GJ, Gollasch M, et al. (1998a). Ca^{2+} channels, ryanodine receptors and Ca^{2+} -activated K^+ channels: A functional unit for regulating arterial tone. *Acta Physiol Scand* **164**, 577--587.
- Jaggari JH, Stevenson AS, Nelson MT. (1998b). Voltage dependence of Ca^{2+} sparks in intact cerebral arteries. *Am J Physiol Cell Physiol* **274**, C1755-C1761.
- Jahromi BS, Aihara Y, Ai J, Zhang ZD, Weyer G, Nikitina E, et al. (2008). Preserved BK channel function in vasospastic myocytes from a dog model of subarachnoid hemorrhage. *J Vasc Res* **45**, 402-15.
- Ji G, Feldman M, Doran R, Zipfel W, Kotlikoff MI. (2006). Ca^{2+} -induced Ca^{2+} release through localized Ca^{2+} uncaging in smooth muscle. *J Gen Physiol* **127**, 225-35.

Jiang Z, Wallner M, Meera P, Toro L. (1999). Human and rodent MaxiK channel beta-subunit genes: Cloning and characterization. *Genomics* **55**, 57-67.

Jones AW, Magliola L, Waters CB, Rubin LJ (1998). Endothelin-1 activates phospholipases and channels at similar concentrations in porcine coronary arteries. *Am J Physiol.* **274**(6), C1583-91.

Kamishima T, McCarron JG. (1997). Regulation of the cytosolic Ca²⁺ concentration by Ca²⁺ stores in single smooth muscle cells from rat cerebral arteries. *J Physiol (Lond)* **501**, 497-508.

Kamishima T, McCarron JG. (1996). Depolarization-evoked increases in cytosolic calcium concentration in isolated smooth muscle cells of rat portal vein. *J Physiol* **492**, 61-74.

Kapicka CL, Carl A, Hall ML, Percival AL, Frey BW, Kenyon JL (1994). *Am J Physiol* **266**, C601-10.

Knaus HG, McManus OB, Lee SH, Schmalhofer WA, Garcia-Calvo M, Helms LM, et al. (1994). Tremorgenic indole alkaloids potently inhibit smooth muscle high-conductance calcium-activated potassium channels. *Biochemistry* **33**, 5819-28.

Kohda M, Komori S, Unno T, Ohashi H. (1997). Characterization of action potential-triggered [Ca²⁺]_i transients in single smooth muscle cells of guinea-pig ileum. *Br J Pharmacol* **122**, 477-86.

Langton PD, Nelson MT, Huang Y, Standen NB. (1991). Block of calcium-activated potassium channels in mammalian arterial myocytes by tetraethylammonium ions. *Am J Physiol* **260**, H927-34.

Large WA, Wang Q. (1996). Characteristics and physiological role of the Ca^{2+} -activated Cl^- conductance in smooth muscle. *Am J Physiol* **271**, C435-54.

Lin MT, Hessinger DA, Pearce WJ, Longo LD. (2003). Developmental differences in Ca^{2+} -activated K^+ channel activity in ovine basilar artery. *Am J Physiol Heart Circ Physiol* **285**, H701-9.

Lippiat JD, Standen NB, Harrow ID, Phillips SC, Davies NW. (2003). Properties of BK(Ca) channels formed by bicistronic expression of hSlo α and beta1-4 subunits in HEK293 cells. *J Membr Biol* **192**, 141-8.

Liu P, Xi Q, Ahmed A, Jaggar JH, Dopico AM (2004). Essential role for smooth muscle BK channels in alcohol-induced cerebrovascular constriction. *Proc Natl Acad Sci USA* **101**(52), 18217-22.

MacMillan D, Chalmers S, Muir TC, McCarron JG. (2005). IP $_3$ -mediated Ca^{2+} increases do not involve the ryanodine receptor, but ryanodine receptor antagonists reduce IP $_3$ -mediated Ca^{2+} increases in guinea-pig colonic smooth muscle cells. *J Physiol* **569**, 533-44.

Marx SO, Reiken S, Hisamatsu Y, Jayaraman T, Burkhoff D, Rosemblyt N, et al. (2000). PKA phosphorylation dissociates FKBP12.6 from the calcium release channel (ryanodine receptor) : Defective regulation in failing hearts. *Cell* **101**, 365-376.

McCarron JG, Bradley KN, MacMillan D, Chalmers S, Muir TC. (2004). The sarcoplasmic reticulum, Ca²⁺ trapping, and wave mechanisms in smooth muscle. *Physiology* **19**, 138-147.

McGahon MK, Dash DP, Arora A, Wall N, Dawicki J, Simpson DA, Scholfield CN, McGeown JG (2007). Diabetes downregulates large-conductance Ca²⁺-activated potassium beta 1 channel subunit in retinal arteriolar smooth muscle. *Circ Res.* **100** (5) 703-11.

McManus OB, Helms LM, Pallanck L, Ganetzky B, Swanson R, Leonard RJ. (1995). Functional role of the beta subunit of high conductance calcium-activated potassium channels. *Neuron* **14**, 645-50.

McManus OB, Magleby KL (1988). Kinetic states and modes of single large-conductance calcium-activated potassium channels in cultured rat skeletal muscle. *J Physiol.* **402**, 79-120.

McManus OB, Magleby KL. (1991). Accounting for the ca(2+)-dependent kinetics of single large-conductance ca(2+)-activated K⁺ channels in rat skeletal muscle. *J Physiol* **443**, 739-77.

Meera P, Wallner M, Jiang Z, Toro L. (1996). A calcium switch for the functional coupling between α (hslo) and β subunits (KV, ca β) of maxi K channels. *FEBS Lett* **382**, 84--88.

Meera P, Wallner M, Toro L. (2000). A neuronal beta subunit (KCNMB4) makes the large conductance, voltage- and Ca²⁺-activated K⁺ channel resistant to charybdotoxin and iberiotoxin. *Proc Natl Acad Sci U S A* **97**, 5562-7.

Michikawa T, Hamanaka H, Otsu H, Yamamoto A, Miyawaki A, Furuichi T, et al. (1994). Transmembrane topology and sites of N-glycosylation of inositol 1,4,5- trisphosphate receptor. *J Biol Chem* **269**, 9184-9189.

Minami K, Hirata Y, Tokumura A, Nakaya Y, Fukuzawa K. (1995). Protein kinase c-independent inhibition of the Ca²⁺-activated K⁺ channel by angiotensin II and endothelin-1. *Biochem Pharmacol* **49**, 1051.

Mironneau J, Martin C, Arnaudeau S, Jmari K, Rakotoarisoa L, Sayet I, et al. (1990). High-affinity binding sites for [3H]saxitoxin are associated with voltage-dependent sodium channels in portal vein smooth muscle. *Eur J Pharmacol* **184**, 315-9.

Mistry DK, Garland CJ. (1998). Characteristics of single, large-conductance calcium-dependent potassium channels (BKCa) from smooth muscle cells isolated from the rabbit mesenteric artery. *J Membrane Biol* **164**, 125-138.

Moss BL, Magleby KL (2001). Gating and conductance properties of BK channels are modulated by the S9-S10 tail domain of the alpha subunit. A study of mSlo1 and mSlo3 wild-type and chimeric channels. *J Gen Physiol* **118**(6), 711-34.

Muraki K, Imaizumi Y, Watanabe M. (1991). Sodium currents in smooth muscle cells freshly isolated from stomach fundus of the rat and ureter of the guinea-pig. *J Physiol* **442**, 351-75.

Murphy RA, Rembold CM. (2005). The latch-bridge hypothesis of smooth muscle contraction. *Can J Physiol Pharmacol* **83**, 857-64.

Nelson MT, Cheng H, Rubart M, Santana LF, Bonev AD, Knot HJ, et al. (1995). Relaxation of arterial smooth muscle by calcium sparks. *Science* **270**, 633-637.

Nelson MT, Patlak JB, Worley JF, Standen NB. (1990). Calcium channels, potassium channels, and voltage dependence of arterial smooth muscle tone. *Am J Physiol Cell Physiol* **259**, C3-C18.

Nelson MT, Quayle JM. (1995). Physiological roles and properties of potassium channels in arterial smooth muscle. *Am J Physiol* **268**, C799-822.

Nelson MT, Standen NB, Brayden JE, Worley JF, 3rd. (1988). Noradrenaline contracts arteries by activating voltage-dependent calcium channels. *Nature* **336**, 382-5.

Nesti E, Everill B, Morielli AD. (2004). Endocytosis as a mechanism for tyrosine kinase-dependent suppression of a voltage-gated potassium channel. *Mol Biol Cell* **15**, 4073-88.

Neylon CB, Richards SM, Larsen MA, Agrotis A, Bobik A. (1995). Multiple types of ryanodine receptor/Ca²⁺ release channels are expressed in vascular smooth muscle. *Biochem Biophys Res Commun* **215**, 814-21.

Nimigean CM, Magleby KL. (1999). The beta subunit increases the Ca²⁺ sensitivity of large conductance Ca²⁺-activated potassium channels by retaining the gating in the bursting states. *J Gen Physiol* **113**, 425-40.

Niu X, Magleby KL. (2002). Stepwise contribution of each subunit to the cooperative activation of BK channels by Ca²⁺. *Proc Natl Acad Sci U S A* **99**, 11441-6.

Ohya Y, Adachi N, Setoguchi M, Abe I, Fujishima M. (1997). Effects of CP-060S on membrane channels in vascular smooth muscle cells from guinea pig. *Eur J Pharmacol* **330**, 93-9.

Park WS, Son YK, Kim N, Ko JH, Kang SH, Warda M, et al. (2007). Acute hypoxia induces vasodilation and increases coronary blood flow by activating inward rectifier K(+) channels. *Pflugers Arch* **454**, 1023-30.

Parker I, Yao Y. (1991). Regenerative release of calcium from functionally discrete subcellular stores by inositol trisphosphate. *Proc Biol Sci* **246**, 269-74.

Patton C. (2003). MaxChelator. <http://www.stanford.edu/~cpatton/maxc.html>

Peng H, Matchkov V, Ivarsen A, Aalkjaer C, Nilsson H. (2001). Hypothesis for the initiation of vasomotion. *Circ Res* **88**, 810-5.

Perez GJ, Bonev AD, Patlak JB, Nelson MT. (1999). Functional coupling of ryanodine receptors to KCa channels in smooth muscle cells from rat cerebral arteries. *J Gen Physiol* **113**, 229-38.

Pluger S, Faulhaber J, Furstenau M, Lohn M, Waldschutz R, Gollasch M, et al. (2000). Mice with disrupted BK channel beta1 subunit gene feature abnormal Ca²⁺ spark/STOC coupling and elevated blood pressure. *Circ Res* **87**, E53-60.

Porter VA, Bonev AD, Knot HJ, Heppner TJ, Stevenson AS, Kleppisch T, et al. (1998). Frequency modulation of Ca²⁺ sparks is involved in regulation of arterial diameter by cyclic nucleotides. *Am J Physiol* **274**, C1346-55.

Rainbow RD, Hardy MEL, Standen NB, Davies NW. (2006). Glucose reduces endothelin inhibition of voltage-gated potassium channels in rat arterial smooth muscle cells. *J Physiol* **575**, 833-844.

Rainbow RD, Standen NB, Davies NW. (2005). PKC independent block of K⁺ channels by 1,2-dioctanoyl-sn-glycerol (DOG). *Biophys J* **88**, 662a-Abstract.

Ross CA, Danoff SK, Schell MJ, Snyder SH, Ullrich A. (1992). Three additional inositol 1,4,5-trisphosphate receptors: Molecular cloning and differential localization in brain and peripheral tissues. *Proc Natl Acad Sci U S A* **89**, 4265-9.

Rothberg BS, Magleby KL (2000). Voltage and Ca²⁺ activation of single large-conductance Ca²⁺-activated K⁺ channels described by a two-tiered allosteric gating mechanism. *J Gen Physiol.* **116**(1), 75-99.

Sadoshima J. (1998). Versatility of the angiotensin II type 1 receptor. *Circ Res* **82**, 1352-1355.

Salamanca DA, Khalil RA. (2005). Protein kinase C isoforms as specific targets for modulation of vascular smooth muscle function in hypertension. *biochem pharm* **70**, 1537-1547.

Saleh S, Yeung SY, Prestwich S, Pucovsky V, Greenwood I. (2005). Electrophysiological and molecular identification of voltage-gated sodium channels in murine vascular myocytes. *J Physiol* **568**, 155-69.

Saleh SN, Greenwood IA. (2005). Activation of chloride currents in murine portal vein smooth muscle cells by membrane depolarization involves intracellular calcium release. *Am J Physiol Cell Physiol* **288**, C122-31.

Schreiber M, Salkoff L. (1997). A novel calcium-sensing domain in the BK channel. *Biophys J* **73**, 1355-63.

Schubert R, Noack T, Serebryakov VN. (1999). Protein kinase C reduces the KCa current of rat tail artery smooth muscle cells. *Am J Physiol Cell Physiol* **276**, C648-C658.

Shin CY, Lee YP, Lee TS, Je HD, Kim DS, Sohn UD. (2002). The signal transduction of endothelin-1-induced circular smooth muscle cell contraction in cat esophagus. *J Pharmacol Exp Ther* **302**, 924.

Shinjoh M, Nakaki T, Otsuka Y, Sasakawa N, Kato R. (1991). Vascular smooth muscle contraction induced by Na⁺ channel activators, veratridine and batrachotoxin. *Eur J Pharmacol* **205**, 199-202.

Shmygol A, Wray S. (2005). Modulation of agonist-induced Ca²⁺ release by SR Ca²⁺ load: Direct SR and cytosolic Ca²⁺ measurements in rat uterine myocytes. *Cell Calcium* **37**, 215-23.

Shuai J, Rose HJ, Parker I. (2006). The number and spatial distribution of IP3 receptors underlying calcium puffs in xenopus oocytes. *Biophysical Journal* **91**, 4033-4044.

Sigworth FJ, Sine SM. (1987). Data transformations for improved display and fitting of single-channel dwell time histograms. *Biophys J* **52**, 1047-54.

Singer JJ, Walsh JV, Jr. (1987). Characterization of calcium-activated potassium channels in single smooth muscle cells using the patch-clamp technique. *Pflugers Arch* **408**, 98-111.

Standen NB, Quayle JM. (1998). K⁺ channel modulation in arterial smooth muscle. *Acta Physiol Scand* **164**, 549-57.

Stefani E, Ottolia M, Noceti F, Olcese R, Wallner M, Latorre R, et al. (1997). Voltage-controlled gating in a large conductance Ca²⁺-sensitive K⁺ channel (hsl_o). *Proc Natl Acad Sci U S A* **94**, 5427-31.

Sterling H, Lin DH, Gu RM, Dong K, Hebert SC, Wang WH. (2002). Inhibition of protein-tyrosine phosphatase stimulates the dynamin-dependent endocytosis of ROMK1. *J Biol Chem* **277**, 4317-23.

Suematsub E, Hirataa M, Hashimotob T, Kuriyamab H. (1984). Inositol 1,4,5-trisphosphate releases Ca²⁺ from intracellular store sites in skinned single cells of porcine coronary artery. *Biochem Biophys Res Commun* **120**, 481-485.

Sun XP, Schlichter LC, Stanley EF (1999). Single-channel properties of BK-type calcium-activated potassium channels at a cholinergic presynaptic nerve terminal. *J Physiol* **518**, 639-51.

Tanaka Y, Koike K, Alioua A, Shigenobu K, Stefani E, Toro L. (2004). Beta1-subunit of MaxiK channel in smooth muscle: A key molecule which tunes muscle mechanical activity. *J Pharmacol Sci* **94**, 339-47.

Toro L, Wallner M, Meera P, Tanaka Y. (1998). Maxi-K(ca), a unique member of the voltage-gated K channel superfamily. *News Physiol Sci* **13**, 112-7.

Tripathy A, Meissner G. (1996). Sarcoplasmic reticulum luminal Ca²⁺ has access to cytosolic activation and inactivation sites of skeletal muscle Ca²⁺ release channel. *Biophys J* **70**, 2600-15.

Wagner-Mann C, Hu Q, Sturek M. (1992). Multiple effects of ryanodine on intracellular free Ca²⁺ in smooth muscle cells from bovine and porcine coronary artery: Modulation of sarcoplasmic reticulum function. *Br J Pharmacol* **105**, 903-11.

Wallner M, Meera P, Ottolia M, Kaczorowski GJ, Latorre R, Garcia ML, et al. (1995). Characterization of and modulation by a beta-subunit of a human maxi KCa channel cloned from myometrium. *Receptors Channels* **3**, 185-99.

Wallner M, Meera P, Toro L. (1999). Molecular basis of fast inactivation in voltage and Ca²⁺-activated K⁺ channels: A transmembrane beta-subunit homolog. *Proc Natl Acad Sci U S A* **96**, 4137-42.

Wallner M, Meera P, Toro L. (1996). Determinant for beta-subunit regulation in high-conductance voltage-activated and ca(2+)-sensitive K⁺ channels: An additional transmembrane region at the N terminus. *Proc Natl Acad Sci U S A* **93**, 14922-7.

Walsh MP. (1994). Calmodulin and the regulation of smooth muscle contraction. *Mol Cell Biochem* **135**, 21-41.

Wang J, Zhou Y, Wen H, Levitan IB. (1999). Simultaneous binding of two protein kinases to a calcium-dependent potassium channel. *J Neurosci* **19**, RC4.

Wei A, Jegla T, Salkoff L. (1996). Eight potassium channel families revealed by the *C. elegans* genome project. *Neuropharmacology* **35**, 805-29.

Wellman GC, Santana LF, Bonev AD, Nelson MT (2001). Role of phospholamban in the modulation of arterial Ca(2+) sparks and Ca(2+)-activated K(+) channels by cAMP. *Am J Physiol Cell Physiol* **281**(3), C1029-37.

White RE, Kryman JP, El-Mowafy AM, Han G, Carrier GO. (2000). cAMP-dependent vasodilators cross-activate the cGMP-dependent protein kinase to stimulate BK ca channel activity in coronary artery smooth muscle cells. *Circ Res* **86**, 897-905.

White C, McGeown JG. (2000). Regulation of basal intracellular calcium concentration by the sarcoplasmic reticulum in myocytes from the rat gastric antrum. *J Physiol* **529**, 395-404.

White C, McGeown JG. (2003). Inositol 1,4,5-trisphosphate receptors modulate Ca²⁺ sparks and Ca²⁺ store content in vas deferens myocytes. *Am J Physiol Cell Physiol* **285**, C195-204.

Xia XM, Ding JP, Lingle CJ. (1999). Molecular basis for the inactivation of Ca²⁺- and voltage-dependent BK channels in adrenal chromaffin cells and rat insulinoma tumor cells. *J Neurosci* **19**, 5255-64.

Xu L, Meissner G. (1998). Regulation of cardiac muscle Ca²⁺ release channel by sarcoplasmic reticulum lumenal Ca²⁺. *Biophys J* **75**, 2302-12.

Yanagisawa M, Kurihara H, Kimura S, Tomobe Y, Kobayashi M, Mitsui Y, et al. (1988). A novel potent vasoconstrictor peptide produced by vascular endothelial cells. *Nature* **332**, 411-5.

Zeng WZ, Babich V, Ortega B, Quigley R, White SJ, Welling PA, et al. (2002). Evidence for endocytosis of ROMK potassium channel via clathrin-coated vesicles. *Am J Physiol Renal Physiol* **283**, F630-9.

Zhang WM, Yip KP, Lin MJ, Shimoda LA, Li WH, Sham JS. (2003). ET-1 activates Ca²⁺ sparks in PASMC: Local Ca²⁺ signaling between inositol trisphosphate and ryanodine receptors. *Am J Physiol Lung Cell Mol Physiol* **285**, L680-90.

Zhou XB, Arntz C, Kamm S, Motejlek K, Sausbier U, Wang GX, et al. (2001). A molecular switch for specific stimulation of the BKCa channel by cGMP and cAMP kinase. *J Biol Chem* **276**, 43239-45.

Zhou R, Liu L, Hu D. (2005). Involvement of BKCa alpha subunit tyrosine phosphorylation in vascular hyporesponsiveness of superior mesenteric artery following hemorrhagic shock in rats. *Cardiovasc Res* **68**, 327-35.

Zhuge R, Fogarty KE, Tuft RA, Walsh JV, Jr. (2002). Spontaneous transient outward currents arise from microdomains where BK channels are exposed to a mean Ca²⁺ concentration on the order of 10 microM during a Ca²⁺ spark. *J Gen Physiol* **120**, 15-27.

ZhuGe R, Tuft RA, Fogarty KE, Bellve K, Fay FS, Walsh JV, Jr. (1999). The influence of sarcoplasmic reticulum Ca^{2+} concentration on Ca^{2+} sparks and spontaneous transient outward currents in single smooth muscle cells. *J Gen Physiol* **113**, 215-28.